

EFFECT OF OPERATING PARAMETERS ON PERFORMANCE OF ADDITIVE/  
ZEOLITE/ POLYMER MIXED MATRIX MEMBRANES

A THESIS SUBMITTED TO  
THE GRADUATE SCHOOL OF NATURAL AND APPLIED SCIENCES  
OF  
MIDDLE EAST TECHNICAL UNIVERSITY

BY

EDİBE EDA ORAL

IN PARTIAL FULFILLMENT OF THE REQUIREMENTS  
FOR  
THE DEGREE OF MASTER OF SCIENCE  
IN  
CHEMICAL ENGINEERING

FEBRUARY 2011

Approval of the thesis:

**EFFECT OF OPERATING PARAMETERS ON PERFORMANCE OF  
ADDITIVE/ZEOLITE/POLYMER MIXED MATRIX MEMBRANES**

submitted by **EDİBE EDA ORAL** in partial fulfillment of the requirements for the degree of **Master of Science in Chemical Engineering Department, Middle East Technical University** by,

Prof. Dr. Canan Özgen  
Dean, Graduate School of **Natural and Applied Sciences**

\_\_\_\_\_

Prof. Dr. Deniz Üner  
Head of Department, **Chemical Engineering**

\_\_\_\_\_

Prof. Dr. Levent Yılmaz  
Supervisor, **Chemical Engineering Dept., METU**

\_\_\_\_\_

Assoc. Prof. Dr. Halil Kalıpçılar  
Co-supervisor, **Chemical Engineering Dept., METU**

\_\_\_\_\_

**Examining Committee Members:**

Prof. Dr. Önder Özbelge  
Chemical Engineering Dept., METU

\_\_\_\_\_

Prof. Dr. Levent Yılmaz  
Chemical Engineering Dept., METU

\_\_\_\_\_

Prof. Dr. Birgül Tantekin Ersolmaz  
Chemical Engineering Dept., ITU

\_\_\_\_\_

Assoc. Prof. Dr. Halil Kalıpçılar  
Chemical Engineering Dept., METU

\_\_\_\_\_

Dr. Ahmet Turhan Ural  
M-D2 Engineering-Recycling-Consultancy- Company

\_\_\_\_\_

**Date:** 04.02.2011

**I hereby declare that all information in this document has been obtained and presented in accordance with academic rules and ethical conduct. I also declare that, as required by these rules and conduct, I have fully cited and referenced all material and results that are not original to this work.**

Name, Last name : Edibe Eda ORAL

Signature :

## **ABSTRACT**

### **EFFECT OF OPERATING PARAMETERS ON PERFORMANCE OF ADDITIVE/ZEOLITE/POLYMER MIXED MATRIX MEMBRANES**

Oral, Edibe Eda

M.Sc., Department of Chemical Engineering

Supervisor : Prof. Dr. Levent Yılmaz

Co-supervisor : Assoc. Prof. Dr. Halil Kalıpçılar

January 2011, 85 pages

Membrane based separation techniques have been widely used and developed over decades. Generally polymeric membranes are used in membrane based gas separation; however their gas separation performances are not sufficient enough for industrial feasibility. On the other hand inorganic membranes have good separation performance but they have processing difficulties. As a consequence mixed matrix membranes (MMMs) which comprise of inorganic particles dispersed in organic matrices are developed. Moreover, to enhance the interaction between polymer and zeolite particles ternary mixed matrix membranes are introduced by using low molecular weight additives as third component and promising results were obtained at 35 °C. Better understanding on gas transport mechanism of these membranes could be achieved by studying the effect of preparation and operating parameters.

This study investigates the effect of operation temperature and annealing time and temperature on gas separation performance of MMMs. The membranes used in this study consist of glassy polyethersulfone (PES) polymer, SAPO-34 particles and 2-

hidroxy 5-methyl aniline (HMA) as compatibilizer. The membranes fabricated in previous study were used and some membranes were used as synthesized while post annealing (at 120°C, 0.2atm, N<sub>2</sub> atm, 7-30 days) applied to some membranes before they are tested. The temperature dependent gas transport properties of the membranes were characterized by single gas permeation measurements of H<sub>2</sub>, CO<sub>2</sub>, and CH<sub>4</sub> gases between 35 °C-120 °C. The membranes also characterized by scanning electron microscopy (SEM), thermal gravimetric analysis (TGA) and differential scanning calorimetry (DSC).

Annealing time and temperature affected the reproducibility and stability of the mixed matrix membranes and by applying post annealing step to mixed matrix membranes at higher temperatures and longer times, more stable membranes were obtained. For pure PES membranes thermally stable performances were obtained without any need of extra treatment.

The permeabilities of all studied gases increased with increasing operation temperature. Also the selectivities of H<sub>2</sub>/CO<sub>2</sub> were increased while CO<sub>2</sub>/CH<sub>4</sub>, H<sub>2</sub>/CH<sub>4</sub> selectivities were decreased with temperature. The best separation performance belongs to PES/SAPO-34/HMA mixed matrix membrane at each temperature. When the temperature increased from 35 °C to 120 °C H<sub>2</sub>/CO<sub>2</sub> selectivity for PES/SAPO-34/HMA membrane was increased from 3.2 to 4.6 and H<sub>2</sub> permeability increased from 8 Barrer to 26.50 Barrer. This results show that for H<sub>2</sub>/CO<sub>2</sub> separation working at higher temperatures will be more advantageous. The activation energies were found in the order of; CH<sub>4</sub> > H<sub>2</sub> > CO<sub>2</sub> for all types of membranes. Activation energies were in the same order of magnitude for all membranes but the PES/SAPO-34 membrane activation energies were slightly lower than PES membrane. Furthermore, PES/SAPO-34/HMA membrane has activation energies higher than PES/SAPO-34 membrane and is very close to pure membrane which shows that HMA acts as a compatibilizer between two phases.

Keywords: Mixed Matrix Membrane, Gas Separation, Temperature, Activation Energy, Polyethersulfone, SAPO-34.

## ÖZ

### KATKILI/ZEOLİT/POLİMER KARIŞIK MATRİSLİ MEMBRANLARIN PERFORMANSINA ÇALIŞMA KOŞULLARININ ETKİSİ

Edibe Eda, Oral

Yüksek Lisans, Kimya Mühendisliği Bölümü

Tez Yöneticisi: Prof. Dr. Levent Yılmaz

Ortak Tez Yöneticisi: Doç. Dr. Halil Kalıpçılar

Şubat 2011, 85 sayfa

Membranlı ayırım teknikleri uzun yıllardır yaygın bir şekilde kullanılmakta ve geliştirilmektedir. Genellikle gaz ayırım membranı olarak polimerik membranlar kullanılırlar ancak polimerik membranların gaz ayırım performansları endüstriyel uygulanabilirlik için yeterli değildir. Buna karşın inorganik membranların yüksek gaz ayırım performansları vardır ancak onların da işletim zorlukları vardır. Bu nedenle inorganik parçacıkların polimer matrise dağılmasından oluşan karışık matrisli membranlar geliştirilmiştir. Bunlara ek olarak polimer ve zeolit arasındaki etkileşimi zenginleştirmek için üçüncü bir bileşen olarak düşük molekül ağırlıklı uyumlaştırıcıların kullanıldığı üçlü karışık matrisli membranlar ortaya çıkmış ve 35 °C’de ümit vaat edici sonuçlar elde edilmiştir. Bu membranların gaz geçiş mekanizmasına daha iyi bir anlayış, hazırlanış ve işletim koşullarının incelenmesiyle elde edilebilir.

Bu çalışmada işletim sıcaklığının ve tavlama süresi ile sıcaklığının karışık matrisli membranların performansına etkisi incelenmiştir. Kullanılan karışım polimer olarak

camsı polietersulfon (PES), zeolit olarak SAPO-34 ve uyumlaştırıcı olarak 2-hidroksi-5-metil anilin (HMA)'den oluşmaktadırlar. Önceki çalışmada üretilen membranlar kullanılmıştır ve bazı membranlar sentezlendiği halde kullanılırken, bazı membranlara test edilmeden önce son tavlama işlemi uygulanmıştır (120°C, 0.2 atm., N<sub>2</sub> atm., 7-30 gün). Membranların sıcaklığa bağlı gaz geçirme özellikleri H<sub>2</sub>, CO<sub>2</sub> ve CH<sub>4</sub> gazlarının 35 °C- 120 °C arasında tek gaz geçirgenliklerinin ölçülmesiyle karakterize edilmiştir. Membranlar ayrıca taramalı elektron mikroskobu (SEM), diferansiyel taramalı kalorimetre (DSC) ve termal gravimetrik analiz (TGA) ile de karakterize edilmişlerdir.

Tavlama süresi ve sıcaklığı karışık matrisli membranların tekrarlanabilirliklerini ve kararlılıklarını etkilemiştir ve son tavlama işleminin karışık matrisli membranlara daha yüksek sıcaklıklarda ve daha uzun sürelerde uygulanması ile daha kararlı membranlar elde edilmiştir. Saf PES membranlarda ise ek bir işleme gerek kalmadan kararlı performanslar elde edilmiştir.

Çalışılan tüm gazların geçirgenlikleri işletim sıcaklığının artması ile artmıştır. Ayrıca sıcaklıkla H<sub>2</sub>/CO<sub>2</sub> seçiciliği artmış, CO<sub>2</sub>/CH<sub>4</sub>, H<sub>2</sub>/CH<sub>4</sub> seçicilikleri ise düşmüştür. Tüm sıcaklıklarda en iyi gaz ayırım performansı PES/SAPO-34/HMA karışık matrisli membranlara aittir. Sıcaklık 35 °C'den 120 °C'ye çıkarıldığında PES/SAPO-34/HMA üçlü karışık matrisli membranın H<sub>2</sub>/CO<sub>2</sub> ideal seçicilik değeri 3.2'den 4.6'ya yükselmiş ve H<sub>2</sub> geçirgenlik değeri 8 Barrer'dan 26.50 Barrer'a yükselmiştir. Bu sonuçlar H<sub>2</sub>/CO<sub>2</sub> ayırımı için yüksek sıcaklıklarda çalışmanın daha avantajlı olacağını göstermektedir. Aktivasyon enerjileri tüm membranlarda şu sırada bulunmuştur; CH<sub>4</sub> > H<sub>2</sub> > CO<sub>2</sub>. Tüm membranların aktivasyon enerjileri aynı mertebededir ancak PES/SAPO-34 membranın aktivasyon enerjisi PES membrandan daha düşüktür. Ayrıca PES/SAPO-34/HMA membranın aktivasyon enerjisi PES/SAPO-34 membranından yüksek ve PES membranına yakındır bu da HMA'nın iki faz arasında uyumlaştırıcı görevi yaptığını göstermektedir.

Anahtar Kelimeler: Karışık Matrisli Membran, Gaz Ayırımı, Sıcaklık, Aktivasyon enerjisi, Polietersülfon, SAPO-34.

*To my dearest family & fiancé*



## ACKNOWLEDGEMENTS

I want to thank to people who helped me through this graduate education. This M. Sc. study gave me the chance to know great people.

Although it is difficult to overstate my gratitude, I want to express my deepest appreciations and thanks to my supervisor Prof. Dr. Levent Yılmaz and my co-supervisor Assoc. Prof. Dr. Halil Kalıpçılar for their help, guidance and encouragements. Studying with them was a great chance for me since I have learned so much about both research and life under their tutelage.

I would like to thank to specialists Mıhrıcan Açıkgöz and Gülten Orakçı. I also thank to the technicians of Chemical Engineering Department.

I want to thank Ahmet Turhan Ural, Aslı Baysal and all employees of M-D2 Engineering-Recycling-Consultancy Company since they let me working on exciting projects and also since they have showed me a friendly face of business life.

I gained very good friendships throughout this study. I want to thank Sena and Berk for our sister/brotherhoods which kept me going on when I feel down. I want to thank Emre Y., Emre B., Bahar, Merve, Gamze, Berna, Aslı, Efe, Seçil, Didem, İrem, Seda, Emre T., Gökhan for their beautiful and enjoyable friendships. I also want to thank my dear sisters Bengi, İlksen and Sevgi for their lovely friendships. I would like to thank my colleague Ülgen and Elif who conveyed me their laboratory experiences. I also want to thank Dr. Berna Topuz for her support and kind friendship.

I want to record my special thanks and indebtedness to my family. I would like to thank my lovely parents Sevim-Davut ORAL, my dear sister Seda ORAL SEYHAN and her husband Ali Erdi SEYHAN since they always supported me and made me the person that I am now. Last but not least, I want to thank my fiancé Çağrı GÜNALTAY not only for his endless love, but also for his encouragement, support, friendship and understanding. I also want to thank his family for encouraging me through every decision I made.

## TABLE OF CONTENT

ABSTRACT .....	iv
ÖZ .....	vi
ACKNOWLEDGEMENTS.....	ix
TABLE OF CONTENTS .....	x
LIST OF TABLES .....	xii
LIST OF FIGURES .....	xiv
LIST OF SYMBOLS AND ABBREVIATIONS .....	xvii
CHAPTERS	
1. INTRODUCTION .....	1
2. LITERATURE SURVEY .....	4
2.1 Gas Separation Membranes.....	4
2.2 Mixed Matrix Membranes (MMMs).....	7
2.3 Effect of Annealing on Membrane Performance.....	13
2.4 Effect of Operating Temperature on Performance of Membranes.....	15
3. EXPERIMENTAL.....	21
3.1 Membrane Preparation Methodology.....	21
3.2 Membrane Characterization.....	22
3.3 Gas Permeability Measurements.....	23
3.3.1 Experimental Set-up and Procedure.....	23
3.3.2 Permeability and Selectivity Calculations.....	26
4. RESULTS AND DISCUSSION.....	27
4.1 Membrane Characterization.....	27
4.1.1 DSC Results.....	27
4.1.2 TGA RESULTS.....	29
4.1.3. SEM Results.....	33
4.2 Gas Permeation.....	35
4.2.1. Repeatability and Reproducibility of the Results.....	35

4.2.2 Effect of Annealing on Membranes Performance.....	43
4.2.3. Effect of Operating Temperature on Membranes Performance.....	46
4.2.4 Activation Energies of the Membranes.....	58
5. CONCLUSIONS.....	62
REFERENCES.....	63
APPENDICES.....	70
A. SINGLE GAS PERMEABILITY CALCULATONS.....	70
B. DSC THERMOGRAMS.....	72
C. TGA THERMOGRAMS.....	76
D. PERMEABILITY AND SELECTIVITY DATA OF TESTED MEMBRANES.....	80

## LIST OF TABLES

### TABLES

Table 1.1 Main Industrial Applications of Membrane Gas separation.....	2
Table 3.1 Membrane codes and annealing conditions.....	22
Table 4.1 Glass transition temperatures of post annealed and not post annealed membranes.....	28
Table 4.2 Weight losses of the post annealed and not post annealed membranes determined by TGA.....	30
Table 4.3 Repeatability results of the PES-n (M1) and PES/SAPO-34-n (M2) membrane performances.....	36
Table 4.4 Effect of gas order on reproducibility of PES/SAPO-34-n (M3) membrane performance.....	37
Table 4.5 Effect of temperature on reproducibility of PES/SAPO-34-n (M2) membrane performance.....	38
Table 4.6 Ideal selectivities of PES-n (M4) membrane with respect to temperature cycles at 35 °C and 90 °C.....	40
Table 4.7 Ideal Selectivities of PES/SAPO-34-n (M3) membrane with respect to temperature cycles at 35 °C and 90 °C.....	43
Table 4.8 Ideal Selectivities of PES/SAPO-34-p (M5) membrane with respect to temperature cycles at 35 °C and 90 °C.....	45
Table 4.9 Single gas permeabilities and ideal selectivities of PES/SAPO-34-n and PES/SAPO-34-p membranes at 35 °C.....	46
Table 4.10 Activation energies of membranes.....	59
Table D.1 Single gas permeabilities of PES-n (M6) membrane obtained from temperature cycles at 35 °C and 90 °C, 1month long period.....	80

Table D.2 Selectivities of PES-n (M6) membrane obtained from temperature cycles at 35 °C and 90 °C, 1month long period.....	80
Table D.3 Permeabilities of PES-SAPO-34-n (M3) membrane obtained from temperature cycles at 35 °C and 90 °C, 2 month long period.....	81
Table D.4 Ideal selectivities of PES-SAPO-34-n (M3) membrane obtained from temperature cycles at 35 °C and 90 °C, 2 month long period.....	81
Table D.5 Single gas permeabilities of PES/SAPO-34-p (M5) membrane obtained from temperature cycles at 35 °C and 90 °C.....	82
Table D.6 Ideal selectivities PES/SAPO-34-p (M5) membrane obtained from temperature cycles 35 °C and 90 °C.....	82
Table D.7 Effect of operating temperature on permeabilities of PES-n (M6) membrane.....	83
Table D.8 Effect of operating temperature on selectivities of PES-n (M6) membrane.....	83
Table D.9 Effect of operating temperature on permeabilities of PES/HMA-p (M7) membrane.....	83
Table D.10 Effect of operating temperature on selectivities of PES//HMA-p (M7) membrane.....	83
Table D.11 Effect of operating temperature on permeabilities of PES/SAPO-34-p (M5) membrane.....	84
Table D.12 Effect of operating temperature on selectivities of PES/SAPO-34-p (M5) membrane.....	84
Table D.13 Effect of operating temperature on permeabilities of PES-SAPO-34/HMA-p (M8) membrane obtained , 2 month long period.....	85
Table D.14 Effect of operating temperature on selectivities of PES-SAPO-34/HMA-p (M8) membrane obtained, 2 month long period.....	85

## LIST OF FIGURES

### FIGURES

Figure 2.1 Upper-bound trade-off curve of polymeric membranes for CO <sub>2</sub> /CH <sub>4</sub> .....	8
Figure 3.1 Schematic representation of the gas permeation set-up.....	25
Figure 4.1 TGA thermograms of post annealed and not post annealed (a) PES membrane, (b) PES/HMA membrane.....	31
Figure 4.2 TGA thermograms of post annealed and not post annealed (a) PES/SAPO-34, (b) PES/SAPO-34/HMA Mixed Matrix Membranes.....	32
Fig. 4.3 SEM images of (a) PES-p, (b) PES-n, (c) PES/HMA-p, (d) PES/HMA-n membranes.....	33
Fig. 4.4 SEM images of (a) PES-SAPO-34-p, (b) PES-SAPO-34-n, (c) PES/HMA-SAPO-34-p, (d) PES/HMA-SAPO-34-n membranes.....	34
Figure 4.5 Permeabilities of (a)H <sub>2</sub> , (b)CO <sub>2</sub> , (c) CH <sub>4</sub> gases through PES-n (M4) membrane with respect to temperature cycles at 35 °C and 90 °C.....	39
Figure 4.6 Permeabilities of (a)H <sub>2</sub> , (b)CO <sub>2</sub> , (c) CH <sub>4</sub> gases through PES-SAPO-34-n (M3) membrane with respect to temperature cycles at 35 °C and 90 °C.....	42
Figure 4.7 Permeabilities of (a)H <sub>2</sub> , (b)CO <sub>2</sub> , (c)CH <sub>4</sub> gases through PES/SAPO-34-p (M5) membrane with respect to temperature cycles at 35 °C and 90 °C.....	44
Figure 4.8 Effect of operation temperature on permeabilities of PES-n (M6) membrane.....	47
Figure 4.9 Effect of operation temperature on (a) CO <sub>2</sub> /CH <sub>4</sub> and H <sub>2</sub> /CH <sub>4</sub> , (b) H <sub>2</sub> /CO <sub>2</sub> selectivities of PES-n (M6) membrane.....	48

Figure 4.10 Effect of operation temperature on permeabilities of PES/HMA-p (M7) membrane.....	49
Figure 4.11 Effect of operation temperature on (a) CO <sub>2</sub> /CH <sub>4</sub> and H <sub>2</sub> /CH <sub>4</sub> , (b) H <sub>2</sub> /CO <sub>2</sub> selectivities of PES/HMA-p (M7) membrane.....	50
Figure 4.12 Effect of operation temperature on permeabilities of PES/SAPO-34-p (M5) mixed matrix membrane.....	51
Figure 4.13 Effect of operation temperature on (a) CO <sub>2</sub> /CH <sub>4</sub> and H <sub>2</sub> /CH <sub>4</sub> , (b) H <sub>2</sub> /CO <sub>2</sub> selectivities of PES/SAPO-34-p (M5) mixed matrix membrane.....	52
Figure 4.14 Effect of operation temperature on permeabilities of PES/SAPO-34/HMA-p (M8) mixed matrix membrane.....	53
Figure 4.15 Effect of operation temperature on (a) CO <sub>2</sub> /CH <sub>4</sub> and H <sub>2</sub> /CH <sub>4</sub> , (b) H <sub>2</sub> /CO <sub>2</sub> selectivities of PES/SAPO-34/HMA-p (M8) mixed matrix membrane.....	54
Figure 4.16 CO <sub>2</sub> /CH <sub>4</sub> gas separation performance of membranes on the predicted upper bound curves as a function of temperature.....	56
Figure 4.17 H <sub>2</sub> /CO <sub>2</sub> gas separation performance of membranes on the predicted upper bound curves as a function of temperature.....	57
Figure 4.18 Activation energy curves for (a)PES (M6), (b) PES/HMA (M7) membranes.....	58
Figure 4.19 Activation Energy curves for (a)PES/SAPO-34 (M5), (b)PES/SAPO-34/HMA (M8) membranes.....	59
Figure A.1 Single gas permeability calculation.....	71
Figure B.1 DSC Thermogram for PES-n membrane.....	72
Figure B.2 DSC Thermogram for PES-p membrane.....	72
Figure B.3 DSC Thermogram for PES/HMA-n membrane.....	73
Figure B.4 DSC Thermogram for PES/HMA-p membrane.....	73
Figure B.5 DSC Thermogram for PES/SAPO-34-n membrane.....	74
Figure B.6 DSC Thermogram for PES/SAPO-34-p membrane.....	74
Figure B.7 DSC Thermogram for PES/SAPO-34/HMA-n membrane.....	75
Figure B.8 DSC Thermogram for PES/SAPO-34/HMA-p membrane.....	75

Figure C.1 TGA Thermogram for PES-n membrane.....	76
Figure C.2 TGA Thermogram for PES-p membrane.....	76
Figure C.3 TGA thermogram for PES/HMA-n membrane.....	77
Figure C.4 TGA thermogram for PES/HMA-p membrane.....	77
Figure C.5 TGA thermogram for PES/SAPO-34-n membrane.....	78
Figure C.6 TGA thermogram for PES/SAPO-34-p membrane.....	78
Figure C.7 TGA thermogram for PES/SAPO-34/HMA-n membrane.....	79
Figure C.8 TGA thermogram for PES/SAPO-34/HMA-p membrane.....	79



## LIST OF SYMBOLS AND ABBREVIATIONS

A	: Effective membrane area (cm <sup>2</sup> )
dn/dt	: Molar flow rate (mol/s)
dp/dt	: Pressure increase
D	: Diffusion coefficient
D <sub>o</sub>	: pre-exponential factor
E <sub>a</sub>	: Activation energy for permeation
E <sub>d</sub>	: Activation energy for diffusion
J	: Flux (cm <sup>3</sup> /cm <sup>2</sup> .s)
ΔH <sub>s</sub>	: Heat of sorption
K	: adjustable parameter
M	: Molecular weight of the gas
P	: Permeability (Barrer)
P <sub>D</sub>	: Permeability of the dispersed zeolite phase
P <sub>o</sub>	: Front factor
P <sub>M</sub>	: Permeability of the continuous polymer matrix
P <sub>MM</sub>	: Permeability of the mixed matrix membrane
p <sub>f</sub>	: Feed side pressure (cmHg)
p <sub>p</sub>	: Permeate side pressure (cmHg)
R	: Ideal gas constant
S	: Solubility coefficient
T	: Temperature (°C)
T <sub>g</sub>	: Glass transition temperature (°C)
V <sub>d</sub>	: Dead volume (cm <sup>3</sup> )

### *Greek Letters*

$\alpha$	: Selectivity
$\Phi_D$	: Volume fraction of the zeolite phase
$\beta_{A/B}$ and $\lambda_{A/B}$	: Empirical parameters
$\rho$	: Density of the gas
$v$	: Volumetric flow rate (cm <sup>3</sup> /s)
$\Delta p$	: Transmembrane pressure difference (cmHg)
$\gamma$	: The upper bound position change with temperature
$\beta_{0,A/B}$	: Front factor

### *Abbreviations*

APTMS	: aminopropyltrimethoxysilane
DMF	: Dimethyl formamide
DMSO	: Dimethyl sulfoxide
DSC	: Differential scanning calorimetry
HMA	: 2-hydroxy 5-methyl aniline
LMWA	: Low molecular-weight additive
MMM	: Mixed matrix membrane
-n	: Not Post Annealed
NBR	: Nitrile-butadiene rubber
-p	: Post annealed
PC	: Polycarbonate
PDMS	: Poly(dimethylsiloxane)
PEMA	: Polyethylmethacrylate
PES	: Polyethersulfone
PBI	: Polybenzimidazole
PI	: Polyimide
pNA	: p-nitroaniline
PPZ	: Polyphosphazene
PSF	: Polysulfone
SEM	: Scanning electron microscopy
STP	: Standard temperature and pressure

TAP	: 2,4,6-triamino pyrimidine
TGA	: Thermal gravimetric analyzer
TMHFPC	: Tetramethyl hexafluoro polycarbonate
TMPC	: Tetramethyl polycarbonate

## **CHAPTER 1**

### **INTRODUCTION**

The separation of gases using membranes has received commercial interest and competes well with other traditional methods such as cryogenic distillation and pressure swing adsorption. Membrane based gas separation offer many advantages such as [1, 2]:

- i) Simplicity and ease of installation operation
- ii) Low maintaince requirements and low capital investment,
- iii) Low space and weight requirements since membrane systems are compact and modular,
- iv) Can be operated under mild conditions,
- v) Can be combined with other systems for effective hybrid processes.

As a result gas separation membranes are of interest for various industrial applications. Some examples of these applications are summarized in Table 1.1 [3].

Most commonly used membranes in gas separation are glassy polymeric membranes, but their usage is limited since polymeric membranes with high selectivity gives low permeability and low permeability gives high selectivity. Robeson et al. [4] plotted this relationship between permeability and selectivity for polymeric materials and obtained an upper bound limit trade off curve. Although polymeric membranes are studied widely and improvements in polymeric membrane conventional performances obtained, the separation performances of polymers could not surpass this upper bound [5, 6]. The Freeman model explains the theoretical reason of this limitation for polymeric membranes [5].

Table 1.1 Main Industrial Applications of Membrane Gas separation, adopted list from ref. [3].

Separation	Process
H <sub>2</sub> /N <sub>2</sub>	Ammonia purge gas
H <sub>2</sub> /CO	Syngas ratio adjustment
H <sub>2</sub> /hydrocarbons	Hydrogen recovery in refineries
O <sub>2</sub> /N <sub>2</sub>	Nitrogen generation, oxygen-enriched air production
CO <sub>2</sub> /hydrocarbons (CH <sub>4</sub> )	Natural gas sweetening, landfill gas upgrading
H <sub>2</sub> S/hydrocarbons	Natural gas dehydration
He/hydrocarbons	Sour gas treating
He/N <sub>2</sub>	Helium separation
Hydrocarbons/air	Helium recovery
H <sub>2</sub> O/air	Hydrocarbons recovery, pollution control, air dehumidification
Volatile organic species / light gases	Polyolefin purge gas purification

Polymeric- inorganic MMMs have been developed to overcome this trade off for polymers [7, 8]. However the material selection and the compatibility between the polymer and zeolite are very important for MMMs [8]. Because of the incompatibility between the polymer and zeolite, defects can occur at the interface such as; voids occurring at the interface [9-11] rigidification of the polymer [7, 12, 13] blockage of the zeolite pores [14, 15]. MMMs prepared from glassy polymers and inorganic particles commonly have voids at the interface. Many methods have been developed to modify this structure. Using low molecular weight additives with multifunctional groups as a third agent has been studied in literature and by our group. The results obtained for low molecular weight additive ternary MMMs are very promising at 35 °C [16-19].

However measuring the membrane performance at only one temperature is not sufficient to understand the separation performance and gas transport mechanism of the membranes. The permeation is an activated process so the operation temperature influences the permeation properties of gases through the membranes. Moreover the gas separations occurs at different temperatures in industry and the temperature dependent gas transport behaviors of these membranes should be investigated to see the influence of temperature. The effect of temperature strongly depends on membrane type and gas mixtures that will be separated. The studies investigating the effect of temperature on performance of ternary MMMs are very limited in literature [20].

The objective of this study is to investigate the temperature effect on performance of polymer/zeolite/additive MMMs. The membranes used in this study are pure PES membrane, PES/HMA (4 %w/w) membrane, PES/SAPO-34 (20%w/w) MMM, PES/SAPO-34 (20%w/w)/HMA (4%w/w) MMM which were formulated and synthesized in previous studies of our group [16]. The membranes used in this study are characterized by scanning electron microscopy (SEM), differential scanning calorimetry (DSC) and thermal gravimetric analysis (TGA). The influence of operation temperature on membrane performance was measured by single gas permeation experiments.

## CHAPTER 2

### LITERATURE SURVEY

#### 2.1 Gas Separation Membranes

Gas separation membrane is a semi-permeable barrier between two phases which separates the one or more gases from a multicomponent gas mixture by permitting the transport of certain molecules under the influence of chemical potential such as pressure or concentration gradient [1].

The performance of a membrane can be defined in terms of permeability and selectivity. Permeability is the normalized flux of the penetrant gas and the permeability of a penetrant A can be defined by the following equation [1];

$$P_A = \frac{N_A \ell}{\Delta p_A} \quad (2.1)$$

where  $N_A$  is the flux of gas passing through the membrane,  $\ell$  is the membrane thickness and  $\Delta p_A$  is the pressure difference between high and low pressure sides. Permeability is usually given in units of Barrer, defined as:

$$\text{Barrer} = 1 * 10^{-10} \frac{\text{cm}^3(\text{STP}) \cdot \text{cm}}{\text{cm}^2 \cdot \text{s} \cdot \text{cmHg}} \quad (2.2)$$

In a temperature range where no transition occurs, the temperature dependence of permeability can be described by an Arrhenius type equation [21].

$$P = P_o \times \exp\left(\frac{-E_a}{R \times T}\right) \quad (2.3)$$

Where  $P_o$  is the front factor,  $R$  is the universal gas constant,  $T$  is the temperature and  $E_a$  is the activation energy for permeation.  $E_a$  shows the effect of temperature on permeation. The higher the activation energy, higher the influence of temperature on permeation.

Selectivity is the ability of a membrane to separate gas molecules. The ideal selectivity of a membrane for a gas pair can be obtained from the ratio of the single gas permeabilities of two gases [1, 22]:

$$\alpha_{A/B} = \frac{P_A}{P_B} \quad (2.4)$$

Both high permeable and high selective membranes are desired. High permeability gives high fluxes and low membrane area, so decreases the capital cost of membrane units and increases the production capacity. High selectivity increases the efficiency of the process, decreases the required driving force so lowers the cost of the separation system and gives high purity products [23]. In addition to high permeability and selectivity the ability to form mechanically stable, thin, low-cost membranes that can be packaged into high- surface-area modules are needed for industrial feasibility [24].

Most widely used membranes in commercial gas separation are polymeric solution diffusion membranes since they have ease of processability and are more economical. Polymeric membranes are more economical because they can be easily spun in to hollow fiber or spiral wound modules due to their ease of processability [23].

The gas transport mechanism across dense polymeric membranes is widely explained by solution diffusion mechanism. According to this model transport



occurs in three steps first the gas molecules are adsorbed at the feed side of the membrane, then diffuse through the membrane and lastly desorbed at the other side of the membrane. Hence the permeability equals to the product of the solubility coefficient (S) and diffusion coefficient (D), in a given membrane [1,25]:

$$P = S \times D \quad (2.5)$$

Diffusion coefficient D, is a kinetic parameter and is a measure of the mobility of the penetrant gases in the membrane. Diffusion coefficient defines the rate of transport of a gas penetrant through the membrane. Solubility coefficient S, is a thermodynamic parameter which is expressed by the condensability of the gases, by the interactions between polymer and penetrant gases and by the excess volume present in the membrane. Solubility gives the amount of penetrant gases adsorbed by the membrane under equilibrium conditions [26]. These coefficients are dependent on temperature, pressure and pressure gradient of the penetrants.

In polymeric membranes diffusion occurs in the presence of free volumes which are good sorption sites for gases. The polymer segments that are encircled with adsorbed gases can displace by thermal fluctuations and diffusion occurs by the transient gaps between polymer matrixes. Since thermal fluctuations in polymer matrix are increasing with temperature the diffusivity is also increasing with temperature which can be described by Arrhenius type expression [27].

$$D = D_0 \exp\left(\frac{-E_d}{RT}\right) \quad (2.6)$$

Where  $D_0$  is the pre exponential factor and  $E_d$  is the activation energy for diffusion. In zeolitic membranes, the diffusion occurs by the pore windows. The motions in polymeric membranes are not effective here, in this mechanism the diffusional jumps of the penetrant gases between zeolite cages exist. The diffusivity is increasing with temperature like polymers and can be explained by Arrhenius type equation. Also the diffusivity constant can be measured by time lag method [1,28].

$$D = \frac{l^2}{6\theta} \quad (2.7)$$

$\theta$  can be estimated from the plot of permeate pressure versus time graph, the intercept of time axis gives  $\theta$  and  $l$  is the membrane thickness.

There are generally two types of membranes as porous and non-porous. Solution diffusion model is suitable for non-porous membranes. In the porous membranes gas mechanism can be defined by molecular sieving mechanism in which the molecules are separated by the size discrimination [2]. Furthermore new models are required to explain the gas transport mechanism in mixed matrix membranes, since they are combinations of two different phases, polymers and zeolites.

## 2.2 Mixed Matrix Membranes (MMMs)

As stated before generally polymeric membranes are used in gas separation applications. However, they have a trade-off between their permeability and selectivity, a high selective membrane have low permeation rate and vice versa. [3]. This behavior was analyzed by Robeson by plotting the available data in literature with various polymers for different gas pairs and an upper bound curve was obtained for polymers, Figure 2.1 represents this relation for CO<sub>2</sub>/CH<sub>4</sub> gas pair [4].

The upper bound permeability and selectivity characteristic is described by Robeson as;

$$\alpha_{A/B} = \frac{\beta_{A/B}}{P_A^{\lambda_{A/B}}} \quad (2.8)$$

where  $\beta_{A/B}$  and  $\lambda_{A/B}$  are empirical parameters which depend on the gas pairs and are reported by Robeson for various common gas pairs [4]. The upper bound relation

was updated by Robeson, for high performance polymeric membranes developed for overcoming the upper bound limitation [29]. Freeman et al. [5] developed a fundamental theory to define the upper bound performance behavior. Due to their theory  $\lambda_{A/B}$  depends only on penetrant gases kinetic diameters;  $\beta_{A/B}$  depends on condensability of gases, one adjustable parameter and  $\lambda_{A/B}$ . In this study it is concluded that the slope of the upper bound curves,  $\lambda_{A/B}$ , are independent from polymer structure since  $\lambda_{A/B}$  is only related to ratio of the gases kinetic sizes. Hence making developments in polymer structures are improbable to change the slopes of the upper bound curves.

Industrially attractive region is above the Robeson upper bound curve and in the upper right hand corner of this figure. On the other hand inorganic membranes have properties lying far beyond this upper bound curve near the industrially attractive region but they are very brittle and making a crack free large surface area with an inorganic membrane is very difficult [30-31].

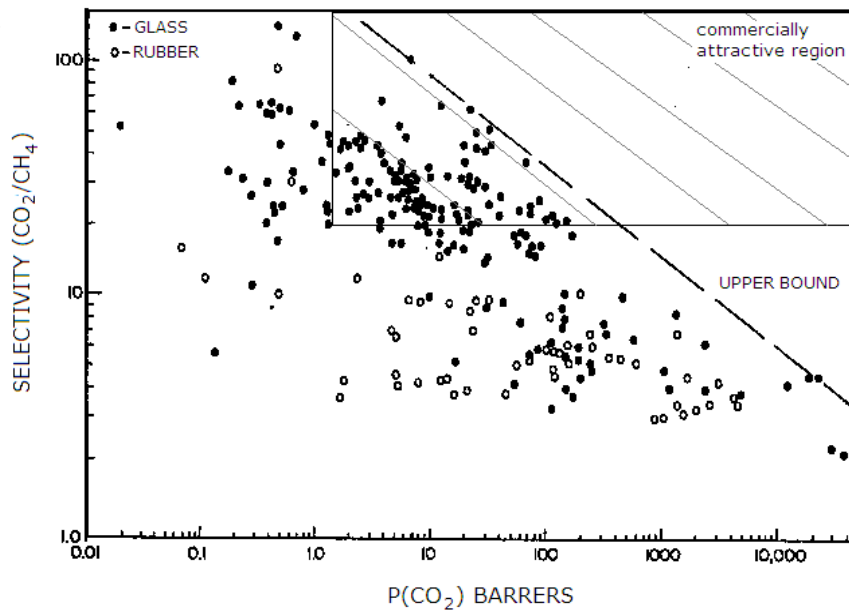


Figure 2.1 Upper-bound trade-off curve of polymeric membranes for CO<sub>2</sub>/CH<sub>4</sub>, adopted from ref. [16].

In order to combine the attractive properties of both polymeric and inorganic membranes and to create a synergy Mixed Matrix Membranes were developed [8]. Mixed-matrix membranes (MMMs) are based on polymeric membranes filled with inorganic particles in order to improve the gas separation performance of the polymeric membranes [7]. MMMs combine the easy processability of polymers and excellent gas separation performances of inorganic particles. The aim is to prepare a high separation performance membrane with mechanical strength, thermal and chemical stability and processability. MMMs have been examined for various gas separations like air separation (e.g.,  $O_2/N_2$ ), natural gas purification (e.g.,  $CO_2/CH_4$ ), hydrogen recovery (e.g.,  $H_2/CO_2$ ,  $H_2/N_2$ , and  $H_2/CH_4$ ), and hydrocarbon separation (e.g., i-pentane/n-pentane, and n-butane/ $CH_4$ ) [32].

Glassy or rubbery polymers can be used as continuous phase while molecular sieves, metal organic frameworks or carbon molecular sieves can be used as inorganic particles. Mixed matrix membranes prepared from rubbery polymers showed better performances than pure polymeric membranes. However, their performances were still weak in comparison with pure glassy polymers since rubbery polymers have properties lying far below the upper bound curve.

Duval et al. [33] employed different types of rubbery polymers as matrix and different zeolites as fillers. Membranes prepared from zeolite 3A, 4A and 5A showed no improvement in gas separation performances with respect to pure polymeric membranes. Improvement observed only with silicalite and zeolite Y zeolites filled membranes.

Jha et al. [34] studied with SAPO-34 filled polyphosphazene (PPZ) membranes. No improvement was observed with the addition of 25%w SAPO-34 incorporated PPZ membranes at 22°C. The  $CO_2$  permeability and  $CO_2/H_2$  selectivity decreased where the  $CO_2/CH_4$  and  $CO_2/N_2$  selectivities slightly increased.

Although some improvements observed with rubbery polymers, they are not commercially attractive since glassy polymers have higher mechanical stability and transport properties especially at higher temperatures. Thus, these studies lead

researchers to prepare mixed matrix membranes with glassy polymers. Studies done with glassy polymers showed that with the incorporation of zeolites to glassy polymers either the separation performance of the membrane (selectivity) or the free volume of the membrane (permeability) is increasing [32]. The performances are promising and higher than the pure polymeric membranes but still not as high as expected. The adhesion problem between polymer and zeolite causes some difficulties. The selection of proper polymer-inorganic phase is very important while developing MMMs. The difficulties resulted from weak interaction between polymer and zeolite interface which causes non selective voids between these interfaces. The non selective voids allow flow of the both gases in a mixture, which decreases the separation performance [35]. To overcome this problem and heal the mixed matrix membranes some methods have been proposed like modification of zeolite surface, using silane coupling agent, addition of plasticizer, annealing the membranes at high temperatures [36-38].

The silanation of zeolite surface by using a silane coupling agent is one approach. One reactive end of the silane agent reacts with the zeolite surface while the second end attaches to polymer chain. So, the silanes act as a coupling bonding agent between these two phases and improves the compatibility. The silane agent can be reacted to the surface [39]. However, the performances of mixed matrix membranes prepared from silanated zeolites showed no improvement.

Another method is incorporation of plasticizers in mixed matrix membranes like RDP Fyroflex, dibutyl phthalate and 4-hydroxy benzophenone [33]. The plasticizer reduces the  $T_g$  of the polymer and as a result the polymer chains become more flexible and mobile while preparation of the membranes. However the results reveal that although the compatibility between polymer and zeolite is good, the performances were not improved.

Casting membranes above the glass transition temperature of the polymer is another approach [18-19, 40-41]. Since at temperatures above the  $T_g$ , the polymer chains become more flexible and mobile, the polymer matrix and zeolite particles can adhere better. Studies done by Huang et al.[40] showed no improvement while

İsmail et al.[41] reported that selectivities were improved by annealing above  $T_g$  of the polymer matrix. They studied with zeolite 4A incorporated PES/PI mixed matrix membranes and observed that the gas separation performances of MMMs increased with permeability loss by applying above  $T_g$  annealing which is an indication of good adhesion between polymer and zeolite.

The incorporation of multifunctional low molecular weight additives is a promising approach [16-18, 37]. Yong et al.[37] used 2, 4, 6-triaminopyrimidine (TAP) low molecular weight additive as a compatibilizer between polymer-zeolite interface to reduce the non selective voids. The permeabilities of all studied gases decreased where the ideal selectivities increased significantly with TAP addition. It is stated that the TAP addition improved the adhesion between polymer and zeolite. Although the TAP was used as an additive the content of TAP to polymer was at least 21% of polymer. At this high concentration the compatibilizer becomes as a main material instead of being an additive. Also the permeabilities are decreasing with addition of compatibilizer and become very low at high loadings. Şen et al.[17] used p-nitroaniline(pNA) as a compatibilizer between polycarbonate(PC) and zeolite 4A. They observed that even at very small concentrations like 1-2%w/w pNA behaved as a compatibilizer and significantly improved the gas separation performance but the permeabilities of ternary membranes were below the pure PC membranes.

Recently Çakal et al. [16] studied with additive/zeolite/polymer ternary mixed matrix membranes. They used 2-hydroxy 5-methylaniline (HMA) as additive between polyethersulfone(PES) and SAPO-34 particles. Dimethyl formamide (DMF) was used as solvent and the particle size of the SAPO-34 particles were between  $1\mu\text{m} - 2\mu\text{m}$ . The membranes were annealed below  $T_g$  of the polymer, at  $100\text{ }^{\circ}\text{C}$ . HMA acted as a compatibilizer between two phases by reducing the non selective voids. The selectivities were increased significantly than PES and PES/SAPO-34 membranes. However the permeabilities were lower compared to pure PES membrane in PES/SAPO-34/HMA ternary mixed matrix membranes.

Karatay et al.[19] also studied with membranes that have similar formulations with Çakal et al. [16]. Different from them, Karatay et al. [19] used dimethyl sulfoxide

(DMSO) as solvent and the particle sizes of the zeolite particles were  $< 1 \mu\text{m}$ . Furthermore, they annealed the membranes above the  $T_g$  of the polymer, at  $220^\circ\text{C}$ . They again observed that the addition of HMA to PES/SAPO-34 mixed matrix membranes increased the selectivities and decreased the permeabilities. However the permeability of PES/SAPO-34/HMA MMM was still higher than pure PES membrane. This difference in two studies can be related to annealing membranes above  $T_g$  of the polymer, using different solvents or using zeolite particles in different sizes. Using sub micron zeolites can be the reason of this difference since sub-micron sizes can cause more polymer/zeolite interface and enhance the polymer zeolite interaction [42]. Also annealing the membranes above their  $T_g$  may improve the adhesion between polymer and zeolite. [38]

As a result studies showed that incorporation of low molecular weight additives, even at very low concentrations, increase the separation performance of polymer/zeolite MMMs significantly by creating a synergistic combination. The performances of ternary mixed matrix membranes move through the upper bound curve with selectivity improvement thus these membranes can be a promising tool to surpass the upper bound limit.

In order to predict the permeability of the heterogeneous mixed matrix membranes many models have been described in literature [27] and two phases Maxwell Model is the most widely used model:

$$P_{MM} = P_M \left[ \frac{P_D + 2P_M - 2\phi_D(P_M - P_D)}{P_D + 2P_M + \phi_D(P_M - P_D)} \right] \quad (2.9)$$

where,  $P_{MM}$  is permeability of the mixed matrix membrane,  $P_D$  is the permeability of the dispersed zeolite phase,  $P_M$  is the permeability of the continuous polymer matrix,  $\phi_D$  is the volume fraction of the zeolite phase. In this model it is assumed that the interface is continuous and the molecular sieves are dispersed. However Maxwell Model does not take in to account the particle size distribution, particle shape and

particle aggregation. This model is valid for filler concentrations smaller than 0.2 [43]. Also three phase Maxwell Model has been investigated by Koros and Mahajan [10] in which interfacial layer is also taken into consideration but it has the same limitations as in two phase model.

### **2.3 Effect of Annealing on Membrane Performance**

It has been known that casting conditions such as solvent type, casting solvent, solution conditions, evaporation conditions, annealing temperature and period strongly influences the membrane performance [44, 45]. Annealing is a thermal treatment which is applied to membranes to remove the remaining solvent in the membrane and to release the stresses from the membrane. The studies showed that annealing conditions and the effect of residual solvent in the membrane have different effects on membrane performance depending on the membrane type [45-49].

Fub et al. [46] studied the effect of residual solvent on performance of polyimide membranes and they observed that the solvent remaining in the membrane acts as a plasticizer. The membranes were treated at 25 °C and 150°C between 0 to 12 days and with increasing treatment time the gas permeabilities decreased. Membranes treated at 25°C had higher permeabilities due to plasticization effect. However when the residual solvent in the membrane is less than 1.5%, the solvent starts to act as an antiplasticizer rather than a plasticizer.

The same observations were reached by Hacıoğlu et al. [45]. They employed pure polycarbonate (PC) membranes and investigated the effect of annealing time on membrane performances. Membranes annealed at 50 °C for different times such as 8, 24, 72, and 154 hours. Increasing the annealing time decreased the permeabilities of the membranes. The membrane structure became denser with longer annealing times. However, after 72 hours annealing the permeabilities stayed nearly constant with increase in annealing time. They concluded that after 24 h annealing period the loosening of the membrane stopped.



On the contrast Joly et al. [47] studied the effect of residual solvent remaining in the 6FDA-mPDA polyimide membranes. The residual solvent is eliminated with longer annealing time. The permeability and solubility coefficient increases with decrease in residual solvent whereas the diffusion coefficient decreases. This behavior attributed to elimination of the solvent imprints in the membrane with longer thermal treatment. They also stated that the solvents with high molar volume leave more imprints in the membrane.

Shen et al. [48] studied the effect of heat treatment on the P84 polyimide membranes. The membranes are annealed at different temperatures. Membrane annealed at 315°C was cracked due to thermal stresses on the membrane. The membranes annealed at 80 °C and 200 °C showed that with increasing annealing temperature the selectivities increased where permeabilities (He, N<sub>2</sub>, O<sub>2</sub>, and CO<sub>2</sub>) decreased. This behavior is related to densification of the membrane structure. By annealing the membrane at higher temperatures the free volume of the membrane is reduced so the selectivity is increased where permeability is decreased.

Moe et al. [49] studied with fluorinated polyimide (1,5ND-6F) membrane and investigated the effect of annealing on membrane performance. They annealed some membranes at 240 °C for 6h and did not anneal some others. They found that with applying annealing to membrane, H<sub>2</sub> permeability increased where CO<sub>2</sub> permeability decreased. They relate this behavior to antiplasticization effect occurring from the removal of the solvent residue which leads decreases in gas sorption levels and mobilities. They conclude that heat treatment caused relaxations in polymer segments thus changes occurred in free volume of the polymer. This free volume redistribution can also be the reason of the complexities in permeabilities after annealing.

Hibshman et al. [50] investigated the effect of annealing with polyimide-organosilicate hybrid membranes. They conducted annealing at 400 °C to improve the gas separation performance of the membranes. The permeabilities of the membranes were increased with annealing and the selectivities were decreased. The increases in permeabilities were higher in hybrid membranes than pure

membrane. The permeability increase was related to increases in diffusivities also to increases in free volumes. The increase in free volume in pure polymeric membrane was attributed to degradation of anhydride end groups and the free volume increase in hybrid materials related to release of sol-gel condensation products.

Studies investigating the effect of annealing on membrane performance and characterization generally used pure polymeric membranes and as a result the membrane characteristics generally related to residual solvent in the membrane which is very dependent on polymer/solvent type and concentration. However in MMMs in addition to these parameters the effect of membrane morphology, the polymer and zeolite interaction and void formation should be considered.

## **2.4 Effect of Operating Temperature on Performance of Membranes**

Most of the permeation and separation measurements of various gas separation membranes were carried out at a very narrow temperature range (25 °C-35 °C). well known Robeson upper bound curve was plotted based on the results obtained at these narrow temperature ranges [4] and the effect of temperature on these upper bound curves has been developed recently [51]. In industrial applications, processes occur at much wider temperature ranges. Therefore measuring membrane permeability and selectivity at one temperature may not be enough for determination of membrane performance. Temperature dependent gas separation performances of membranes should be known to obtain high performance membranes for various gas separation applications.

There are a limited number of studies investigating the effect of temperature on different polymeric membranes and similar trends have been observed in literature, that is permeability increase with temperature. The permeabilities in polymeric membranes are related to polymer structure like free volume, chain stiffness and also the polymer penetrant interactions which are influenced by temperature strongly [51]. Increase in temperature causes increase in segmental motions of polymers which results in increase in molecular diffusion rates.

Koros et al. [21] investigated the permeability and selectivity trends of bisphenol-A polycarbonate (PC), tetramethyl polycarbonate (TMPC), and tetramethyl hexafluoro polycarbonate (TMHFPC) between 35 °C- 125 °C. As temperature increases the permeability of the membranes increased with selectivity losses. Solubility coefficients of the studied gases were also measured and with increasing temperature sorption of the gases where decreased especially for CO<sub>2</sub> gas. The CO<sub>2</sub>/CH<sub>4</sub> and He/N<sub>2</sub> permselectivity loss is related to decreases in solubility and diffusivity selectivities. Solubility and diffusivity selectivities were also decreased with increasing temperature. Activation energies of diffusions  $E_d$  for penetrant gases is increased with increasing penetrants sizes. They found  $E_a$  of H<sub>2</sub> as 12.56 kJ/mole and CH<sub>4</sub> as 25.96 kJ/mole. Heats of sorptions ( $\Delta H_s$ ) were related to critical temperatures of the gases. CO<sub>2</sub> with the highest critical temperature influenced much from temperature and it has lowest  $\Delta H_s$  value. The trends of activation permeation energies  $E_a$ , are similar to  $E_d$  values since the absolute value of  $E_d$  is larger than  $\Delta H_s$ . CO<sub>2</sub> is out of this trend because of its lowest  $\Delta H_s$  value, the decrease in CO<sub>2</sub> solubility predominates the increase in its diffusivity.

Freeman et al. [52] investigated the temperature dependent gas transport properties of poly(ethylene oxide) for a large number of gases at 25 °C, 35 °C and 45 °C. The permeabilities of He, H<sub>2</sub>, O<sub>2</sub>, N<sub>2</sub>, CO<sub>2</sub>, CH<sub>4</sub>, C<sub>2</sub>H<sub>4</sub>, C<sub>2</sub>H<sub>6</sub>, C<sub>3</sub>H<sub>6</sub> and C<sub>3</sub>H<sub>8</sub> were increased with temperature. The selectivities were higher at low temperatures. The H<sub>2</sub> permeability was measured again at 35 °C, after making measurements at 45 °C to check that whether or not gas transport properties changed irreversibility and no changes were observed.

Chung et al. [53] studied 6FDA-durene polyimide membranes and investigated the influence of temperature on gas transport properties of He, H<sub>2</sub>, O<sub>2</sub>, N<sub>2</sub>, CH<sub>4</sub>, and CO<sub>2</sub> gases between 30 °C- 50 °C. They calculated the solubility and diffusivity coefficients by time lag method. They found that as temperature increased the permeabilities and diffusivities again increased while solubilities and permselectivities were decreased. Activation energies were calculated and the activation energies of the gases were found to increase with increasing kinetic diameters of the studied gases

Wang et al.[ 54] studied the effect of temperature on performance of silicone coated asymmetric PES membranes. The H<sub>2</sub>, He, CO<sub>2</sub>, O<sub>2</sub>, and N<sub>2</sub> gas permeabilities increased with increase in temperature while the H<sub>2</sub>/N<sub>2</sub>, He/N<sub>2</sub>, CO<sub>2</sub>/N<sub>2</sub>, and O<sub>2</sub>/N<sub>2</sub> selectivities decreased.

Açıklan et al. [55-56] studied the effect of temperature on poly (ethyl methacrylate) PEMA membranes between 25 °C-75 °C which includes the T<sub>g</sub> of the membrane. They observed a discontinuity in the slope of logarithmic permeability versus inverse temperature graph and obtained two different permeation activation energies. They measured the permeabilities between 25 °C- 45 °C and observed that the permeabilities were increasing. The Ar/N<sub>2</sub>, O<sub>2</sub>/N<sub>2</sub>, H<sub>2</sub>/N<sub>2</sub> selectivities decreased till 35 °C and then increased slightly and H<sub>2</sub>/CO<sub>2</sub> selectivity did not change significantly. This behavior is related to differences in gas solubilities of the penetrant gases with temperature increase. They found the order of the activation energies as; H<sub>2</sub>>CO<sub>2</sub>> Ar > N<sub>2</sub>>O<sub>2</sub> and the E<sub>a</sub> values were very close to each other.

Rowe et al.[51] investigated the effect of temperature on Robeson upper bound for polymeric membranes. They modified the upper bound relation by including the temperature effect on Equation (2.8) and for a given gas pair upper bound can be defined by:

$$\alpha_{A/B} = \frac{\beta_{0,A/B} e^{\gamma/T}}{P_A^{\lambda_{A/B}}} \quad (2.10)$$

In equation 2.10  $\beta_{0,A/B}$  is a front factor and  $\gamma$  is a parameter which defines the change in upper bound position with respect to temperature. They concluded that upper bound curve shifts vertically with temperature and the direction is related to size and condensability of the gas molecules. The upper bound shifts downwards as temperature increases for CO<sub>2</sub>/H<sub>2</sub>, CO<sub>2</sub>/CH<sub>4</sub>, H<sub>2</sub>/N<sub>2</sub>, CO<sub>2</sub>/N<sub>2</sub> separations and upward for H<sub>2</sub>/CO<sub>2</sub> separations. They stated that when the difference between the molecule size of the penetrants increases the influence of temperature on diffusivity

selectivity is more sensitive and when the condensabilities of the penetrants difference is increasing the effect of temperature on solubility selectivity is more effective.

The temperature effect on zeolitic membranes also studied but the trends are very different than polymeric membranes. Poshusta et al. [57] investigated SAPO-34 zeolitic membranes and investigated the effect of temperature on single and binary gas permeabilities between 300 K- 470 K. The permeability of CO<sub>2</sub> decreased, CH<sub>4</sub> permeability increased continuously. Also the H<sub>2</sub> and N<sub>2</sub> permeabilities decreased and showed minima between 360 K and 390 K, then increased. The CO<sub>2</sub>/CH<sub>4</sub>, CO<sub>2</sub>/N<sub>2</sub>, N<sub>2</sub>/CH<sub>4</sub>, H<sub>2</sub>/CH<sub>4</sub> ideal selectivities decreased with increasing temperature where H<sub>2</sub>/CO<sub>2</sub> selectivity increased and H<sub>2</sub>/N<sub>2</sub> selectivity stayed nearly constant. Difference effects of temperature on studied gases explained by different kinetic diameters of the gas molecules. According to this study CH<sub>4</sub> gas permeability increased with increasing temperature. Since its kinetic diameter was close to SAPO-34 pores it has highest activation energy for diffusion. CO<sub>2</sub> has smaller kinetic diameter so its diffusion activation energy was smaller. With increasing temperature the adsorption capacity decreased and the permeability of CO<sub>2</sub> also decreased.

Falconer et al. [58] studied the effect of temperature also with MFI type membranes. They investigated the temperature effect on three membranes, two of them are silicalite and one is H-ZSM-5 membrane. They changed the permeation temperature from 20 to 200 °C. The single gas permeabilities of ZSM-5 zeolite was decreased with temperature and the gas permeabilities of silicalite membrane was exhibit a minimum at around 120 °C. They related different behaviors of the membranes to non zeolitic pores of the membranes and conclude that different procedures can caused differences in zeolitic and non zeolitic pores. Moreover they conclude that, where the permeability shows minimum with temperature the diffusion becomes gas translational diffusion from surface diffusion. In general as temperature increases the diffusivity increases and hence the adsorbed amount gradient increases to a maximum which leads permeability increase. To explain the minima in gas permeabilities, they used a model in which the gas translational model is used. According to this model with increasing temperature first surface coverage amount

decreases until gas translational diffusion becomes dominant which is increasing with increasing temperature and as a result a minima is observed.

The temperature dependent gas transport properties of MMMs were also studied recently but the studies are very limited and no systematic approach has been followed in these studies.

Jha et al. [34] studied with SAPO-34 filled rubbery poly dimethyl sulfoxide (PDMS) MMMs and investigated the effect of temperature between -15-22 °C. They observed that the CO<sub>2</sub>/CH<sub>4</sub> and CO<sub>2</sub>/N<sub>2</sub> selectivities are decreasing with increasing temperature and highest selectivity was found at -15 °C. They relate this to increased sorption of CO<sub>2</sub> or decreased diffusivities of CH<sub>4</sub> and N<sub>2</sub> at low temperature.

Choi et al. [44] studied the H<sub>2</sub>/ CO<sub>2</sub> selectivity of polybenzimidazole (PBI), swollen AMH-3 and proton-exchanged AMH-3 incorporated PBI composite membranes in a temperature range of 35 °C-200 °C. At 35 °C the selectivities of composite membranes were nearly two times higher than PBI membranes since the CO<sub>2</sub> permeability reduced with the incorporation of inorganic particles. However, when temperatures increased up to 200 °C both H<sub>2</sub> and CO<sub>2</sub> permeability increased but the selectivities of composite membranes approached to pure PBI membranes since the reduction in CO<sub>2</sub> permeability came close to H<sub>2</sub> permeability. This behavior was related to mismatch of properties of polymer and inorganic phases at high temperatures.

Clarizia et al. [14] prepared rubbery polymer polydimethylsiloxane (PDMS) based hybrid membranes to investigate the effect of fillers and temperature on performance of PDMS membranes. NaA, NaX, silicalite-1 used as inorganic fillers and temperature changed between 15-65 °C. The gas permeabilities increased in pure PDMS films where the selectivities decreased as temperature is increased. Carbon dioxide, the most permeable gas did not affected much with temperature. They observed that the inorganic fillers incorporated to membrane have different effects

on activation energies of the gases. Generally with the addition of fillers the activation energies decreased.

The only study done with ternary mixed matrix membranes were reported by Khan et al. [20] to our best knowledge. They used acrylate modified polysulfone as polymer matrix, zeolite 3A as inorganic filler and aminopropyltrimethoxysilane (APTMS) as coupling agent. They investigated the effect of temperature on H<sub>2</sub>/ CO<sub>2</sub> separation. They observed that H<sub>2</sub> permeability was increased while the H<sub>2</sub>/ CO<sub>2</sub> selectivity was decreased with increasing temperature. They conclude that the diffusivity of gas molecules increased with increasing temperature due to increased flexibility of the polymer and the increase in CO<sub>2</sub> was higher than H<sub>2</sub> hence the H<sub>2</sub>/CO<sub>2</sub> selectivity decreased.

Literature studies investigating effect of operating temperature on membrane performances showed that temperature influence on membrane performances depend on membrane types. The investigation of temperature dependent gas transport properties is important for understanding the separation performance of the membranes in more detail. Moreover in industrial applications the membranes are operated at various temperatures and since gas permeability is an activated process the temperature effect on membranes should be investigated. Also ternary mixed matrix membranes are promising materials for gas separation applications and studied by our group at 25 °C -35 °C [16-19], but the systematic studies dealing with temperature effect on these membranes are very rare.

So in this study the influence of annealing time and temperature and operating temperature on performance of pure polymeric, binary and ternary mixed matrix membranes are investigated systematically with single gas permeabilities of H<sub>2</sub>, CO<sub>2</sub> and CH<sub>4</sub> gases.

## CHAPTER 3

### EXPERIMENTAL

#### 3.1 Membrane Preparation Methodology

The membranes used in this study were synthesized in a previous study of our group in our laboratory [16]. The membranes were fabricated by using solution casting method.

Solvent-evaporation method was used during preparation of the membranes and the methodology was given Appendix D. In this study only post annealing step applied to some membranes at 120 °C, 0.2 atm., N<sub>2</sub> atm., for 7-30 days. Post annealing carried out to enhance the stability and reproducibility of the gas permeation performances of the membranes which will be discussed in Chapter 4 in more detail.

Four types of membranes were employed which are pure polymeric (PES), polymer/zeolite (PES/SAPO-34) mixed matrix, polymer/additive (PES/HMA) and polymer/ zeolite/ additive (PES/SAPO-34/HMA) ternary mixed matrix membranes. The membrane compositions were selected considering the gas performances in previous study [16]. The compositions of membranes used in this study are given below:

The concentration of PES in DMF was 20% (w/v).

The concentration of SAPO-34 relative to polymer was 20% (w/w).

The concentration of HMA relative to polymer was 4 % (w/w).



Also the membrane codes and annealing conditions were tabulated in Table 3.1

Table 3.1 Membrane codes and annealing conditions.

Membrane Code	Membrane Type	Annealing Condition
M1	PES	Not Post Annealed
M2	PES/SAPO-34	Not Post Annealed
M3	PES/SAPO-34	Not Post Annealed
M4	PES	Not Post annealed
M5	PES/SAPO-34	Post annealed
M6	PES	Not Post annealed
M7	PES/HMA	Post annealed
M8	PES/SAPO-34/HMA	Post annealed

Post annealed membranes and not post annealed membranes were abbreviated by -p and -n respectively.

### 3.2 Membrane Characterization

Similar to previous studies [16-19, 59] membranes were characterized by differential scanning calorimetry (DSC, Shimadzu DSC60) to determine the glass transition temperatures ( $T_g$ ) of the membranes. Small samples of the membranes were placed in alumina DSC pans and heated from 30°C to 250°C at a rate of 10°C/min in N<sub>2</sub> atmosphere where the N<sub>2</sub> flow rate was 75 ml/min. After 250°C the membranes were cooled down to 30°C for second scan. The second scan was conducted again by the same procedure. The first scan was done in order to erase the thermal history and the second scan was used to obtain the  $T_g$ .

Membranes were also characterized by a thermal gravimetric analyzer (TGA, Shimadzu DTG-60H) to determine the thermal stability of the membranes and the

amount of residual solvent remaining in the membranes. For TGA analysis the samples were heated from 30 °C to 250 °C at 10 °C/min heating rate in N<sub>2</sub> atmosphere and the flow rate of the N<sub>2</sub> was 75ml/min.

The morphological characterizations of the membranes were done using scanning electron microscopy (SEM), FEI Quanta-400 F. The membranes were sectioned in liquid N<sub>2</sub> for this characterization. Membranes were placed in the aluminum holders with electrically conductive tapes and the cross sections were analyzed at this fractured end of the film. Before analysis the membrane samples were coated with gold/palladium to improve the SEM images.

### **3.3 Gas Permeability Measurements**

#### **3.3.1 Experimental Set-up and Procedure**

The single gas permeation experiments were done using the single gas permeation set up for flat type membranes shown in Fig.3.1 [16-19]. Constant volume variable pressure technique was used. In this system the pressurized feed gases permeate through the membrane and pressure increase in the permeate side, which was initially at vacuum, is measured to calculate the permeability.

Membrane module used in this study is a commercial module Millipore filter holder (Millipore, part no.XX45 047 00) with a double-Viton O-ring seal. The effective membrane area was 9.6 cm<sup>2</sup> and the dead volume of the set-up was 7.1 cm<sup>3</sup>, which is the volume occupied by the permeate gas from permeate side of the membrane cell to pressure transducer and measured by filling the described volume by water. The pressure increase in the permeate side was measured with a pressure transducer (BD Sensors, DMP331, 0–4 bar pressure range, 0.001 bar sensitivity). In order to control the operation temperature, the membrane module was placed in a silicone oil bath which is isolated and the operation temperature was changed between 35 °C-120 °C. The gases used in this study were purchased from OKSAN which is a local company.

Both feed and permeate sides of the set up were evacuated by a vacuum pump (Model E2M5, Edwards High Vacuum Pump) to less than 0.1 bar (gauge pressure) for at least 1 hour. The pressurized gas first passed through a dehumidifier and fed to the feed tank. The dehumidifier was filled with zeolite 4A particles and was used to reduce the humidity of the feed gases. The feed side pressure in the gas chamber was kept constant at 2.9 bar while the permeate side pressure was  $\sim 0.9$  bar (at vacuum). Gas to be measured fed to the membrane module and passed through the membrane due to 2 bar transmembrane difference. The increase in the permeate side pressure was measured by pressure transducer and the data sent to computer by a data acquisition system. The experimental permeate side pressure as a function of time data was recorded digitally.

The thermal stability of the membranes was tested by applying temperature cycles. The single gas permeability measurements were carried out in the order of  $H_2$ ,  $CO_2$  and  $CH_4$  at 35 °C. Then the temperature was slowly increased to 90 °C and the single gas permeabilities were again measured in the same order. The cycle was terminated by decreasing the temperature to again 35 °C. The single gas permeates were measured again. This cycle was conducted for several times.

The effect of operating temperature was investigated between 35-120 °C. First the single gas permeability measurements were done in the order of  $H_2$ ,  $CO_2$ , and  $CH_4$  at 35 °C. After finishing the measurements at 35 °C, the temperature slowly increased to 50, 70, 90 and 120 °C and the gas permeability experiments were carried out at each temperature. Lastly the investigation of the effect of operating parameters was terminated by decreasing the temperature to again 35 °C and the single gas permeation experiments were repeated to measure the membrane performance stability. The heating and cooling of the membrane module was conducted at very slow heating/cooling rates (15 °C /h). Gas permeability values are reported in terms of Barrer ( $1 \text{ Barrer} = 10^{-10} \text{ cm}^3 \text{ (STP) cm/cm}^2 \text{ s cmHg}$ ).

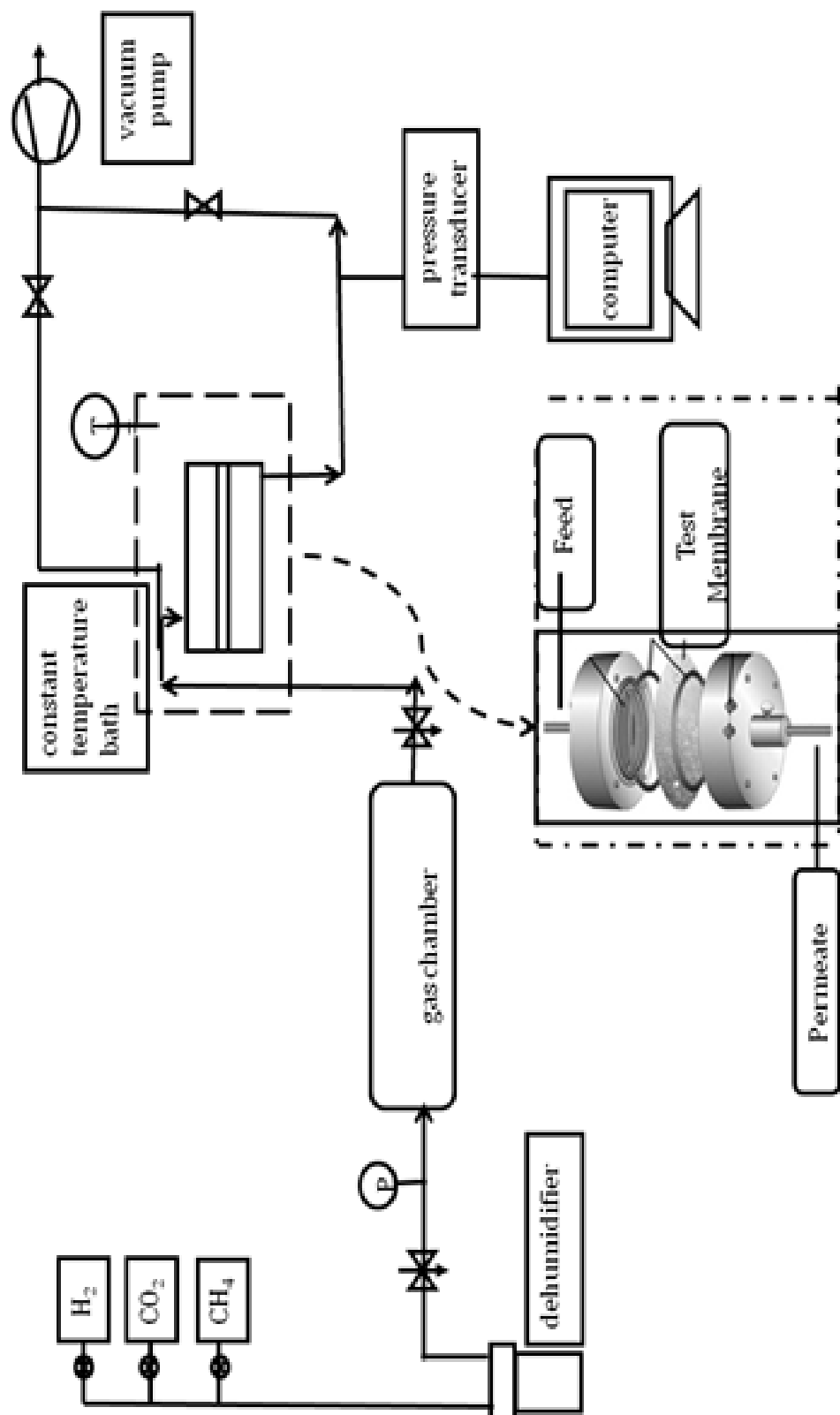


Figure 3.1 Schematic representation of the gas permeation set-up.

### 3.3.2 Permeability and Selectivity Calculations

After completion of the single gas permeation experiments, the permeabilities, selectivities and  $E_a$  values were calculated. Since the calculation steps were given in detail in previous works, it will not be explained in this work again [17,19 ]. The increase in permeate side pressure with respect to experiment time was used to predict the permeability. Equation 2.1 was used to calculate single gas permeabilities. The ideal selectivities were also determined from Equation 2.4.

After permeability calculations, activation energies of the studied gases were also calculated by;

$$\ln P = \ln P_0 - \frac{E_a}{RT} \quad (3.1)$$

The slope of inverse temperature versus  $\ln P$  graph gives the activation energy ( $E_a$ ) over universal gas constant  $R$ .  $E_a$  is reported in terms of kJ/mole.

## CHAPTER 4

### RESULTS AND DISCUSSION

#### 4.1 Membrane Characterization

##### 4.1.1 DSC Results

Glass transitions temperatures ( $T_g$ ) of the membranes were measured with differential scanning calorimetry (DSC) in order to understand the effect of membrane formulation on chain stiffness or chain flexibility. As mentioned before some of the membranes were used as synthesized and some membranes were post annealed to see the annealing effect on membranes. DSC analyses were done both post annealed and not post annealed membrane samples. Post annealing was performed at 120 °C, 0.2 atm.,  $N_2$  atm. for 7 days. The second scan thermograms are given in Appendix B and  $T_g$  of membranes are shown in Table 4.1.

The  $T_g$  of PES membrane was found similar to the literature which is 220 °C [16, 19, 60]. PES/HMA membrane has lower  $T_g$  than PES membrane. This behavior is also reported in the literature; the addition of low molecular weight additives decreases the  $T_g$  of the pure polymeric membranes because of dilution effect [17, 59, 61]. The low glass transition temperatures of the low molecular weight additives (LMWA) decreases the  $T_g$  of the polymer/ LMWA blends even at very low concentrations. The  $T_g$  of the PES/SAPO-34 membrane is the same as pure PES membrane in accordance with the literature [16, 17, 19, 62]. This suggests that there is no substantial interaction at the molecular level between the polymer and zeolite. The  $T_g$  of PES/SAPO-34/HMA membrane is higher than that of PES/HMA membrane [16, 19]. This can be explained by increasing interaction of PES and SAPO-34 with HMA

addition. The post annealing did not make any significant changes in  $T_g$  of membranes, the glass transition temperatures are nearly the same as not post annealed ones. It can be concluded that the changes occurring in the membrane with post annealing is not in the molecular level. Similar to our results Fu et al. [46] did not observe any differences in  $T_g$  of polyimide dense membranes that are annealed at different temperatures for different periods. On the other hand Joly et al. [47] observed that the  $T_g$  of the fluorinated polyimide membranes changed with the amount of residual solvent remaining in the membrane. They observed that solvent free membranes have higher  $T_g$  values and relate these to the reduction in the intermolecular interactions in the presence of solvent residues in the membrane. Moreover Chang et al. [63] performed an energy analysis to polymer chains to determine the intramolecular and intermolecular energies. They stated the effect of remaining solvent in the membrane on the molecular energy is dependent on the solvent amount in the membrane and molar volume of the solvent. They also concluded that residual solvent present in the membrane enhances small scale segmental motions. Therefore effect of annealing on  $T_g$  strongly depend on the polymer and solvent type.

Table 4.1 Glass transition temperatures of post annealed and not post annealed membranes.

Membrane Type	Annealing Condition	
	Post Annealed	Not Post Annealed
	$T_g$ (°C)	$T_g$ (°C)
PES	219	220
PES/HMA	213	212
PES/SAPO-34	219	221
PES/SAPO-34/HMA	217	216

#### 4.1.2 TGA RESULTS

The solvent remaining in the membrane and molecular imprint of removed solvent molecules influence the separation performance of the membrane. In order to analyze the remaining solvent in the membrane, thermal gravimetric analyzer (TGA) was used in this study. Post annealed and not post annealed membranes were tested. The results are given in Table 4.2 and the thermograms were given in Fig. 4.1, Fig. 4.2 and Appendix C.

As can be seen in Table 4.2, the weight of PES-p membrane decreased up to 100°C and above 100 °C no significant weight loss was observed. So this weight loss can be attributed to release of moisture and some solvent sorbed by the membrane. For PES-n membrane the weight loss was nearly the same as post annealed one until 100 °C, however, after 150 °C the weight of PES-n membrane continued decreasing which is related to solvent removal through the membrane or decomposition of the polymer. Again the weight loss of PES/HMA-p membrane decreased slightly till 100 °C and stayed nearly constant up to 250 °C. On the other hand the weight loss of PES/HMA-n membrane decreased significantly after 150 °C which can be related to solvent removal or decomposition of HMA particles present in the membrane. The total weight losses of PES-p and PES/HMA-p membranes were smaller than 1%.

The weights of PES/SAPO-34-p and PES/SAPO-34-n membranes were decreased till 100 °C, after 100 °C no significant change in weight loss of PES/SAPO-34-p membrane was observed while the weight of the PES/SAPO-34-n membrane continued decreasing. The same trend with PES/SAPO-34 membranes was obtained from PES/SAPO-34/HMA membranes. The weight losses through all membranes until 100 °C can be related to moisture that is gained by the membranes. Moe et al.[49] tested how much moisture can be taken from polyimide membranes. After annealing two membranes at 240 °C for five days, they immersed one of the membranes in water for 14 days and left the other one in room conditions for 14 days. The membrane that is exposed to room conditions gained <1% water while the membrane that is immersed in water gained only 1.4% moisture. The weight losses of mixed matrix membranes till 100 °C are higher than polymeric membranes which



can be due to SAPO-34 particles presence in the membranes and created interfaces between polymer and zeolite. Solvents, impurities and moistures may be gained by SAPO-34 particles. As can be seen in Figure 4.1 and Figure 4.2, post annealing provide removal of solvent from the membrane. Post annealed membranes have higher thermal stability than not post annealed ones. The weight losses of not post annealed mixed matrix membranes after 150 °C can be related to solvent removal from the membranes. The boiling point of the solvent used in this study, DMF, is 153 °C so high temperatures are needed to remove the residual solvent in the membranes.

Table 4.2 Weight losses of the post annealed and not post annealed membranes determined by TGA.

Annealing Condition	Membrane Type	Weight loss up to 100°C, (%)	Weight loss up to 150°C, (%)	Total weight loss, up to 250°C, (%)
Post Annealed	PES	0.79	0.82	0.96
	PES/SAPO-34	2.73	2.88	3.03
	PES/HMA	0.62	0.62	0.81
	PES/SAPO-34/HMA	3.43	3.53	3.68
Not Post Annealed	PES	0.99	1.13	3.59
	PES/SAPO-34	3.73	4.02	5.99
	PES/HMA	1.02	1.20	5.16
	PES/SAPO-34/HMA	3.66	4.39	7.77

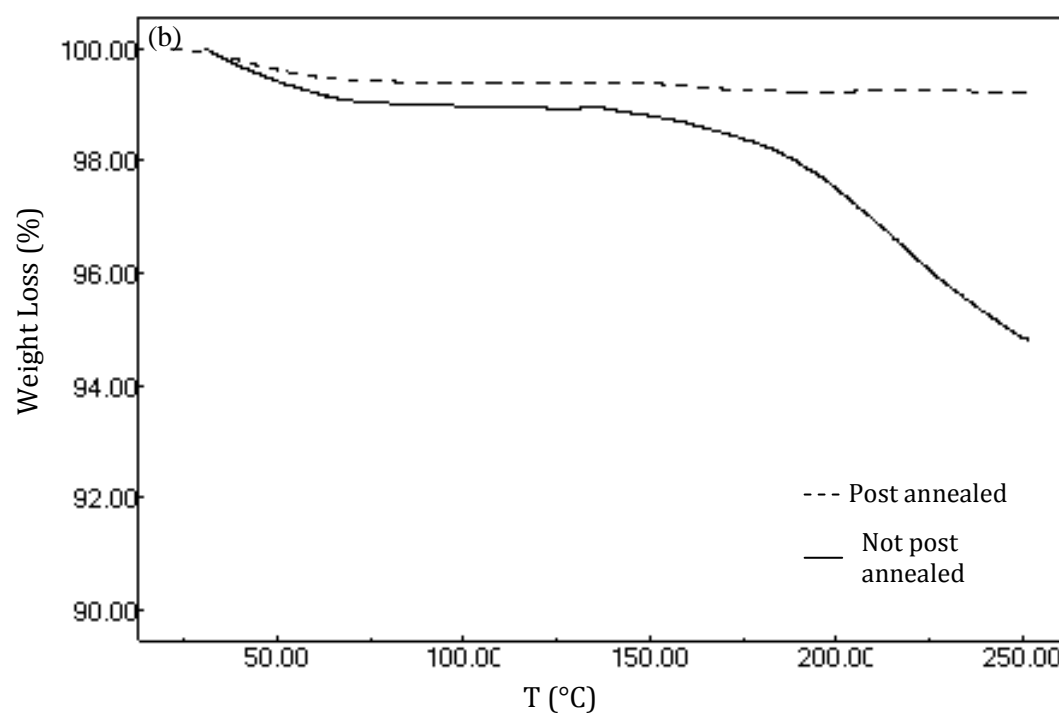
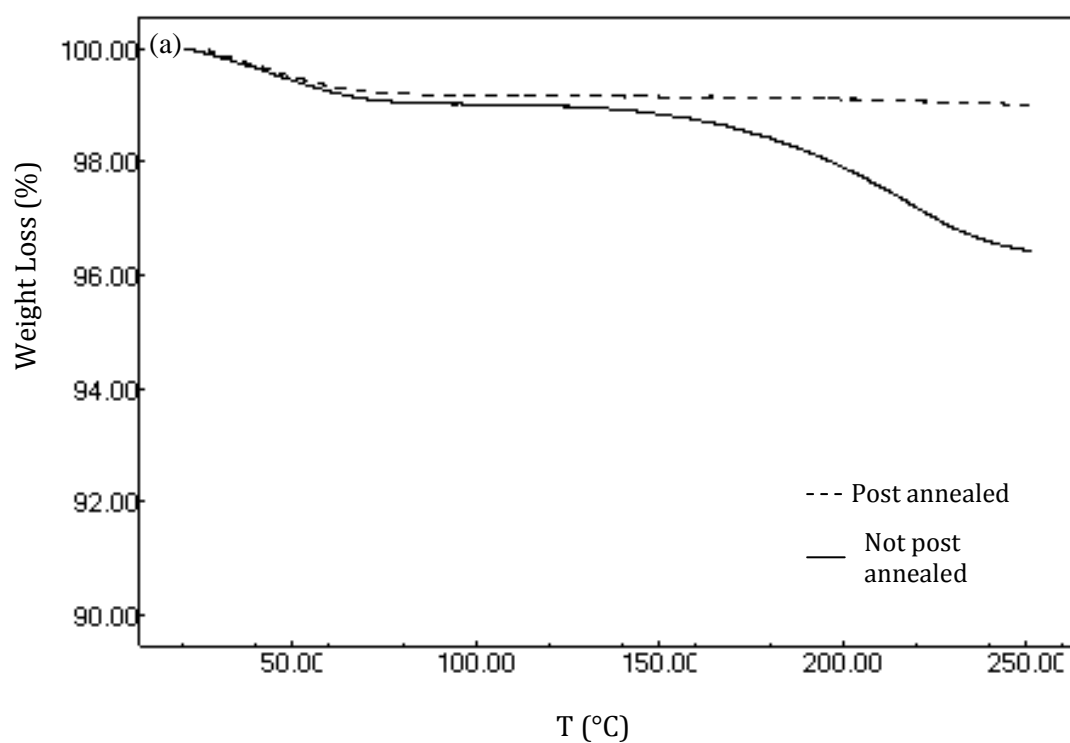


Figure 4.1 TGA thermograms of post annealed and not post annealed (a) PES, (b) PES/HMA membrane

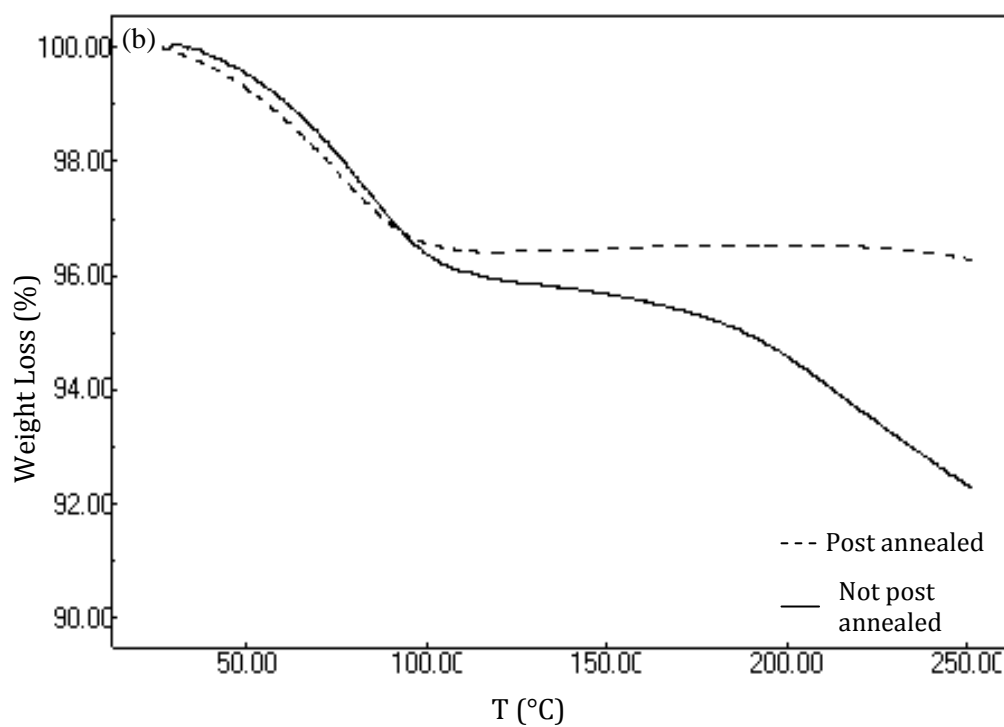
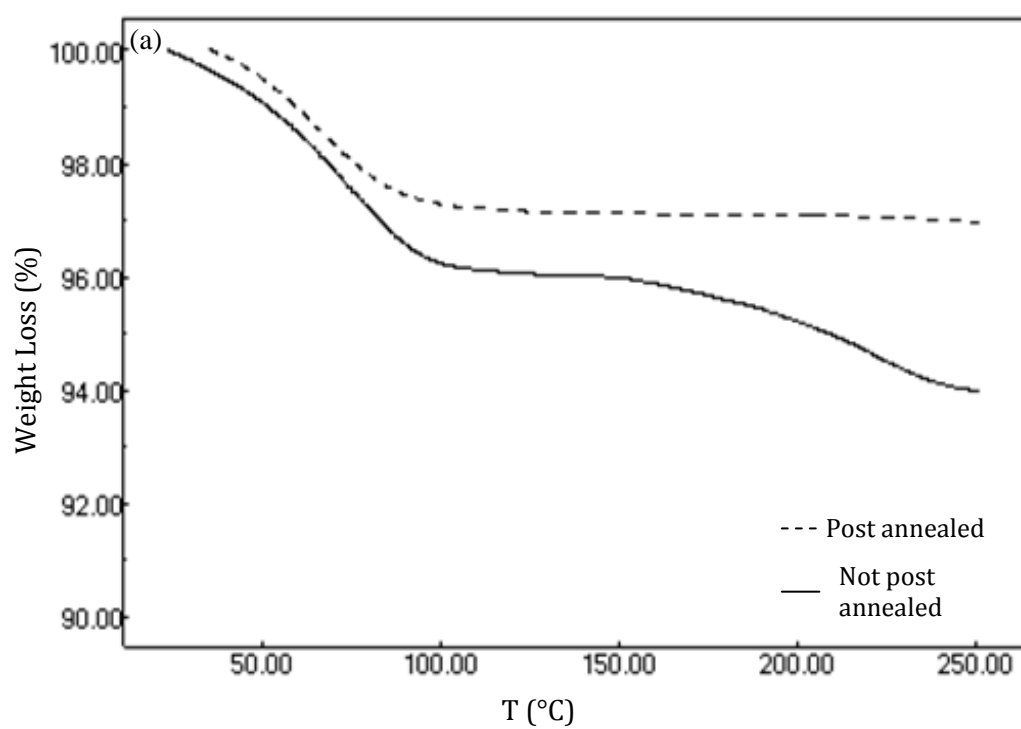


Figure 4.2 TGA thermograms of post annealed and not post annealed (a) PES/SAPO-34, (b) PES/SAPO-34/HMA Mixed Matrix Membranes.

#### 4.1.3. SEM Results

Scanning electron microscopy (SEM) characterization was made in order to investigate the morphologies of the membranes that were used in this study. The aim is to see the effect of post annealing on membrane morphologies. The SEM images of both post annealed and not post annealed PES and PES HMA membranes are given in Fig. 4.3.

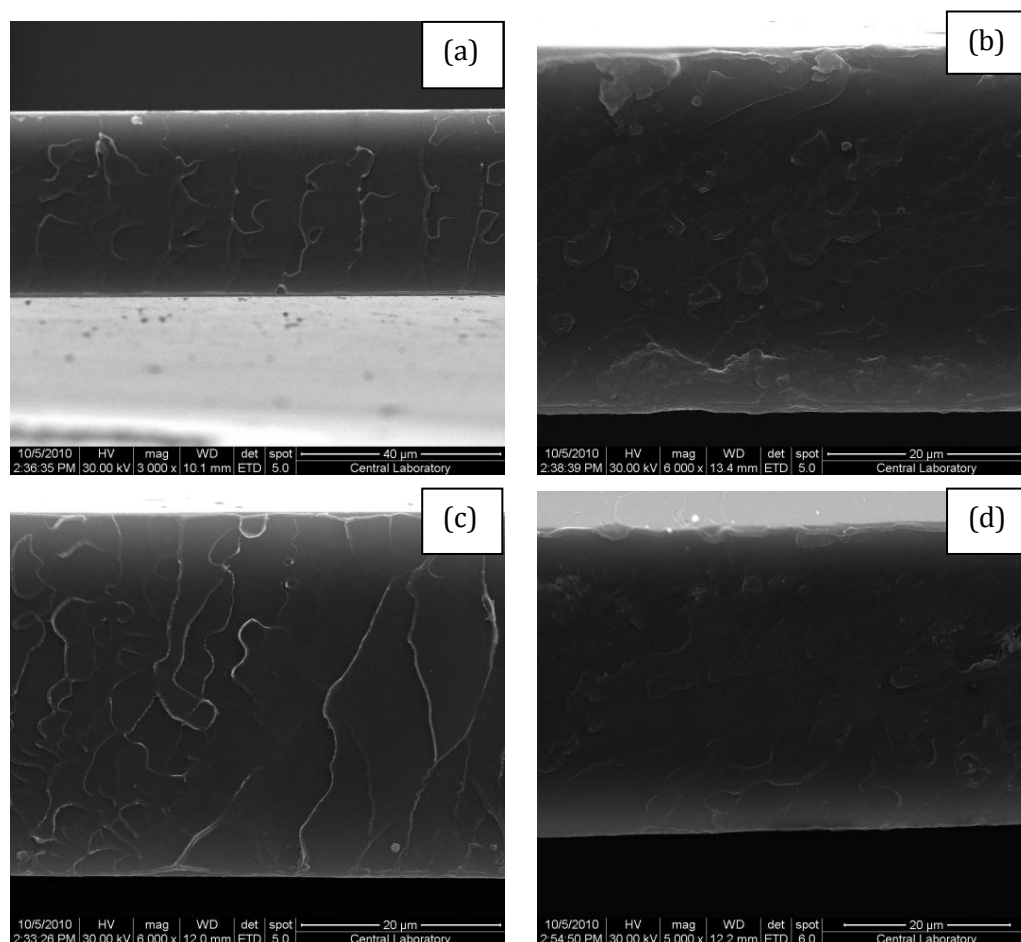


Figure 4.3 SEM images of (a) PES-p, (b) PES-n, (c) PES/HMA-p, (d) PES/HMA-n membranes.

The cross section image of the PES and PES/HMA membrane is smooth as expected and no defects or voids were observed. Furthermore, no changes in the membrane morphologies were seen with post annealing.

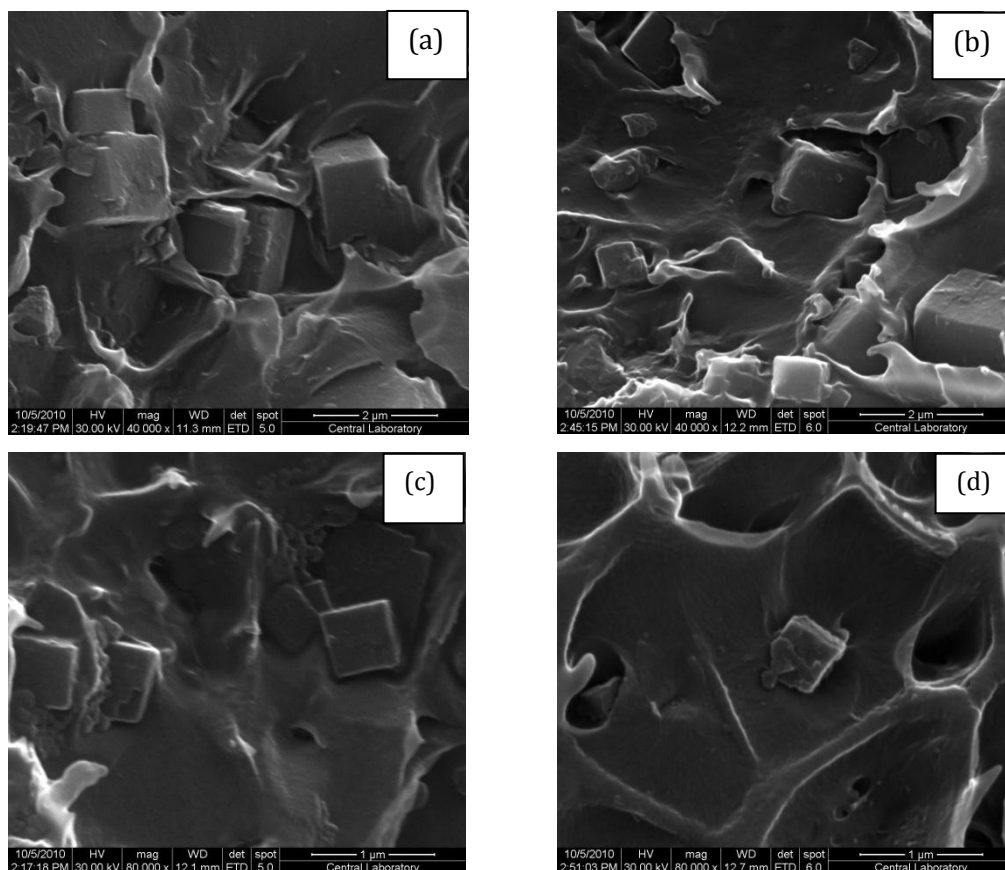


Fig. 4.4 SEM images of (a) PES-SAPO-34-p, (b) PES-SAPO-34-n, (c) PES/HMA-SAPO-34-p, (d) PES/HMA-SAPO-34-n membranes.

The SEM images of SAPO-34 loaded membranes are given in Fig. 4.4. The images (Fig. 4.4 a and b) show that PES/SAPO-34 membranes have some voids and loose structure at the polymer-zeolite interfaces. The ternary mixed membrane including

HMA, shows better adhesion between PES and SAPO-34 particles as can be seen from the figures. These images showed that everything is as expected in these membranes and similar to those reported in Çakal's work. The SEM images of the post annealed membranes are also given and no significant changes in the morphologies have been observed. In literature some studies investigating effect of annealing on mixed matrix membranes structures observed differences from SEM figures [10, 41]. Koros et al. [10] and İsmail et al. [41] both investigated the effect of above and below  $T_g$  annealing on the membrane performances. They observed that by annealing the membranes above  $T_g$  of the polymer, better adherence between polymer and zeolite particles were obtained based on SEM micrographs [10, 41]. At temperatures above  $T_g$  of the polymer, the polymer chain moves more so that the adherence can be improved. However at temperatures below  $T_g$  of the polymer the chain movements are restricted. In this study both annealing treatments (pre and post annealing) were applied below the  $T_g$  of the polymer. So applying post annealing may have caused changes in the membrane structure in very small scales which could not be observed by SEM. The SEM figures, therefore, show that no changes occur in membrane structures in micro scale with post annealing.

## **4.2 Gas Permeation**

### **4.2.1. Repeatability and Reproducibility of the Results**

While determining the membrane performance by gas permeation the repeatability and reproducibility of the measurements are very important. The repeatability of the gas permeability results were investigated by measuring gas permeability of each gas for each membrane twice except  $\text{CH}_4$ . Gas permeability of  $\text{CH}_4$  was not repeated systematically owing to its long permeation time. First  $\text{H}_2$  permeability was measured between 35 °C- 90 °C then  $\text{CO}_2$  gas permeability was measured at each temperature and lastly  $\text{CH}_4$  was tested. As an example some of the repeatability results were reported in Table 4.3 for PES-n and PES/SAPO-34-n membranes. The numerical data of all gas permeation measurements were given in Appendix D. The differences between two runs were found smaller than 10% which is consistent with previous studies [11, 16, 19, 59].

Table 4.3 Repeatability results of the PES-n (M1) and PES/SAPO-34-n (M2) membrane performances.

	T °C	Run	Permeability			Selectivity		
			H <sub>2</sub>	CO <sub>2</sub>	CH <sub>4</sub>	H <sub>2</sub> /CO <sub>2</sub>	CO <sub>2</sub> /CH <sub>4</sub>	H <sub>2</sub> /CH <sub>4</sub>
PES-n (M1)	35	1 <sup>st</sup>	6.63	3.67		1.81		
		2 <sup>nd</sup>	6.78	3.83		1.77		
		Avg:	6.71	3.75		1.79		
		Δ%	2.26	4.35	0.14		26.98	48,28
	50	1 <sup>st</sup>	8.77	4.46		1.97		
		2 <sup>nd</sup>	8.55	4.60		1.86		
		Avg:	8.66	4.53		1.91		
		Δ%	2.5	3.07	0.21		22.32	42.66
	70	1 <sup>st</sup>	11.61	5.68		2.04		
		2 <sup>nd</sup>	11.54	5.66		2.04		
		Avg:	11.56	5.67		2.03		
		Δ%	0.6	0.35	0.34		16.48	33.6
	90	1 <sup>st</sup>	16.74	6.81		2,46		
		2 <sup>nd</sup>	16.83	7.08		2,38		
		Avg:	16.79	6.95		2.42		
		Δ%	0.5	3.8	0.54		13.0	30.9
PES/SAPO- 34-n (M2)	35	1 <sup>st</sup>	11.10	4.60				
		2 <sup>nd</sup>	11.04	4.54		2.41		
		Avg:	11.07	4.57		2.43		
		Δ%	0.54	1.3	0.15	2.42	30.46	73.8
	50	1 <sup>st</sup>	13.55	5.25		2.58		
		2 <sup>nd</sup>	13.93	5.18		2.69		
		Avg:	13.74	5.22		2.63		
		Δ%	2.8	1.3	0.25		20.88	54.96
	70	1 <sup>st</sup>	18.86	6.74		2.80		
		2 <sup>nd</sup>	19.64	6.76		2.90		
		Avg:	19.12	6.75		2.83		
		Δ%	4.14	0.3	0.39		17.31	49.03
	90	1 <sup>st</sup>	26.33	8.76		3.01		
		2 <sup>nd</sup>	26.17	8.43		3.10		
		Avg:	26.25	8.60		3.05		
		Δ%	0.61	3.76	0.66		13.03	39.77

Then the effect of gas order on gas permeation was investigated. First the permeabilities were measured in the order of H<sub>2</sub>, CO<sub>2</sub> and CH<sub>4</sub>, after CH<sub>4</sub> again H<sub>2</sub>, CO<sub>2</sub>, CH<sub>4</sub> gases permeabilities were measured respectively through PES/SAPO-34-n membranes. The results are given in Table 4.4. The differences between two runs

were again found smaller than 10% which means repeatable results can be obtained after changing the gas order and gas order do not have any influence on membrane performance.

Table 4.4 Effect of gas order on reproducibility of PES/SAPO-34-n (M3) membrane performance.

	T °C	Run	Permeability			Selectivity		
			H <sub>2</sub>	CO <sub>2</sub>	CH <sub>4</sub>	H <sub>2</sub> /CO <sub>2</sub>	CO <sub>2</sub> /CH <sub>4</sub>	H <sub>2</sub> /CH <sub>4</sub>
PES/SAPO-34-n (M3)	35	1 <sup>st</sup>	10.6	4.58	0.13	2.31	34.4	79.6
	35	2 <sup>nd</sup>	10.2	4.40	0.13	2.31	33.6	77.5

After testing the effect of gas order on PES/SAPO-34-n membrane performance the temperature effect on reproducibility of the results were tested as shown in Table 4.5. This time again the permeabilities were measured first for H<sub>2</sub> from 35 °C to 90 °C then CO<sub>2</sub> permeability measured and lastly CH<sub>4</sub> permeability measured between 35 °C to 90 °C. After measuring CH<sub>4</sub> permeability, CO<sub>2</sub> permeability was measured again at the studied temperatures and the membrane showed higher CO<sub>2</sub> permeability than previous one. Since differences in permeabilities are significant and it was found that gas order do not have that much influence on gas permeability these deviations must be due to effect of operating temperature on membrane stability.



Table 4.5 Effect of temperature on reproducibility of PES/SAPO-34-n (M2) membrane performance.

Membrane Type	T °C	Permeability (Barrer)				Selectivity		
		H <sub>2</sub>	CO <sub>2</sub>	CH <sub>4</sub>	CO <sub>2</sub>	H <sub>2</sub> /CO <sub>2</sub>	CO <sub>2</sub> /CH <sub>4</sub>	H <sub>2</sub> /CH <sub>4</sub>
PES/SAPO-34-n (M2)	35	11.1	4.57	0.14	5.71	2.42	30.46	73.8
	50	13.7	5.22	0.25	6.77	2.63	20.9	54.9
	70	19.1	6.75	0.39	7.95	2.83	17.3	49.0
	90	26.3	8.60	0.66	9.46	3.05	13.0	39.8

To further investigate this behavior, a cyclic operating temperature program is applied to dense homogenous PES-n membranes as can be seen in Figure 4.5. In the figure the dashed lines shows the temperature cycle period and the continuous lines shows the membrane performances at each temperature. Single gas permeabilities of all gases were measured first at 35 °C in the order of H<sub>2</sub>, CO<sub>2</sub> and CH<sub>4</sub>. Then the temperature was slowly increased to 90 °C and the gas permeabilities were measured again in the same order. Finally the cycle was terminated by measuring the membrane performance at 35 °C again to see the reproducibility of the results. These temperature cycles were done for several times.

The temperature cycles versus permeability graph for each gas through PES-n membrane is given in Figure 4.5 and the selectivities were given in Table 4.6. The figure shows that the permeabilities did not change with temperature. Results showed that stable performance through pure PES membrane can be obtained. The changes in both selectivities and permeabilities are calculated from the highest and lowest results difference obtained from temperature cycles and are tabulated in Appendix D. The changes found smaller than 10% which is an acceptable ratio.

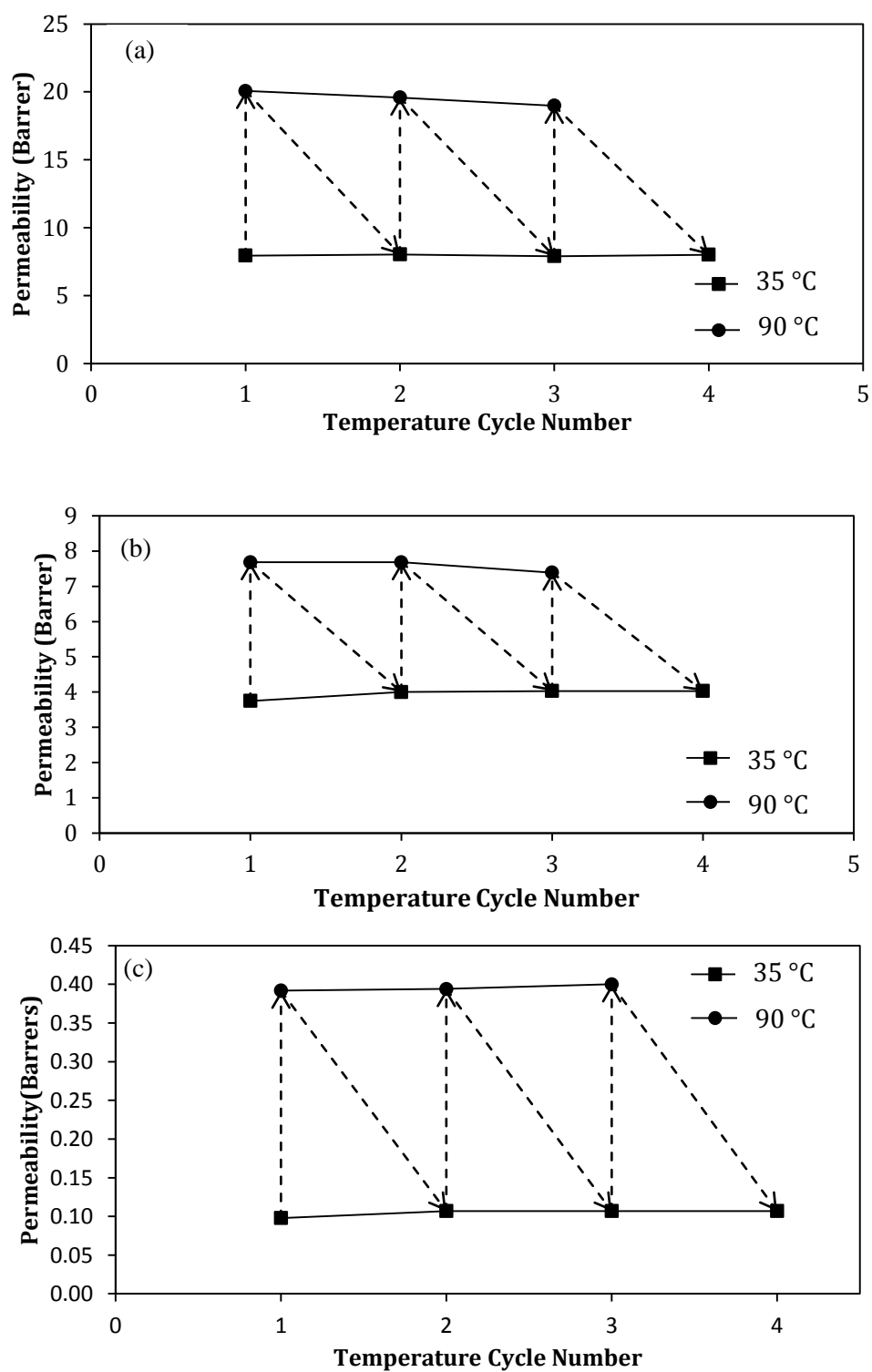


Figure 4.5 Permeabilities of (a)  $H_2$ , (b)  $CO_2$ , (c)  $CH_4$  gases through PES-n (M4) membrane with respect to temperature cycles at 35 °C and 90 °C.

Table 4.6 Ideal selectivities of PES-n (M4) membrane with respect to temperature cycles at 35 °C and 90 °C.

Selectivities	1 <sup>st</sup> Cycle		2 <sup>nd</sup> Cycle		3 <sup>rd</sup> Cycle		4 <sup>th</sup> Cycle
	35 °C	90 °C	35 °C	90 °C	35 °C	90 °C	35 °C
H <sub>2</sub> /CO <sub>2</sub>	2.12	2.61	2.01	2.55	1.96	2.57	1.99
CO <sub>2</sub> /CH <sub>4</sub>	38.27	19.59	37.38	19.49	37.66	18.48	37.66
H <sub>2</sub> /CH <sub>4</sub>	81.12	51.20	75.05	49.70	73.83	47.45	74.85

Secondly a similar cyclic temperature program was applied to PES/SAPO-34-n membrane which was tested again at 35 °C and 90 °C without any additional treatment. The permeability results are plotted in Figure 4.6 and selectivities are given in Table 4.7. Total duration of experiments is longer than one month and the results showed that the permeabilities increased but selectivities decreased after each cycle. The permeability increase was very obvious for CH<sub>4</sub> gas and less significant for H<sub>2</sub>. At 35 °C the CH<sub>4</sub> permeability increased by 8 times while H<sub>2</sub> gas permeability increased by 39%. CH<sub>4</sub> has largest kinetic diameter and so experiences highest resistance to permeation and H<sub>2</sub> experiences lowest resistance so small molecule affected less from the increased motions occurring in the polymer structure [21]. The results also showed that the permeability increase is more pronounced at 35 °C than at 90 °C. The CH<sub>4</sub> gas permeability increases by 2 times and H<sub>2</sub> permeability increase is 19% at 90 °C. At 90 °C the polymer chains become very flexible and mobile but at 35 °C the polymer chains are stiffer so the increase in free volume of the membrane due to solvent removal has more effect on the gas transport at 35 °C.

This heating and cooling effect on membrane performance has also been observed by Woo et al. [64]. They studied with MFI loaded poly(1-trimethylsilyl-1-propyne) composite membranes for *n*-butane/*i*-butane gas separation. They measured the effect of temperature on permeabilities of the membranes first while heating from

25 °C to 200°C and then while cooling down from 200 °C to 25 °C. Different from our results in their study the permeabilities were decreasing and selectivities were increasing with increasing temperature. They observed that first heating the membranes and then cooling them results in different membrane performances, the permeabilities were lower and selectivities were higher during cooling step than those during heating step. They attributed this result to decrease in membrane free volume and desorption of methanol from MFI particles with increasing temperature. However they did not proposed any methods to overcome this behavior.

This trend has not been observed in pure polymeric membranes so it can be related to incorporation of SAPO-34 particles present in the membrane. PES/SAPO-34 MMM has a morphology consisting of polymer, zeolite and the interface between them. Obtaining different behaviors from these two membranes in relation to thermal treatment is not an unexpected result. This increase in gas permeabilities can be related to the removal of residual solvent remained in the membrane with increasing temperature hence increasing the free volume which leads increases in permeabilities. However no change in permeabilities was observed for PES-n membrane, suggesting all solvent was successfully removed from this membrane during annealing while for PES/SAPO-34-n membrane the solvent can be hold by SAPO-34 particles and longer annealing periods and higher temperatures can be required to remove the solvent. Also this large increase in permeation can be attributed to loosened structure of the membrane to some extend with temperature cycles. Also differences in thermal expansion coefficients of the polymer and zeolite particles may cause this behavior. Moore et al. [27] proposed that, the polymeric material generally has higher thermal expansion coefficients than zeolites and with increasing temperature the polymer matrix expands and then with cooling it contracts and voids left between the two phase.

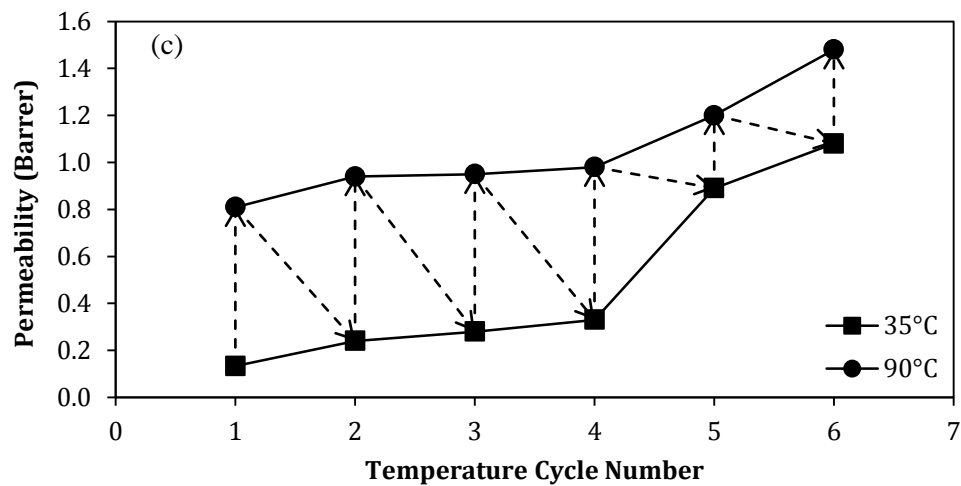
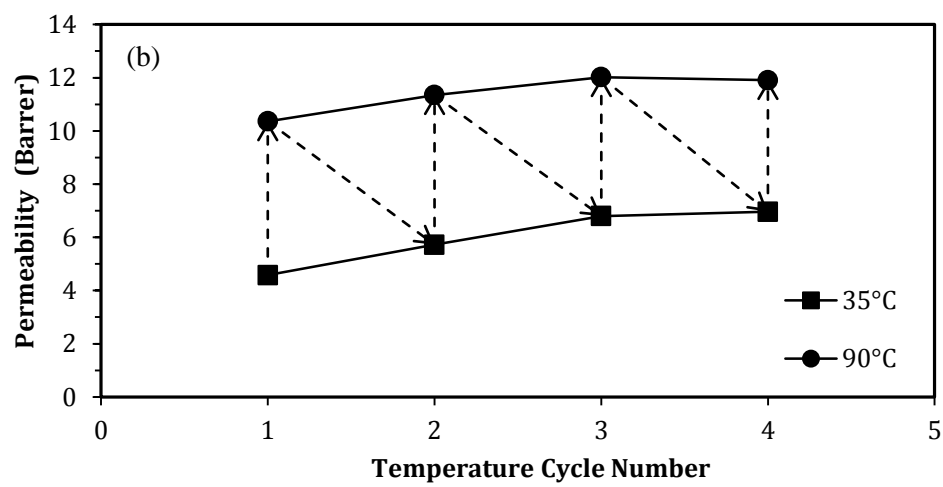
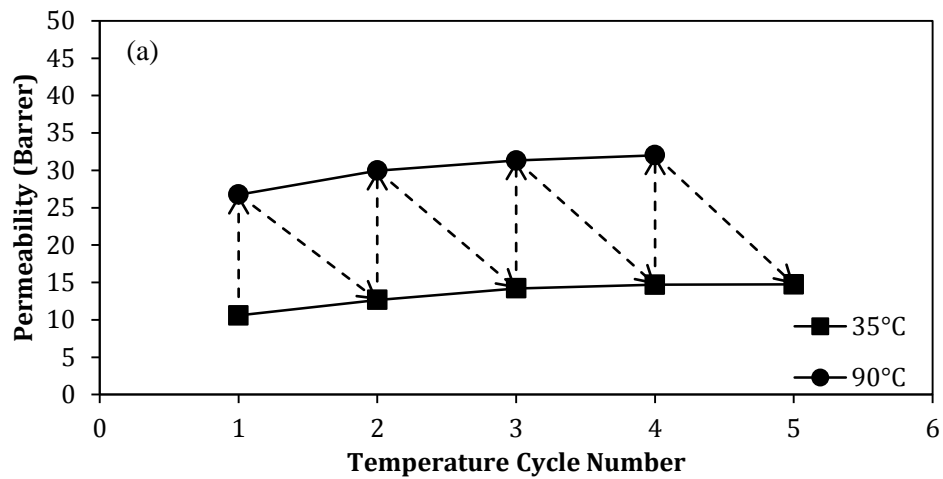


Figure 4.6 Permeabilities of (a) H<sub>2</sub>, (b) CO<sub>2</sub>, (c) CH<sub>4</sub> gases through PES-SAPO-34-n (M3) membrane with respect to temperature cycles at 35 °C and 90 °C.

Table 4.7 Ideal selectivities of PES/SAPO-34-n (M3) membrane with respect to temperature cycles at 35 °C and 90 °C.

Selectivity	1 <sup>st</sup> Cycle		2 <sup>nd</sup> Cycle		3 <sup>rd</sup> Cycle		4 <sup>th</sup> Cycle		5 <sup>th</sup> Cycle
	35 °C	90 °C	35 °C	90 °C	35 °C	90 °C	35 °C	90 °C	35 °C
H <sub>2</sub> /CO <sub>2</sub>	2.31	2.58	2.22	2.64	2.09	2.60	2.11	2.69	2.08
CO <sub>2</sub> /CH <sub>4</sub>	34.4	12.8	23.8	12.1	24.3	12.7	21.1	12.2	7.97
H <sub>2</sub> /CH <sub>4</sub>	79.6	33.0	52.8	31.9	50.7	33.0	44.5	32.7	16.6

#### 4.2.2 Effect of Annealing on Membranes Performance

Generally studies dealing with the effect of membrane casting conditions on membrane performances carried out with homogenous dense polymeric membranes. These studies showed that the solvent residue in the membrane can act as a plasticizer or an antiplasticizer and affect the membrane performance [46-47]. In literature there are no studies investigating the effect of annealing on ternary mixed matrix membranes. Our results suggest that annealing MMMs at 100 °C, 0.2 atm, for 24 h is not enough to remove all solvent from membranes. So it is decided to apply additional annealing step to PES/SAPO-34 membrane called post annealing to investigate the reason of those increases in permeabilities of gases. Thus the post annealing was applied at higher temperatures for longer times to stabilize the membrane performance by erasing the thermal history and stresses in the membrane. So PES/SAPO-34 mixed matrix membrane was annealed again (post annealing) at 120 °C, 0.2 N<sub>2</sub> atm., for 7 days. The post annealed membrane shown by PES-SAPO-34-p.

The permeabilities obtained with PES/SAPO-34-p membranes with a similar cyclic operating temperature program, are shown in Figure 4.7 and selectivities are given in Table 4.8.

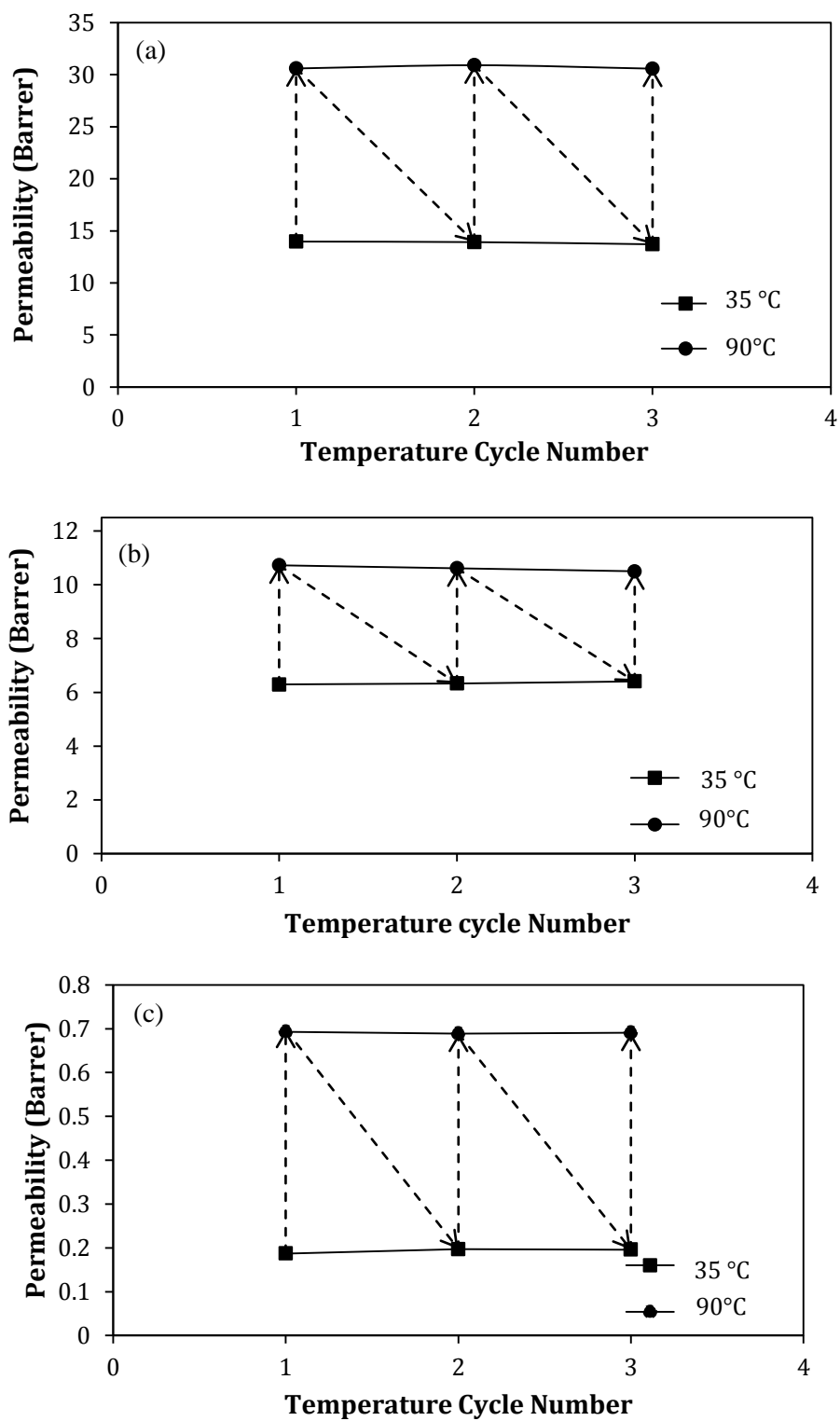


Figure 4.7 Permeabilities of (a)  $H_2$ , (b)  $CO_2$ , (c)  $CH_4$  gases through PES/SAPO-34-p (M5) membrane with respect to temperature cycles at 35 °C and 90 °C.

Table 4.8 Ideal selectivities of PES/SAPO-34-p (M5) membrane with respect to temperature cycles at 35 °C and 90 °C.

	1 <sup>st</sup> Cycle		2 <sup>nd</sup> Cycle		3 <sup>rd</sup> Cycle	
Selectivity	35 °C	90 °C	35 °C	90 °C	35 °C	90 °C
H <sub>2</sub> /CO <sub>2</sub>	2.22	2.85	2.20	2.91	2.14	2.91
CO <sub>2</sub> /CH <sub>4</sub>	33.46	15.37	32.13	15.41	32.70	15.19
H <sub>2</sub> /CH <sub>4</sub>	74.31	43.84	70.66	44.86	69.95	44.25

The permeabilities and selectivities stayed nearly constant after post annealing applied on membrane, showing that to obtain reproducible results the PES/SAPO-34 mixed matrix membranes should be annealed for longer times.

The permeabilities and selectivities of post annealed and not post annealed PES/SAPO-34 membranes at 35 °C are compared in Table 4.9. The data are obtained from the first temperature cycles. Application of post annealing increased the permeabilities while the selectivities did not change or decreased slightly. The increase in permeabilities was ~43% for both CO<sub>2</sub> and CH<sub>4</sub> and 38% for H<sub>2</sub>. Similar results were obtained by Chang et al. [63] and Joly et al. [47], who reported that with increasing annealing time residual solvent in the membrane decreased and the permeabilities increased. Chang et al. [63] made a molecular simulation on polyimide membranes. They observed that the thermal motions of the molecules increase with the removal of solvent remained in the membrane. They compared their results with the experimental data of Joly et al. [47] and the results confirmed each other.

The increases can be due to increased free volumes in the membranes. The increase was smaller for H<sub>2</sub> which means that the transport of smaller gas molecule affected less from the annealing and the increases in free volume of the membrane since it experiences less resistance to flow.



Table 4.9 Single gas permeabilities and ideal selectivities of PES/SAPO-34-n and PES/SAPO-34-p membranes at 35 °C.

	T, °C	Permeabilities (Barrer)			Selectivities		
		H <sub>2</sub>	CO <sub>2</sub>	CH <sub>4</sub>	H <sub>2</sub> /CO <sub>2</sub>	CO <sub>2</sub> /CH <sub>4</sub>	H <sub>2</sub> /CH <sub>4</sub>
PES/SAPO-34-n (M3)	35	10.2	4.40	0.131	2.31	33.6	77.5
PES/SAPO-34-p (M5)	35	14.0	6.29	0.187	2.22	33.6	74.7

So it is decided to post-anneal the SAPO-34 loaded PES membranes before investigating the effect of operating temperature on membrane performances.

#### 4.2.3. Effect of Operating Temperature on Membranes Performance

After eliminating the effect of preparation conditions, annealing time and temperature, the effect of operating temperature on membrane performances were investigated. For these purpose the permeation temperatures changed between 35 °C and 120 °C.

First the effect of temperature on the performance of PES-n membrane was investigated. The membrane was not post annealed since its performance did not show any change after temperature cycles. Single gas permeabilities of H<sub>2</sub>, CO<sub>2</sub> and CH<sub>4</sub> gases were measured at 35 °C, 50 °C, 70 °C and 90 °C, then the permeabilities re-measured at 35 °C. The numerical data are tabulated in Appendix D. The permeability results are shown in Figure 4.8, demonstrating that with increasing temperature the single gas permeabilities of all studied gases increased. After measuring the permeabilities of all gases at 90 °C, the temperature again decreased to 35 °C to check the stability of the membrane performance and the permeabilities nearly stayed constant after one month long experiments. The highest increase in

permeabilities with temperature belongs to CH<sub>4</sub> gas and the lowest belongs to CO<sub>2</sub>. Observed trend of permeability increase with increasing operating temperature also reported in the literature for dense homogenous polymeric membranes [21, 54-56]. This increase in permeabilities with increasing temperature is related to increase in diffusivities of the membranes, which is more dominant than solubility in glassy membranes [24].

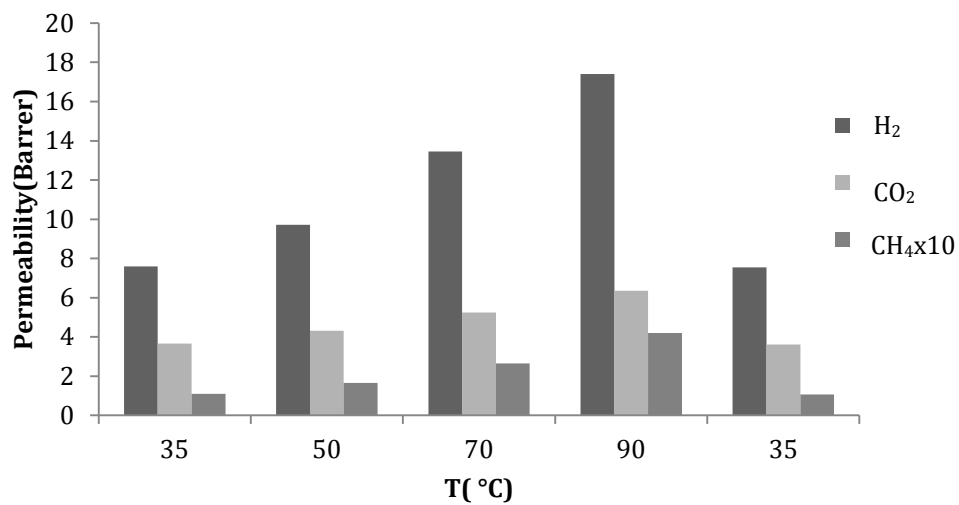


Figure 4.8 Effect of operation temperature on permeabilities of PES-n (M6) membrane.

The selectivities of CO<sub>2</sub>/CH<sub>4</sub> and H<sub>2</sub>/CH<sub>4</sub> gas pairs decreased but H<sub>2</sub>/CO<sub>2</sub> selectivity slightly increased with temperature as shown in Figure 4.9. The CO<sub>2</sub>/CH<sub>4</sub> gas selectivity decreases with increasing temperature because CO<sub>2</sub> has high solubility and diffusivity than CH<sub>4</sub> [51]. So the CH<sub>4</sub> permeability increases more compared to CO<sub>2</sub> permeability. The similar behavior observed for H<sub>2</sub>/CH<sub>4</sub> selectivity. The decrease in CO<sub>2</sub>/CH<sub>4</sub> selectivity was higher than H<sub>2</sub>/CH<sub>4</sub> selectivity since CO<sub>2</sub> permeability increase is smaller than H<sub>2</sub> permeability with respect to temperature. On the other hand temperature effects the H<sub>2</sub>/CO<sub>2</sub> separation in a different way.

Since  $\text{CO}_2$ , the slower gas is more condensable, its solubility decrease with temperature is more influential than  $\text{H}_2$ . The same observations were also concluded by Rowe et al. [51] and the molecular explanations of these behaviors were reported.

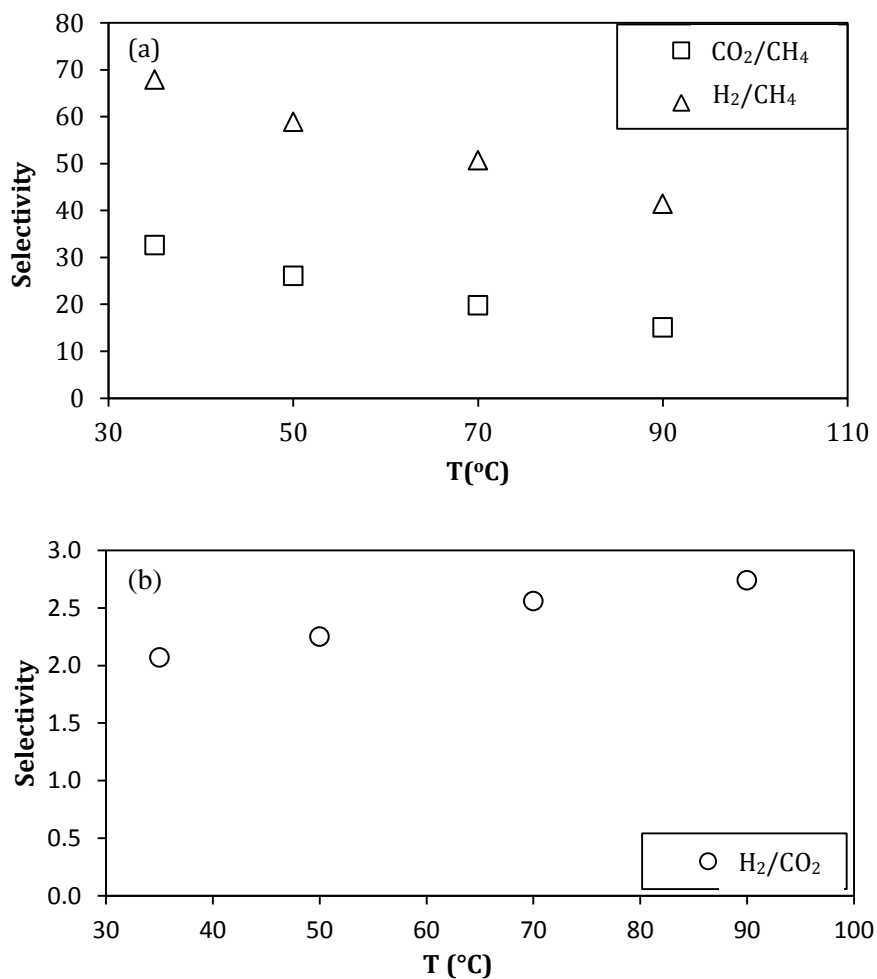


Figure 4.9 Effect of operation temperature on (a)  $\text{CO}_2/\text{CH}_4$  and  $\text{H}_2/\text{CH}_4$ , (b)  $\text{H}_2/\text{CO}_2$  selectivities of PES-n (M6) membrane.

Before investigating the effect of temperature on the performance of PES/HMA membrane, the membrane was post annealed for one month at 120 °C, 0.2 atm. in  $\text{N}_2$  atmosphere to obtain a durable and stable membrane performance. Before testing

the temperature effect, a temperature cycle was applied to same membrane with studied gases and the permeabilities and selectivities were found very close to each other. The results are also tabulated in Appendix D, Table D.9 and D.10. After temperature cycles, effect of operating temperature was investigated in the 35 °C to 120 °C range. The measurements were done by the same systematic with PES membrane. The permeability results are shown in Figure 4.10 and the selectivities are given in Figure 4.11. The similar trends with PES-n membrane observed, permeabilities increased with increasing temperature and the increase in gas permeabilities were again in the same order. However the increase in permeabilities for all gases through PES/HMA-p membrane was higher than PES-n membrane.  $H_2/CO_2$  selectivities increased with increasing temperature and  $CO_2/CH_4$  and  $H_2/CH_4$  selectivities decreased again. The increase in  $H_2/CO_2$  selectivity was also higher than PES membrane. This time again after 90 °C the measurements repeated at 35 °C and it has been observed that the permeabilities nearly stayed constant. After making measurements at 35 °C, it was decided to increase the operation temperature up to 120 °C and the same trend observed but above 120 °C, the membrane deformed and cracks were observed.

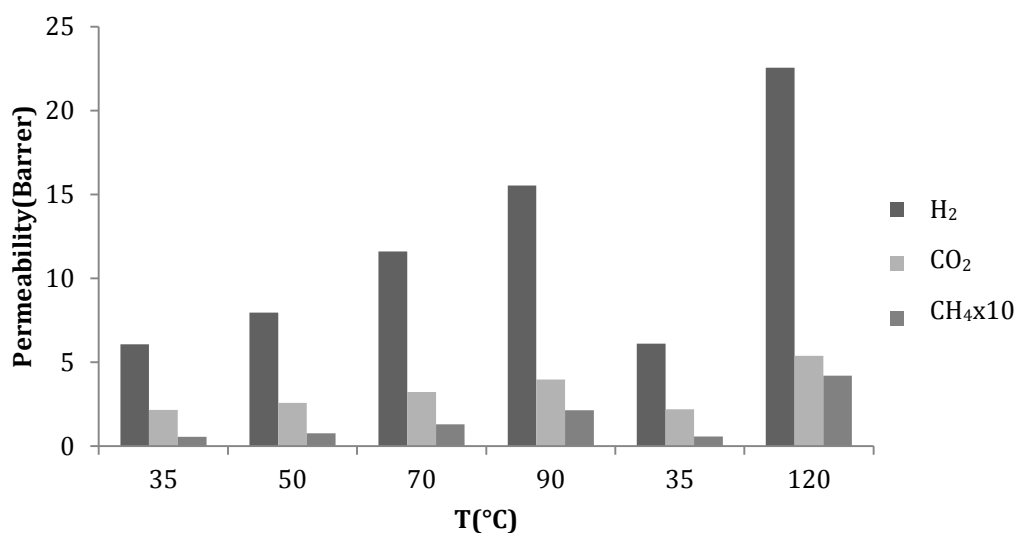


Figure 4.10 Effect of operation temperature on permeabilities of PES/HMA-p (M7) membrane.

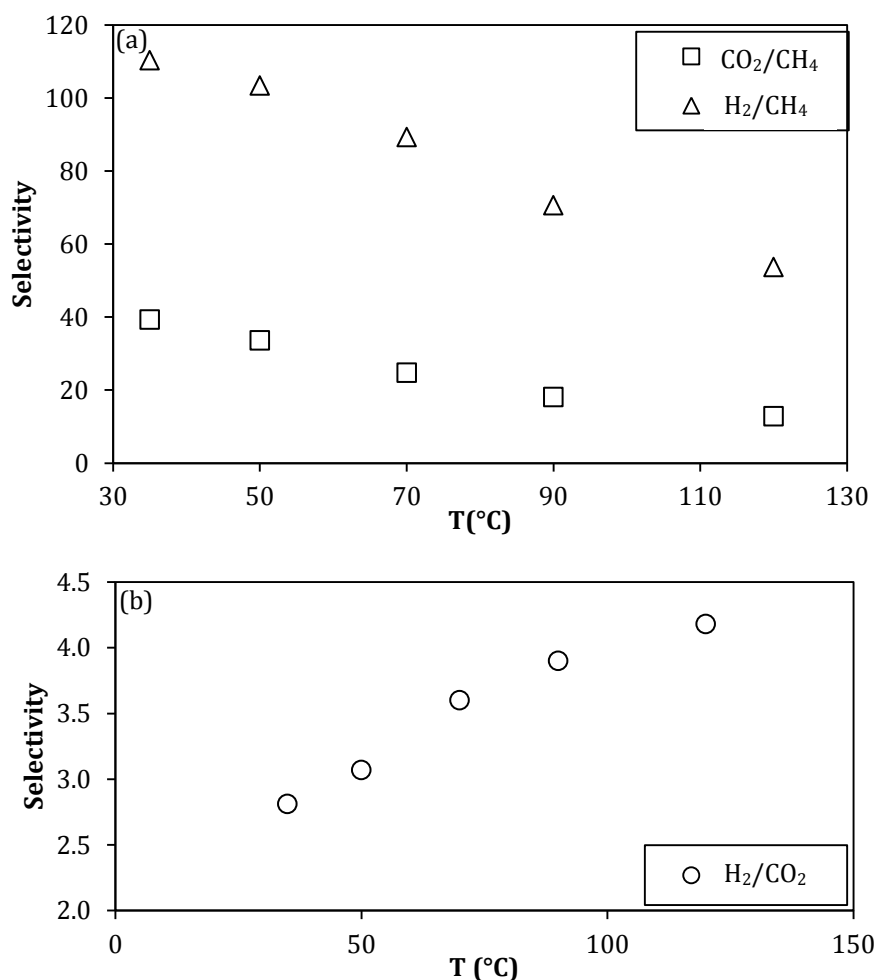


Figure 4.11 Effect of operation temperature on (a)  $\text{CO}_2/\text{CH}_4$  and  $\text{H}_2/\text{CH}_4$ , (b)  $\text{H}_2/\text{CO}_2$  selectivities of PES/HMA-p (M7) membrane.

As mentioned in previous part PES/SAPO-34 membranes were post annealed for 7 days at 120  $^\circ\text{C}$ , 0.2 atm, in  $\text{N}_2$  atmosphere, before measuring single gas permeabilities. The results in Figure 4.12 and Figure 4.13 show that, with increasing temperature, the permeabilities increased but the increases were lower than PES-n and PES/HMA-p membranes.  $\text{H}_2/\text{CO}_2$  selectivity increased with loss of  $\text{CO}_2/\text{CH}_4$  and  $\text{H}_2/\text{CH}_4$  selectivities. The selectivity improvement obtained at 35  $^\circ\text{C}$  observed at each temperature. On the other hand Choi et al. [44] observed that the  $\text{H}_2/\text{CO}_2$  selectivity

improvement obtained at 35 °C with the addition of silicates to PBI polymer could not be achieved at temperatures above 100 °C. At temperatures higher than 100 °C the PBI/ silicalite membrane performances decreased and come close to pure PBI membranes. They relate this behavior to mismatch in transport properties of two phases. However our results showed that the selectivity trends did not change with addition of zeolite particles, so it can be claimed that still diffusion is dominant and there is no mismatch between PES and SAPO-34 particles. Moreover, the decreases in CO<sub>2</sub>/CH<sub>4</sub> and H<sub>2</sub>/CH<sub>4</sub> selectivities were greater and the increase in H<sub>2</sub>/CO<sub>2</sub> selectivity was lower than PES membrane. After 90°C measurements the temperature decreased to 35 °C and single gas permeabilities through this post annealed PES/SAPO-34-p mixed matrix membrane measured and no change in membrane performance observed.

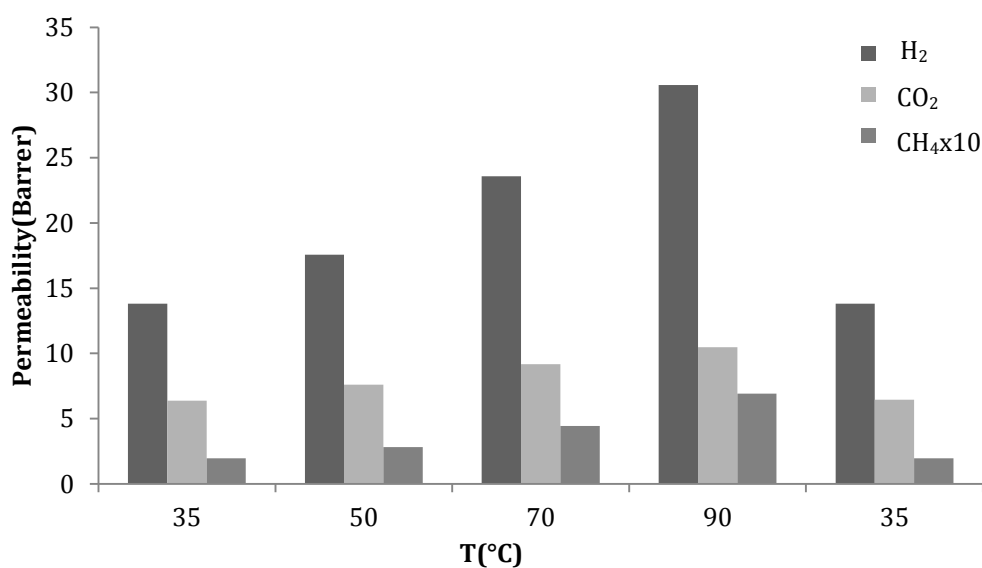


Figure 4.12 Effect of operation temperature on permeabilities of PES/SAPO-34-p (M5) mixed matrix membrane.

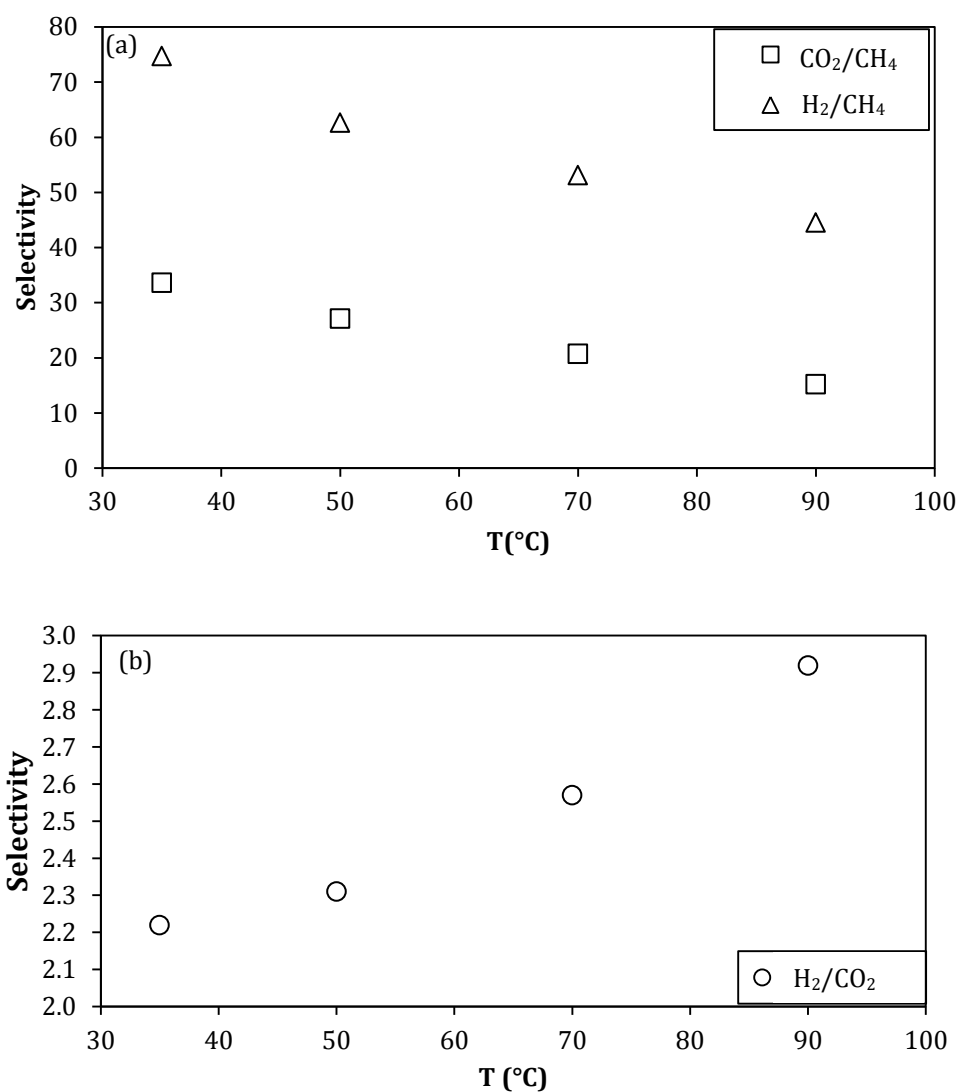


Figure 4.13 Effect of operation temperature on (a) CO<sub>2</sub>/CH<sub>4</sub> and H<sub>2</sub>/CH<sub>4</sub>, (b) H<sub>2</sub>/CO<sub>2</sub> selectivities of PES/SAPO-34-p (M5) mixed matrix membrane.

PES/SAPO/HMA ternary membranes were post annealed for one month to be sure of complete removal of the remaining solvent. The gas permeation experiments between 35 °C – 90 °C were done twice (Table D.13 and D.14) and the average results are plotted in Figure 4.14 and Figure 4.15. As can be seen from Figure 4.14 and 4.15 with increasing temperature a similar trend in permeabilities were obtained. The increases in the gas permeabilities were higher than PES/SAPO-34-p

membranes and close to PES-n membranes.  $H_2/CO_2$  selectivity increase is smaller than PES/HMA-p membrane and close to PES-n membrane. The decreases in  $CO_2/CH_4$  and  $H_2/CH_4$  selectivities were smaller than PES/SAPO-34-p membranes and close to PES-n membrane. After 90°C measurements the temperature is increased slowly to 120 °C and no deformation occurred in the membrane after 120 °C measurement. The ternary membrane could resist up to 120 °C without any deformation. The temperature did not increased to higher temperatures because the single gas permeation set-up was not appropriate for elevated temperatures. After 120 °C again the temperature decreased to 35 °C and it has been observed that after using membrane for 2 month at elevated temperatures, we obtained very similar permeability at 35 °C and the membrane gave reproducible results.

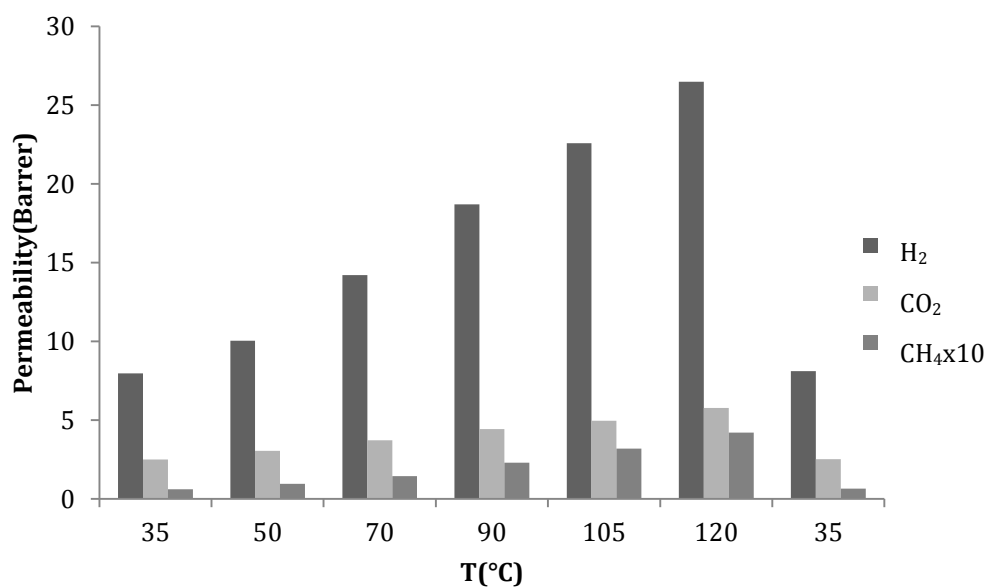


Figure 4.14 Effect of operation temperature on permeabilities of PES/SAPO-34/HMA-p (M8) mixed matrix membrane.



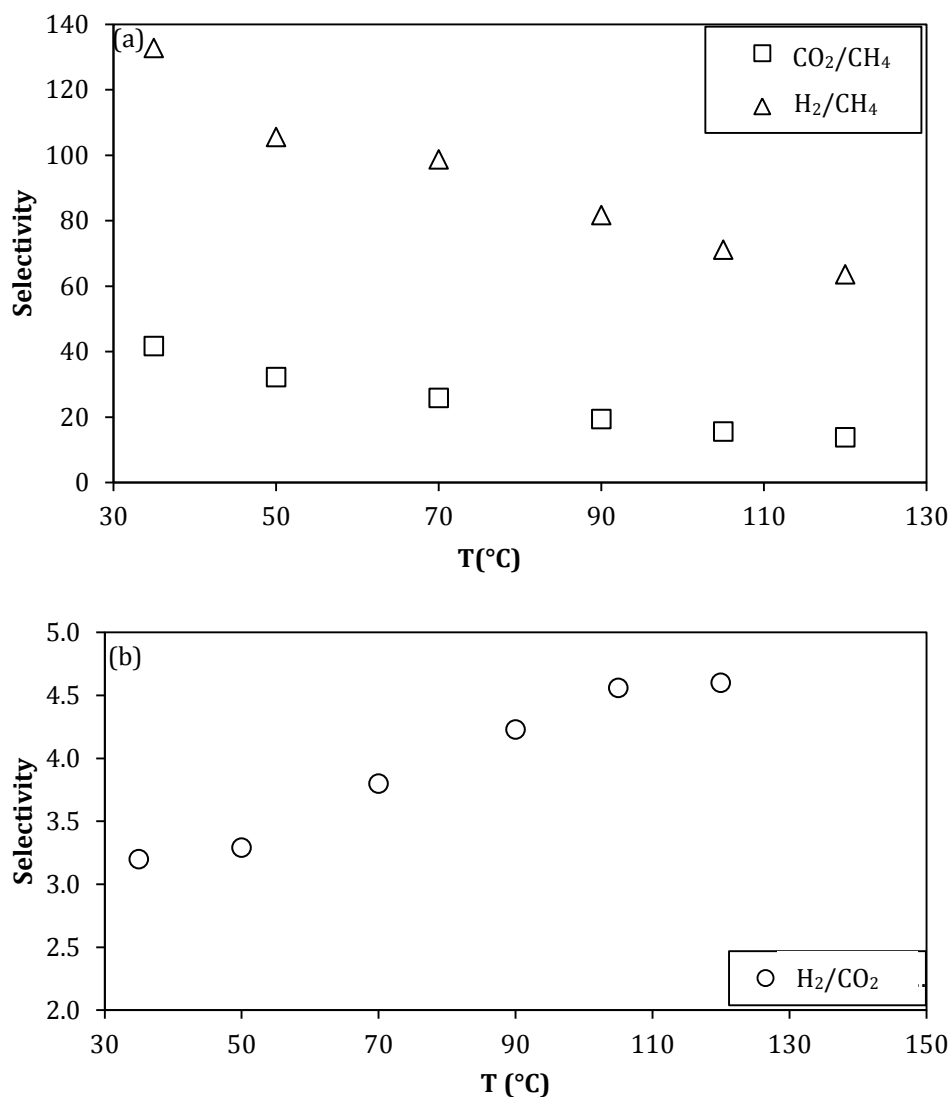


Figure 4.15 Effect of operation temperature on (a)  $\text{CO}_2/\text{CH}_4$  and  $\text{H}_2/\text{CH}_4$ , (b)  $\text{H}_2/\text{CO}_2$  selectivities of PES/SAPO-34/HMA-p (M8) mixed matrix membrane.

Khan et al. [20] also studied with PSf-Ac-Zeolite 3A-APTMS coupling agent incorporated ternary mixed matrix membranes and studied the temperature effect on  $\text{H}_2/\text{CO}_2$  separation. Contrary to our results they observed that the  $\text{H}_2/\text{CO}_2$  selectivity decreases with increasing temperature. It was concluded that the diffusivity increase is more significant for  $\text{CO}_2$  compared to  $\text{H}_2$ . Therefore, the

increase in CO<sub>2</sub> permeability with temperature was higher than increase in H<sub>2</sub> permeability. On the other hand in our case, for PES/SAPO-34/HMA-p membranes as temperature increased from 35 °C to 120°C the selectivity was increased from 3.2 to 4.60, a 44% increase. The diffusivity of the CO<sub>2</sub> is increasing with temperature but the high solubility of the CO<sub>2</sub> gas hinders its permeability from increasing. So it can be concluded that for H<sub>2</sub>/CO<sub>2</sub> separation high temperature operations are more effective.

Rowe et al. [51] studied the temperature effect on the upper bound. They developed a relation to describe the upper bound curve behavior with respect to temperature. By using the data given in that work and using Equation 2.10, the predicted theoretical upper bound curves including the temperature effect for H<sub>2</sub>/ CO<sub>2</sub> and CO<sub>2</sub>/CH<sub>4</sub> gas separation were plotted at studied temperatures. Permeability and selectivity values of PES, PES/HMA, PES/SAPO-34 and PES/SAPO-34/HMA membranes are also given with reference to upper bound curves in Figure 4.16 and Figure 4.17.

For CO<sub>2</sub>/CH<sub>4</sub> gas separation, the performances of our membranes lie below the upper bound curves at each temperature. The upper bound line shifts downward with increasing temperature (Figure 4.16). The performances of our membranes showed similar trend to the predicted upper bound curves indicating the CO<sub>2</sub>/CH<sub>4</sub> selectivity decreased with increasing temperature. The predicted upper bound curve which was obtained by using Equation 2.10 at 35 °C, was compared with the 1991 [4] and 2008 [29] upper bound curves which are plotted from the experimental data obtained at 25°C - 35 °C. The predicted curve fits well with experimental upper bounds.

The membrane performances desired to be above the upper bound line. PES/SAPO-34 membrane performance is close to upper bound curve and the membrane has higher permeability and similar selectivity with PES membrane. This may indicate the existence of voids at the polymer-zeolite interface [10]. Furthermore, the performance of PES/SAPO-34/HMA membrane is also close to the upper bound curve. The membrane performance shifts through the upper bound by adding HMA

which may rigidify the structure. So that selectivity increases but permeability decreases [10]. This rigidification may be due to improved adhesion between polymer and zeolite. So, the ternary mixed matrix membrane is preferable if higher selectivities are desired and binary MMM is preferable if higher permeabilities are desired.

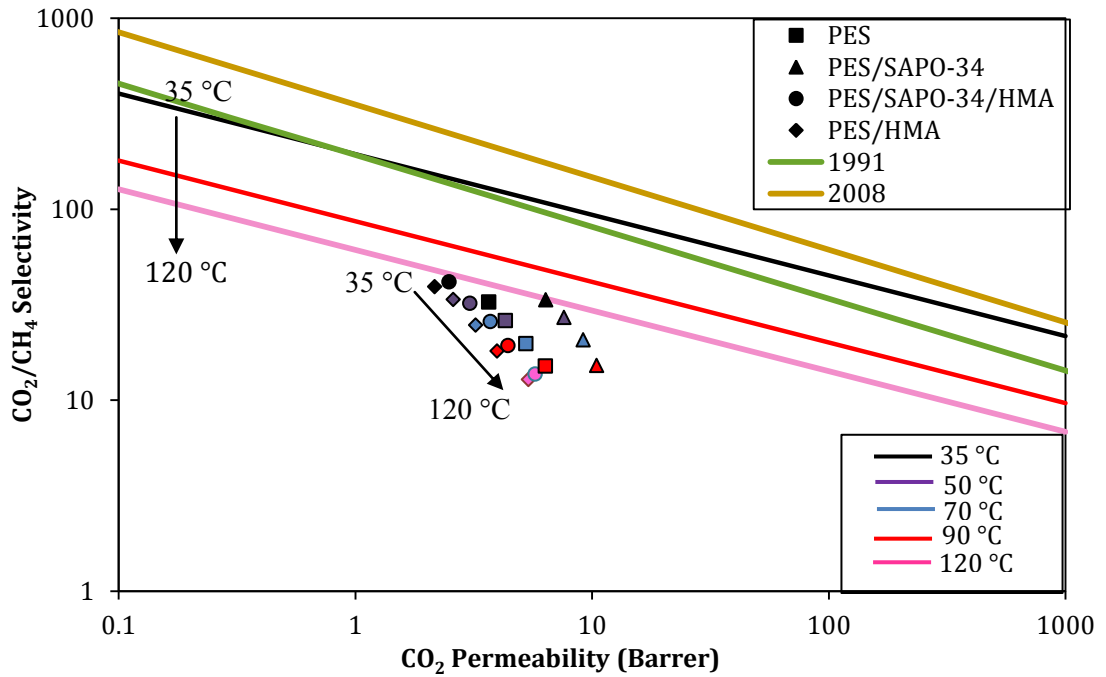


Figure 4.16  $\text{CO}_2/\text{CH}_4$  gas separation performance of membranes on the predicted upper bound curves as a function of temperature.

Figure 4.17 shows that for  $\text{H}_2/\text{CO}_2$  gas pair the upper bound moves upwards with increasing temperature. Also our membrane performances shifts through the right corner of the upper bound curves with increasing temperature which indicates the selectivities increased with temperature. Since there are large differences in condensabilities of  $\text{H}_2$  and  $\text{CO}_2$  gases, the solubility controls the gas separation performance of the membranes.

At each temperature, our membrane performances have gas separation performances above the predicted upper bound curves. In contrast to that, when we compare our membrane performances at 35 °C with the experimental upper bound curves [4,29], we observe that the performances of our membranes lies below the experimental upper bound limits (Figure 4.17). This shows that there is a mismatch between the experimental [4,29] and predicted [51] upper bound curves for H<sub>2</sub>/CO<sub>2</sub> gas separation. The reasons of this mismatch have not been reported yet [51]. However, the trend of the predicted upper bound curve with respect to temperature is in the similar way of our results. Moreover, the similar trends observed when the membrane performances were compared, incorporation of SAPO-34 results in higher permeability while HMA addition results in higher selectivities.

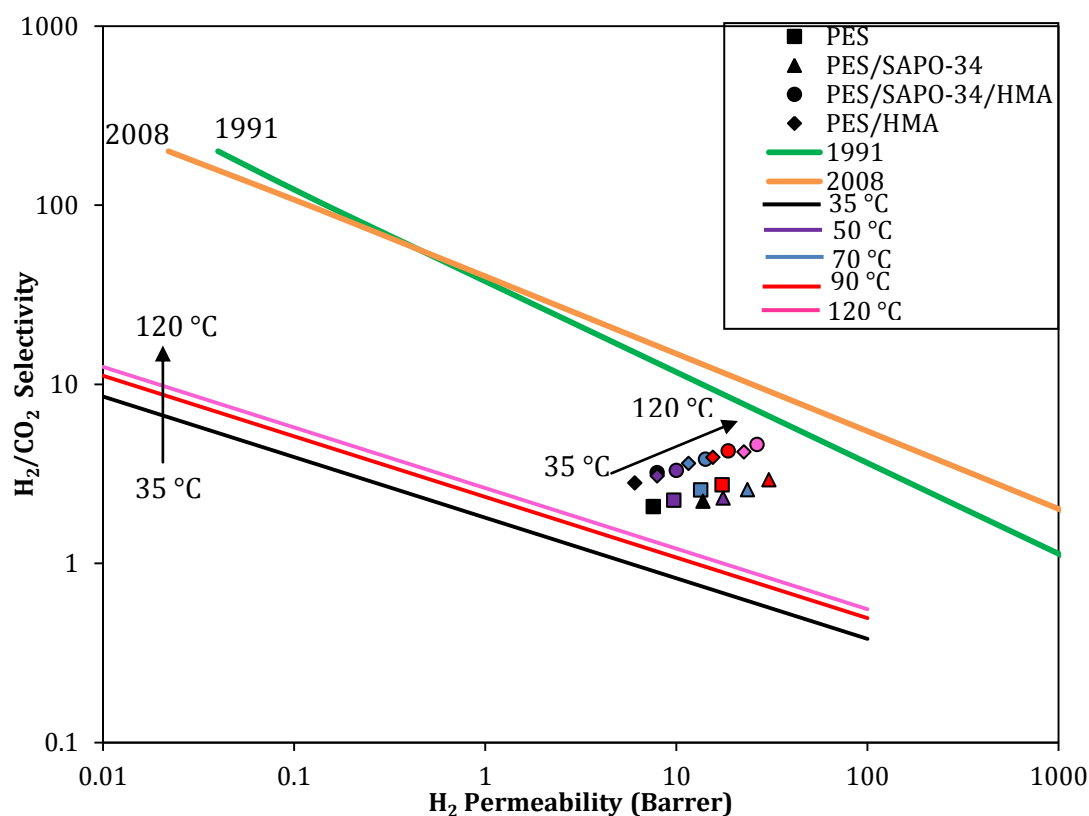


Figure 4.17 H<sub>2</sub>/CO<sub>2</sub> gas separation performance of membranes on the predicted upper bound curves as a function of temperature

#### 4.2.4 Activation Energies of the Membranes

The permeability can be defined in terms of an Arrhenius type equation and the activation energies were calculated from Equation 3.7. As can be seen from Figure 4.18, 4.19 the temperature dependent permeabilities of all gases through all membranes follow the Arrhenius behavior. The activation energy plot of CH<sub>4</sub> gas has the highest slope where CO<sub>2</sub> has the lowest.

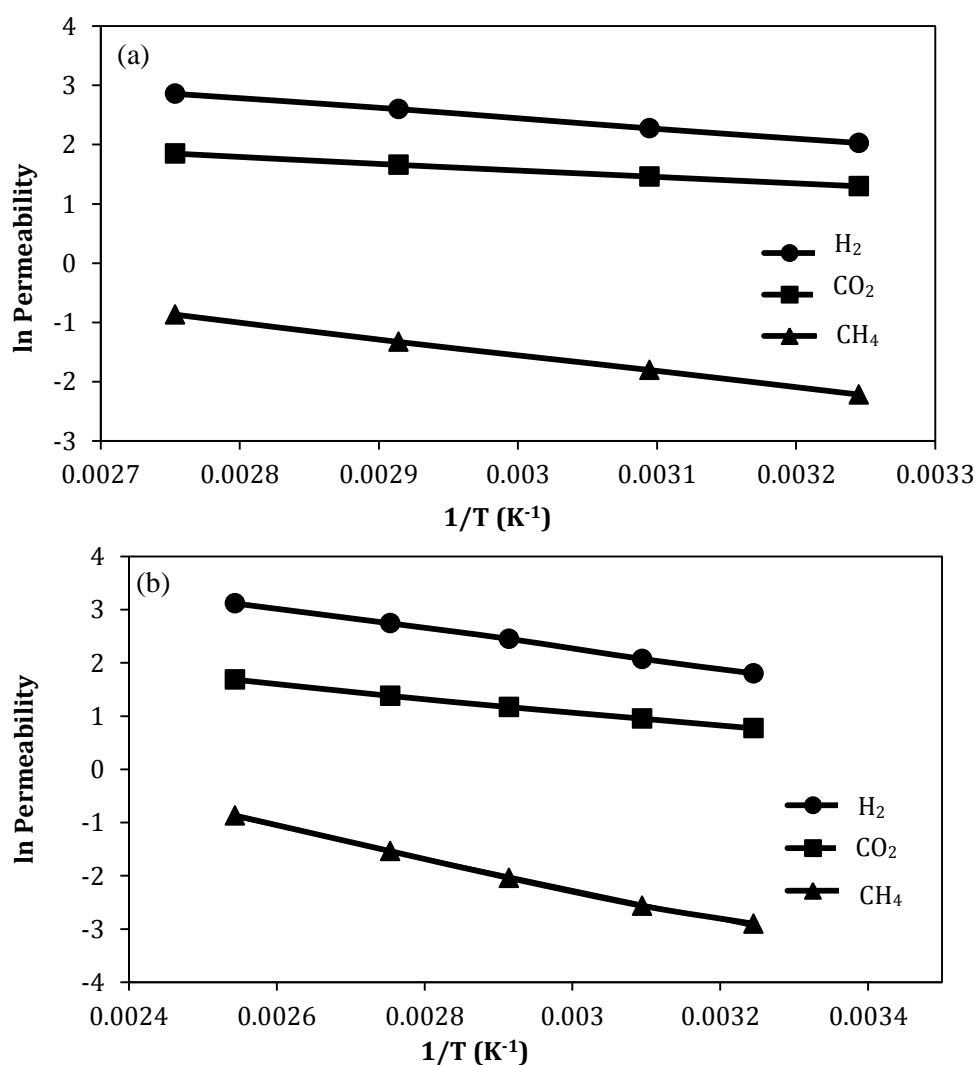


Figure 4.18 Activation energy curves for (a) PES-n (M6), (b) PES/HMA-p(M7) membranes.

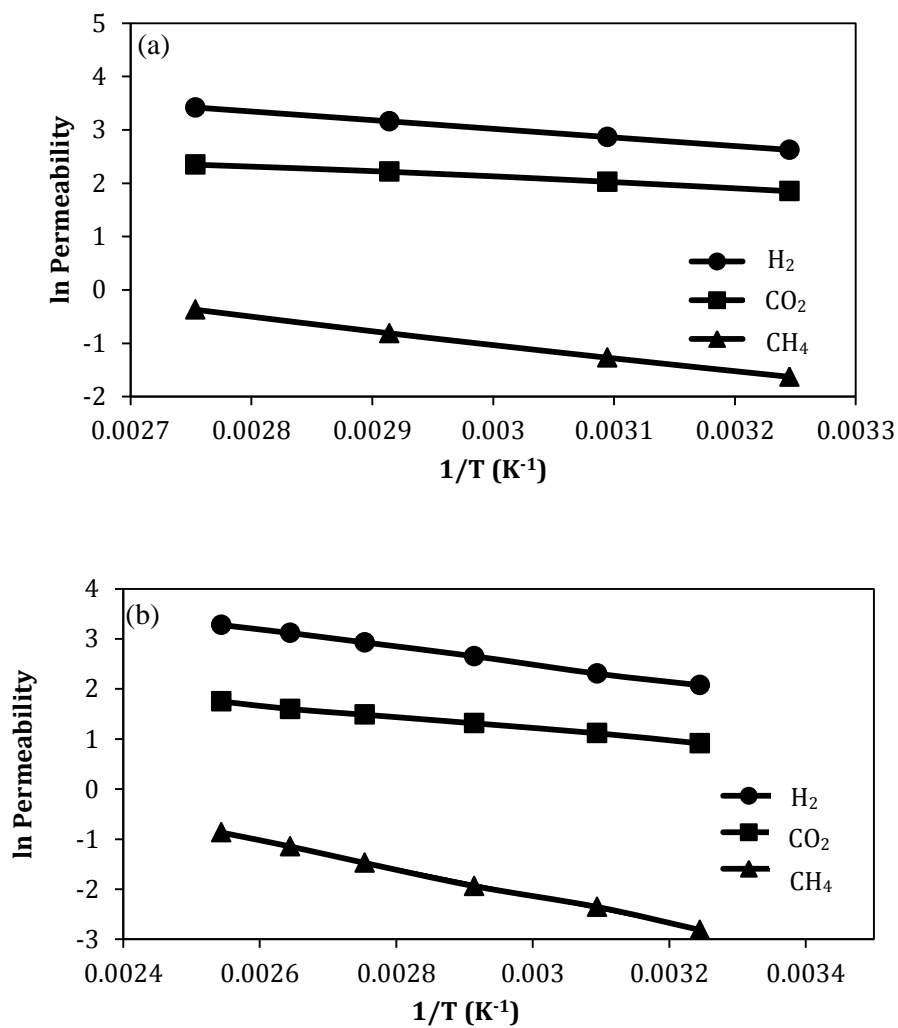


Figure 4.19 Activation Energy curves for (a) PES/SAPO-34-p (M5), (b) PES/SAPO-34/HMA-p (M8) membranes.

Table 4.10 Activation energies of membranes.

	Activation Energies, $E_a$ (kJ/mole)			
	PES-n (M6)	PES/SAPO-34-p (M5)	PES/SAPO-34/HMA-p (M8)	PES/HMA-p (M7)
$H_2$	14.1	13.4	14.5	15.7
$CO_2$	9.30	8.42	9.62	10.7
$CH_4$	22.7	21.3	22.8	24.3

The activation energies are calculated and tabulated in Table 4.10. For PES membrane the highest activation energy belongs to CH<sub>4</sub> gas, which has the largest kinetic diameter. CH<sub>4</sub> has the largest kinetic diameter and it is exposed to highest resistance to make diffusive jumps at 35 °C as a result as temperature is increasing CH<sub>4</sub> permeability affected much from the motions in the membrane structure. However, the lowest activation energy does not belong to H<sub>2</sub>, it belongs to CO<sub>2</sub> gas which is the most condensable gas. CO<sub>2</sub> is the most soluble gas and it is known that solubility decreases with temperature so CO<sub>2</sub> permeability increases less than other gases studied [21, 51]. The activation energy order is CH<sub>4</sub>> H<sub>2</sub>> CO<sub>2</sub>. This trend in activation energy also explains the selectivity trends. In a gas mixture when preferentially permeated molecule has higher activation energy than the others the selectivity increases. The activation energies of PES membrane is found consistent with literature. In literature activation energies of PES membranes were evaluated. Wang et al. reported activation energy of pure PES membrane for H<sub>2</sub> as 16.97 kJ/mole and for CO<sub>2</sub> as 12.67 kJ/mole which is close to our values and follow the same trend. Vijay et al. studied the effect of temperature on PES membrane and calculated the activation energies of H<sub>2</sub> and CO<sub>2</sub> gases. Their activation energies are lower; for H<sub>2</sub> 7.91 kJ/mole, for CO<sub>2</sub> 7.72 kJ/mole and they relate these decrease to structural properties of the membrane [65].

The activation energy of PES/HMA membrane is higher than PES membrane but the E<sub>a</sub> order is the same. Since the HMA particles act as antiplasticizer, they increased the resistance to make active jumps and hence increased the activation energies. PES/SAPO-34 membrane has lowest activation energies in the same trend with PES membranes. With the addition of SAPO-34 particles in PES membranes the activation energies slightly dropped. The decrease in activation energy is more significant for CO<sub>2</sub> than other gases due to strong affinity of CO<sub>2</sub> to SAPO-34 particles. Clarizia et al.[14] showed that the addition silicalite particles in PDMS lowers the activation energies especially for CO<sub>2</sub> which has the highest affinity to NaA and activation energy of CO<sub>2</sub> increases with addition of NaX particles to PDMS membranes. It is concluded that the filler type effect the permeation rate of the gases with temperature. The decrease in activation energies can be due to weak interaction between PES and SAPO-34 particles which enables the penetrant

molecules to permeate more easily. Addition of HMA to PES/SAPO-34 mixed matrix membrane increased the activation energies and the activation energies come close to pure polymeric membrane.



## CHAPTER 5

### CONCLUSIONS

The temperature dependent gas transport properties of mixed matrix membranes that consist of polyethersulfone (PES) as continuous phase, SAPO-34 particles as dispersed phase and HMA as compatibilizer, were investigated in this study. The following conclusions are drawn:

1. Annealing has great influence especially on mixed matrix membranes. More stable performances obtained from membranes which are post annealed before used.
2. As temperature is increased the permeabilities of  $H_2$ ,  $CO_2$  and  $CH_4$  gas increased for all membrane types. The  $H_2/CO_2$  selectivity increased where  $CO_2/CH_4$  and  $H_2/CH_4$  selectivity decreased.
3. For  $H_2/CO_2$  it would be more advantageous to operate at high temperatures since both permeability and selectivity is improved
4. PES/SAPO-34/HMA membrane has higher separation performance at each temperature and can resist up to 120 °C without any changes in gas separation performance.
5. Highest activation energy belongs to PES/HMA membrane and lowest belongs to PES/SAPO-34 membrane. And in each membrane type lowest activation energy belongs to  $CO_2$  and highest belongs to  $CH_4$ .

## REFERENCES

- [1] Mulder, M., "Basic Principles of Membrane Technology", Kluwer Academic Publishers, Second edition, 1997, Dordrecht.
- [2] Yi, L., "Development of Mixed Matrix Membranes for Gas Separation Application", PhD Thesis, Chemical and Biomolecular Engineering Department, National University of Singapore, 2006, China.
- [3] Scott, K., "Handbook of industrial membranes", Elsevier Advanced Technology, 1997, Oxford.
- [4] Robeson, L.M., "Correlation of separation factor versus permeability for polymeric membranes", Journal of Membrane Science, 62, 1991, p. 165-185.
- [5] Freeman, B.D., "Basis of permeability/selectivity tradeoff relations in polymeric gas separation membranes, Macromolecules", 32, 1999, p.375-380.
- [6] Budd, P., McKeown, N., "Highly permeable polymers for gas separation membranes", Polymer Chemistry, 1, 2010, p.63-68.
- [7] Moore, T.T., Mahajan R., Vu, D.Q., Koros, W.J., "Hybrid membrane materials comprising organic polymers with rigid dispersed phases", AIChE J., 50, 2004, p.311-321.
- [8] Chung, T.S., Jiang, L.Y., Li, Y., Kulprathipanja, S., "Mixed matrix membranes (MMMs) comprising organic polymers with dispersed inorganic fillers for gas separation", Prog. Polym. Sci. 32, 2007, p. 483-507.
- [9] Duval, J. M., Kemperman, A. J. B., Folkers, B., Mulder, M. H. V., Desgrandchamps, G., Smolders, C. A., "Preparation of zeolite filled glassy polymer membranes", Journal of Applied Polymer Science, 54, 1994, p.409-418.
- [10] Koros, W. J., Mahajan, R., "Mixed matrix membrane materials with glassy polymers. Part 1". Polym. Eng. Sci., 42, 2002, p.1420-1431.

- [11] Süer, M.G., Baç, N., Yılmaz, L., "Gas permeation characteristics of polymer-zeolite mixed matrix membranes", *Journal of Membrane Science*, 91, 1994, p. 77-86.
- [12] Moore, T.T., Koros, W. J. , "Non-ideal effects in organic-inorganic materials for gas separation membranes", *J. Mol. Struct.*, 739, 2005, p.87-98.
- [13] Hillock, A. M. W., Miller, S. J., Koros, W. J., "Cross-linked mixed matrix membranes for the purification of natural gas: Effects of sieve surface modification", *Journal of Membrane Science*, 314, 2008, p.193-199.
- [14] Algeria, F.C., Drioli, E., Clarizia, G., "Filler-polymer combination: a route to modify gas transport properties of a polymeric membrane" *Polymer*, 45, 2004, p. 5671-5681.
- [15] Y. Li, T. S. Chung, C. Cao, S. Kulprathipanja, "The effects of polymer chain rigidification, zeolite pore size and pore blockage on polyethersulfone (PES)-zeolite A mixed matrix membranes", *Journal of Membrane Science*, 260, 2005, p.45- 55.
- [16] Çakal, U., "Natural Gas Purification by zeolite filled polyethersulfone based mixed matrix membranes", MSc Thesis, Middle East Technical University, 2009.
- [17] Şen, D., Kalıpçılar, H., Yılmaz, L., "Development of polycarbonate based zeolite 4A filled mixed matrix gas separation membranes", *Journal of Membrane Science*, 303, 2007, p. 194-203.
- [18] Karatay, E., Kalıpçılar, H., Yılmaz, L., " Preparation and performance assessment of binary and ternary PES-SAPO 34-HMA based gas separation membranes", *Journal of Membrane Science*, 364, 2010, p. 75-81.
- [19] Karatay, E., "Effect of Preparation and Operation Parameters on Performance of Polyethersulfone Based Mixed Matrix Gas Separation Membranes", MSc Thesis, Middle East Technical University, 2009.
- [20] Khan, A.L., Cano-Odena, A., Gutierrez, B., Minguillon, C., Vankelecom, F.J., "Hydrogen separation and purification using polysulfone acrylate-zeolite mixed matrix membranes", *Journal of Membrane Science*, 350, 2010, p.340-346.
- [21] Costello, L.M. , Koros, W.J., "Effect of Structure on the Temperature Dependence of Gas Transport and Sorption in a Series of Polycarbonates", *Journal of Polymer Science*, 32, 1994, p.701-713.

- [22] Moore, T.T., Damle, S., Wallace, D., Koros, W.J., "The Engineering Handbook", 2<sup>nd</sup> edition, CRC Press LLC, 2005.
- [23] W.J. Koros, R. Mahajan , "Pushing the limits on possibilities for large scale gas separation: which strategies?", Journal of Membrane Science, 175, 2000, p.181–196.
- [24] Baker, W.R., "Future Directions of Membrane Gas Separation Technology", Ind. Eng. Chem. Res., 41(6), 2002, p.1393-1411.
- [25] Costello, L.M., Koros, W.J., "Temperature dependence of gas sorption and transport properties in polymers: measurement and applications" Ind. Eng. Chem. Res., 31 (12), 1992, p.2708-2714.
- [26] Staudt-Bickel, C., Koros, W.J., "Improvement of CO<sub>2</sub>/CH<sub>4</sub> separation characteristics of polyimides by chemical crosslinking", Journal of Membrane Science, 155, 1999, p.145-154.
- [27] Moore, T.T., "Effects of Materials, Processing, And Operating Conditions On The Morphology And Gas Transport Properties Of Mixed Matrix Membranes", PhD Thesis, The University of Texas, December 2004.
- [28] Tremblay, P., Vermette, J., Savard, M.M., "Gas permeability, diffusivity and solubility of nitrogen, helium, methane, carbon dioxide and formaldehyde in dense polymeric membranes using a new on-line permeation apparatus" Journal of Membrane Science, 282, 2006, p.245–256.
- [29] Robeson, L.M., "The upper bound revisited", Journal of Membrane Science, 320, 2008, p.390–400.
- [30] Vu, D.Q., Koros, W.J., Miller, S.J., "Mixed matrix membranes using carbon molecular sieves, I. Preparation and experimental results", Journal of Membrane Science, 211, 2003, p.311– 334.
- [31] Vu, D.Q., Koros, W.J., Miller, S.J., "Mixed matrix membranes using carbon molecular sieves, II. Modeling permeation behavior", Journal of Membrane Science, 211, 2003, p.335–348.
- [32] Bernardo, A.P., Drioli, E., Golemme, G., "Membrane Gas Separation: A Review/State of the Art" Ind. Eng. Chem. Res., Vol. 48, No. 10, 2009

- [33] Duval, J. M., Folkers, B., Mulder, M. H. V., Desgrandchamps, G., Smolders, C. A., "Adsorbent-filled membranes for gas separation. Part 1. Improvement of the gas separation properties of polymeric membranes by incorporation of microporous adsorbents.", *Journal of Membrane Science*, 1993, 80, p.189-198.
- [34] Jha, P., Way, J.D., "Carbon dioxide selective mixed-matrix membranes formulation and characterization using rubbery substituted polyphosphazene", *Journal of Membrane Science*, 324, 2008, p. 151-161.
- [35] Hillock, A.M.W., "Crosslinkable Polyimide Mixed Matrix Membranes for Natural Gas Purification", PhD Thesis, Georgia Institute of Technology, December 2005.
- [36] Mahajan, R., Burns, R., Schaeffer, M., Koros, W.J., "Challenges in forming successful mixed matrix membranes with rigid polymeric materials", *Journal of Applied Polymer Science*, 86, 2002, p. 881-890.
- [37] Yong, H.H., Park, H.C., Kang, Y.S., Won, J., Kim, W.N., "Zeolite-filled polyimide membrane containing 2,4,6-triaminopyrimidine", *Journal of Membrane Science*, 188, 2001, p. 151-163.
- [38] Mahajan, R., Koros, W.J., "Mixed matrix membrane materials with glassy polymers. Part 2", *Polymer Engineering and Science*, 42, 2002, p. 1432-1441.
- [39] A.F. Ismail, T.D. Kusworo, A. Mustafa, "Enhanced gas permeation performance of polyethersulfone mixed matrix hollow fiber membranes using novel Dynasylan Amino silane agent", *J. Membr. Sci.*, 319, 2008, p.306-312.
- [40] Huang, Z., Li, Y., Wen, R., Teoh, M.M., Kulprathipanja, S., "Enhanced gas separation properties by using nanostructured PES-zeolite 4A mixed matrix membranes", *Journal of Applied Polymer Science*, 101, 2006, p. 3800-3805.
- [41] Ismail, A.F., Rahim, R.A., Rahman, W.A.W.A., "Characterization of polyethersulfone/Matrimid 5218 miscible blend mixed matrix membranes for O<sub>2</sub>/N<sub>2</sub> gas separation", *Separation and Purification Technology*, 63, 2008, p. 200-206.
- [42] Aroon, M., Ismail, A.F., Matsuura, T., Montazer-Rahmati, M.M., "Performance studies of mixed matrix membranes for gas separation: A review", *Separation and Purification Technology* 75, 2010, p. 229-242

- [43] Rajinder Pal, "Permeation models for mixed matrix membranes" , Journal of Colloid and Interface Science, 317, 2008, p.191–198
- [44] Choi, S., Coronas, J., Lai, Z., Yust, D., Onorato, F., Tsapatsis, M., "Fabrication and gas separation properties of polybenzimidazole (PBI)/nanoporous silicates hybrid membranes", Journal of Membrane Science, 316, 2008, p.145–152.
- [45] Hacarlioglu, P., Toppare, L., Yilmaz, L., "Effect of preparation parameters on performance of dense homogenous polycarbonate gas separation membranes", Journal of Applied Polymer Science, 90, 2002, p. 776-785.
- [46] Fu, Y.J., Hu, C.C., Qui, H., Lee, K.R., Lai, J.Y., "Effects of residual solvent on gas separation properties of polyimide membranes", Separation and Purification Technology, 62, 1, 2008, p.175-182.
- [47] Joly, C., Cerf, D., Chappay, C., Langevin, D., Muller, G., "Residual solvent effect on the permeation properties of fluorinated polyimide films", Separation and Purification Technology, 16, 1999, p.47–54.
- [48] Shen, Y., Lua, A.C., "Effects of Membrane Thickness and Heat Treatment on the Gas Transport Properties of Membranes Based on P84 Polyimide", Journal of Applied Polymer Science, 116, 2010, p.2906–2912
- [49] Moe, M., Koros, W.J., Hoehn, H.H., Husk, G.R., "Effects of film history on gas transport in a fluorinated aromatic polyimide", Journal of Applied Polymer Science, 36, 1988, p. 1833-1846.
- [50] Hibshman, C., Cornelius, C.J., Marand, E., "The gas separation effects of annealing polyimide–organosilicate hybrid membranes", Journal of Membrane Science, 211, 2003, p. 25–40.
- [51] Rowe, B.W., Robeson, L.M., Freeman, B.D., Paul, D.R., "Influence of temperature on the upper bound: Theoretical considerations and comparison with experimental results" Journal of Membrane Science, 360, 2010, p.58–69.
- [52] Lin H., Freeman B.D., "Gas solubility, diffusivity and permeability in poly(ethylene oxide)", Journal of Membrane Science, 239, 2004, p.105– 117.

- [53] Chung, T.S., Lin, W.H., "Gas permeability, diffusivity, solubility, and aging characteristics of 6FDA-durene polyimide membranes", *Journal of Membrane Science* 186, 2001, p.183–193.
- [54] Wang, D., Li, K., Teo, W.K., "Gas Permselection Properties in Silicone-Coated Asymmetric Polyethersulfone Membranes" *Journal of Applied Polymer Science*, 66, 1997, p.837–846.
- [55] Açıklın S., "Effect of Temperature on Gas Permeation Properties of Polymeric Membranes", MSc Thesis, Middle East Technical University, 1996.
- [56] Açıklın, S., Yılmaz, L., "Effect of Temperature and Membrane Preparation Parameters on Gas Permeation Properties of Polymetacrylates", *Journal of Polymer Science*, 45, 2007, p. 3025-3033.
- [57] Poshusta, J.C., Tuan, V.A., Falconer, J.L., Noble, R.D., "Synthesis and Permeation Properties of SAPO-34 Tubular Membranes", *Journal of Industrial Chemical Engineering*, 37, 1998, p.3924-3929.
- [58] Poshusta, J.C., Noble, R.D., Falconer, J.L., "Temperature and pressure effects on CO<sub>2</sub> and CH<sub>4</sub> permeation through MFI zeolite membranes", *Journal of Membrane Science*, 160, 1999, p.115-125.
- [59] Şen, D., Kalıpçılar, H., Yılmaz, L., "Gas separation performance of Polycarbonate membranes modified with multifunctional low molecular-weight additives", *Separation Science and Technology*, 41, 2006, p.1813-1828.
- [60] Radel Resins Design Guide, Solvay Advanced Polymers, L.L.C., 2004.
- [61] Ruiz-Treviño, F.A., Paul, D.R., "Gas permselectivity properties of high free volume polymers modified by a low molecular weight additive", *Journal of Applied Polymer Science*, 68, 1998, p. 403-415.
- [62] Battal, T., Baç, N., Yılmaz, L., "Effect of feed composition on the performance of polymer-zeolite mixed matrix gas separation membranes", *Separation Science and Technology*, 30, 1995, p. 2365-2384.
- [63] Chang, K. S., Hsiung, C. C., Lin, C. C., Tung, K. L., "Residual Solvent Effects on Free Volume and Performance of Fluorinated Polyimide Membranes: A Molecular Simulation Study", *Journal of Physical Chemistry*, 113, 2009, p. 10159–10169.

[64] Woo, M., Choi, J., Tsapatsis, M., "Poly(1-trimethylsilyl-1-1 propyne)/MFI composite membranes for butane separation", Microporous and Mesoporous Materials, 110, 2008, p.330-338.

[65] Kulshrestha, V., Awasthi, K., Acharya, N. K., Singh, M., Vijay, Y.K., "Effect of temperature and  $\alpha$ -irradiation on gas permeability for polymeric membrane" Bulletin of Materials Science, 28, 7, 2005, p.643-646.



## **APPENDIX A**

### **SINGLE GAS PERMEABILITY CALCULATIONS**

The pressure rise at the permeate side versus permeation time data are recorded by computer at certain time periods (10 seconds). From the slope of the permeate pressure versus time graphs the permeabilities were calculated as shown in Figure A.1.

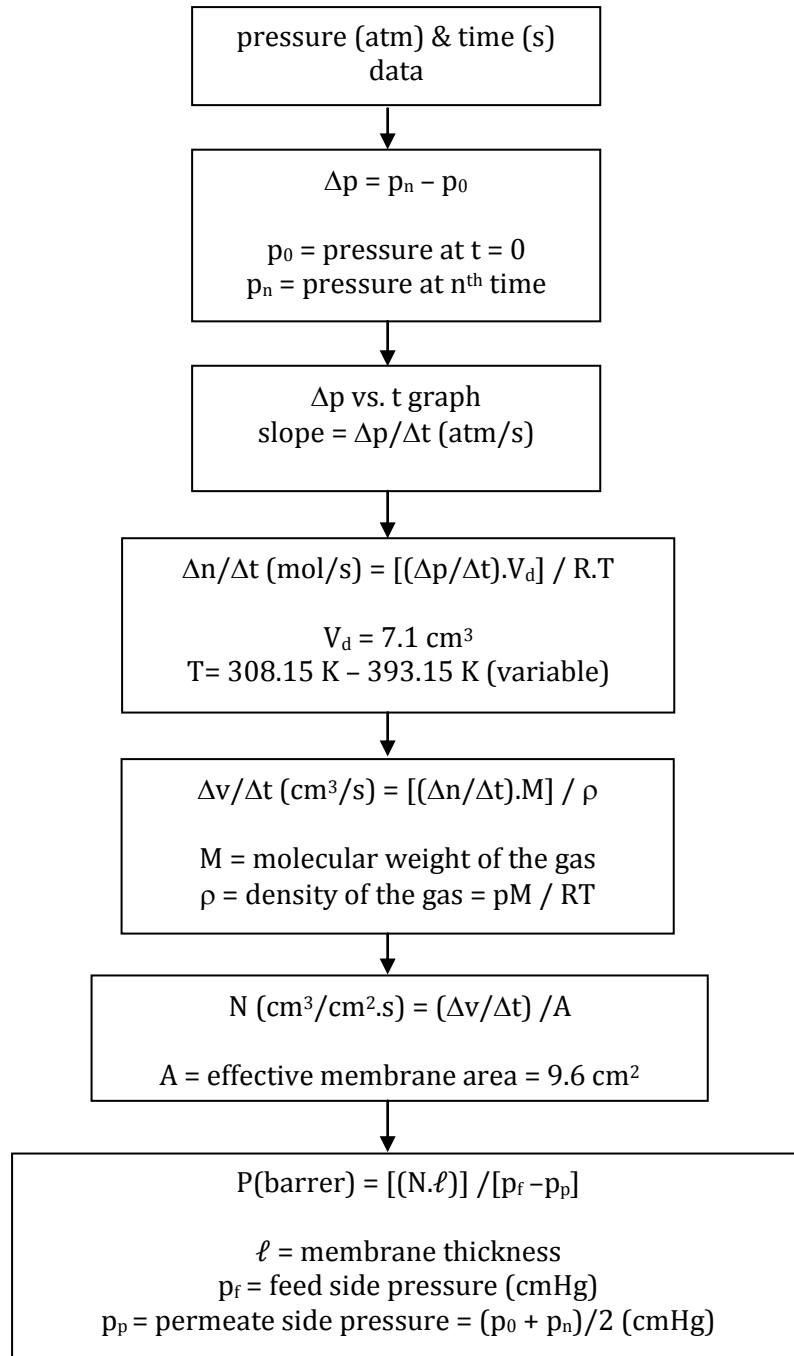


Figure A.1 Single gas permeability calculation.

## APPENDIX B

### DSC THERMOGRAMS

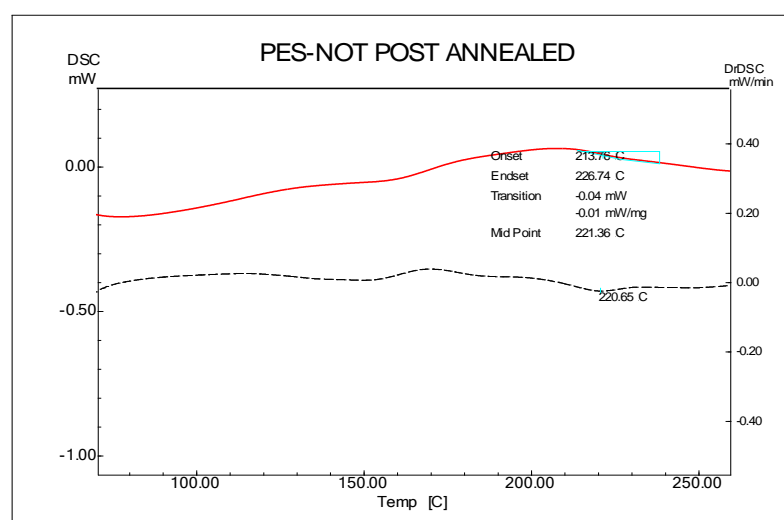


Figure B.1 DSC Thermogram for PES-n membrane

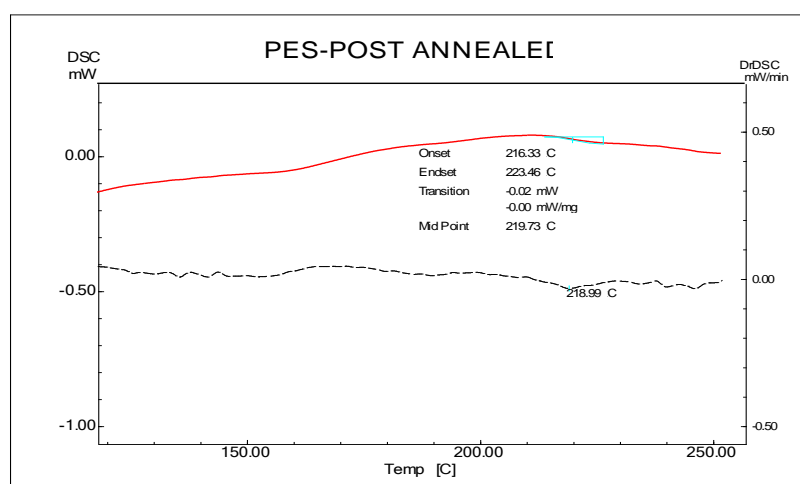


Figure B.2 DSC Thermogram for PES-p membrane

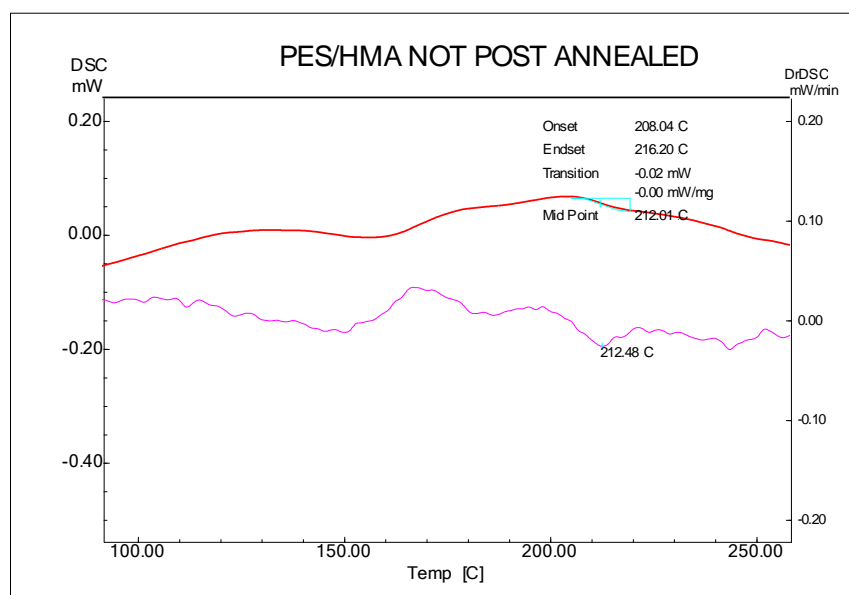


Figure B.3 DSC Thermogram for PES/HMA-n membrane

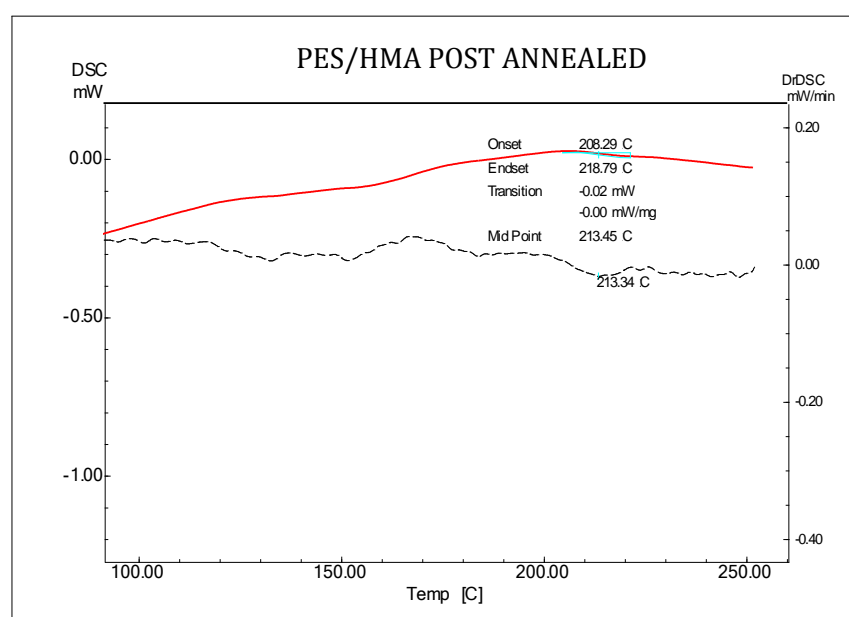


Figure B.4 DSC Thermogram for PES/HMA-p membrane

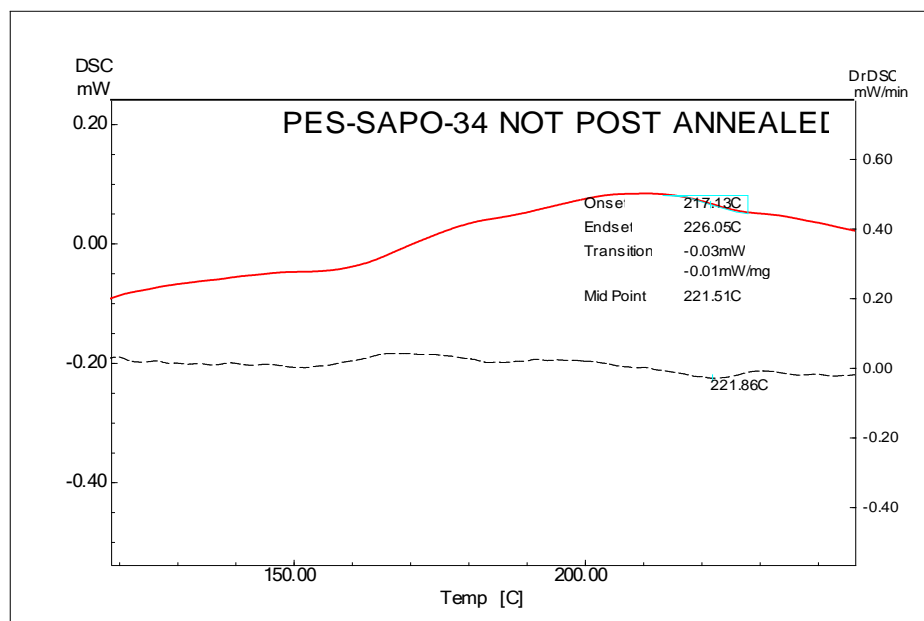


Figure B.5 DSC Thermogram for PES/SAPO-34-n membrane.

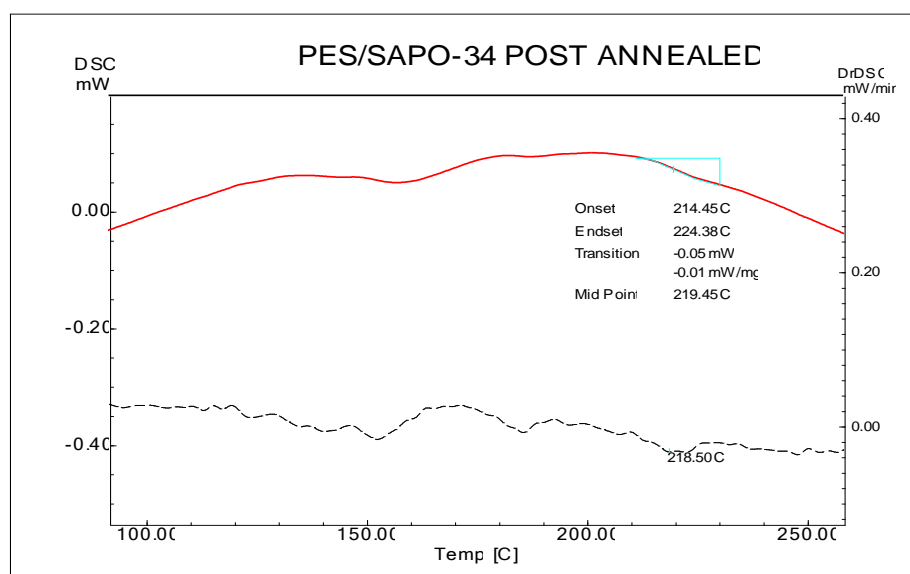


Figure B.6 DSC Thermogram for PES/SAPO-34-p membrane.

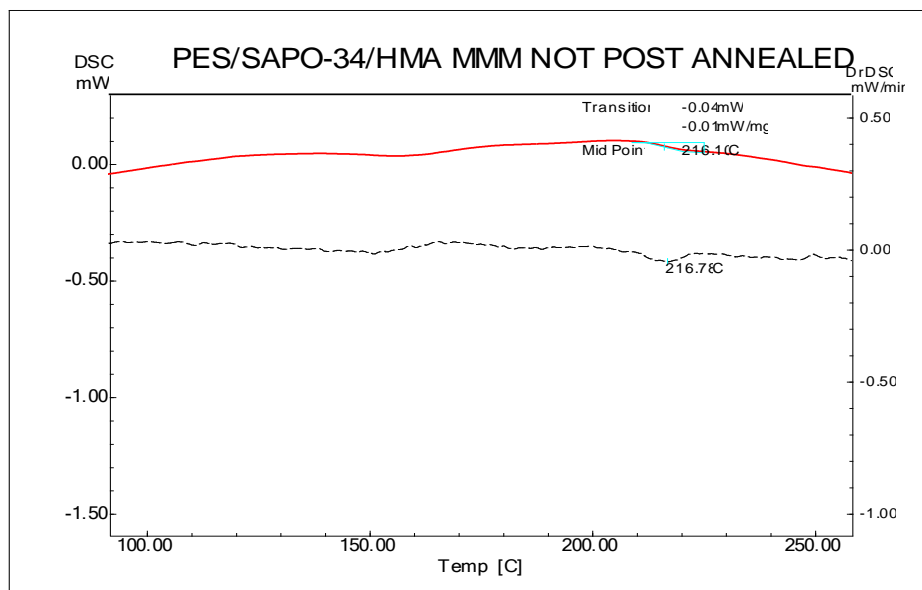


Figure B.7 DSC Thermogram for PES/SAPO-34/HMA-n membrane.

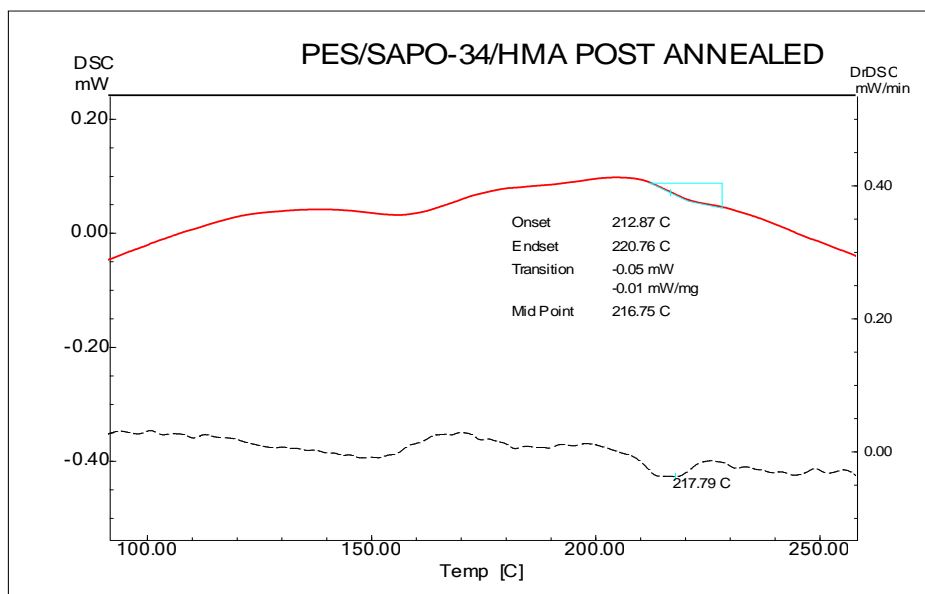


Figure B.8 DSC Thermogram for PES/SAPO-34/HMA-p membrane.

## APPENDIX C

### TGA THERMOGRAMS

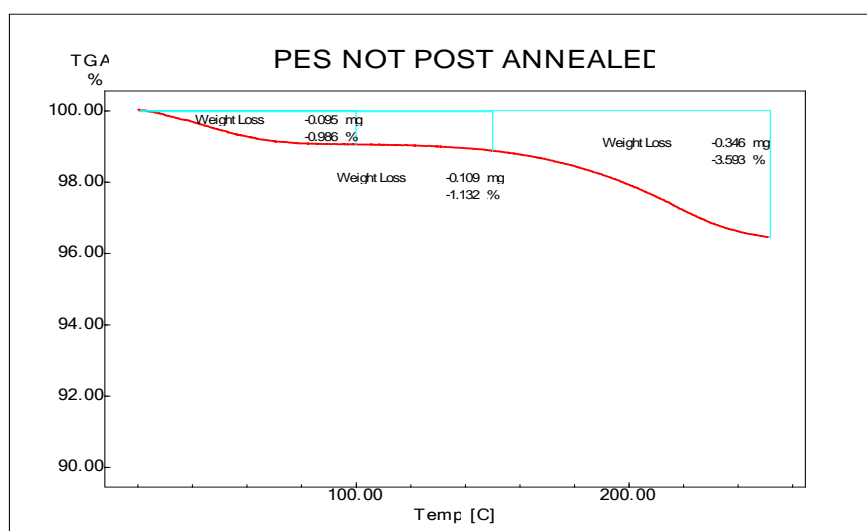


Figure C.1 TGA Thermogram for PES-n membrane.

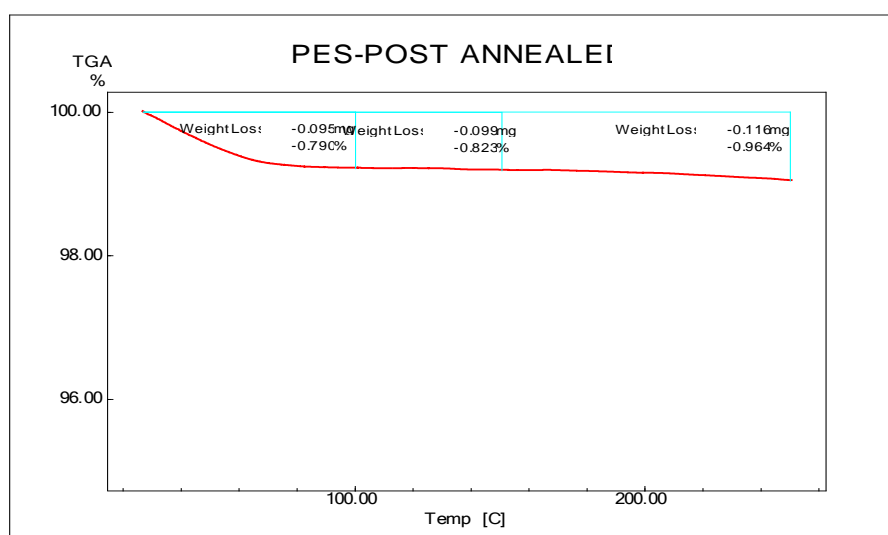


Figure C.2 TGA Thermogram for PES-p membrane.

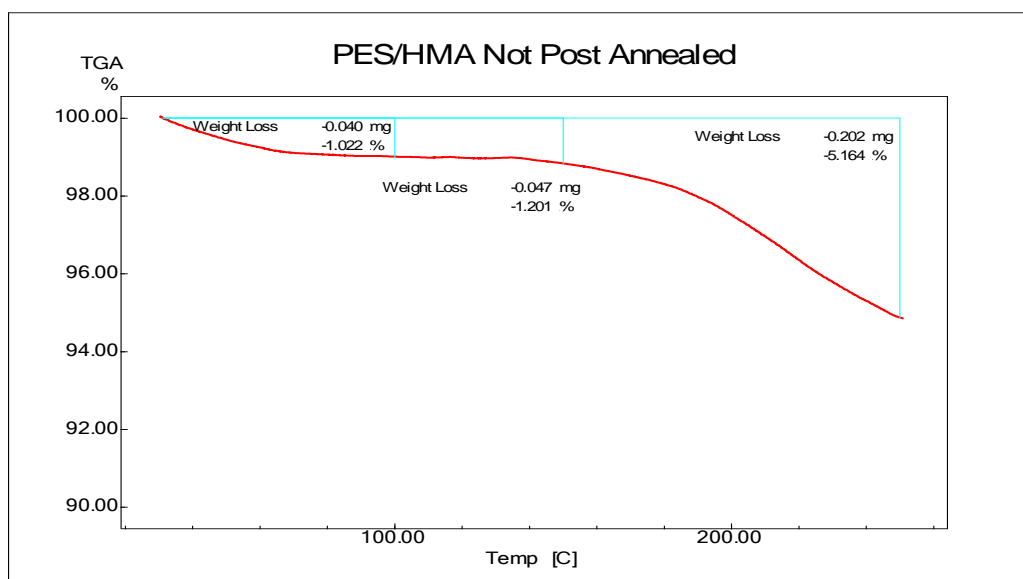


Figure C.3 TGA thermogram for PES/HMA-n membrane.

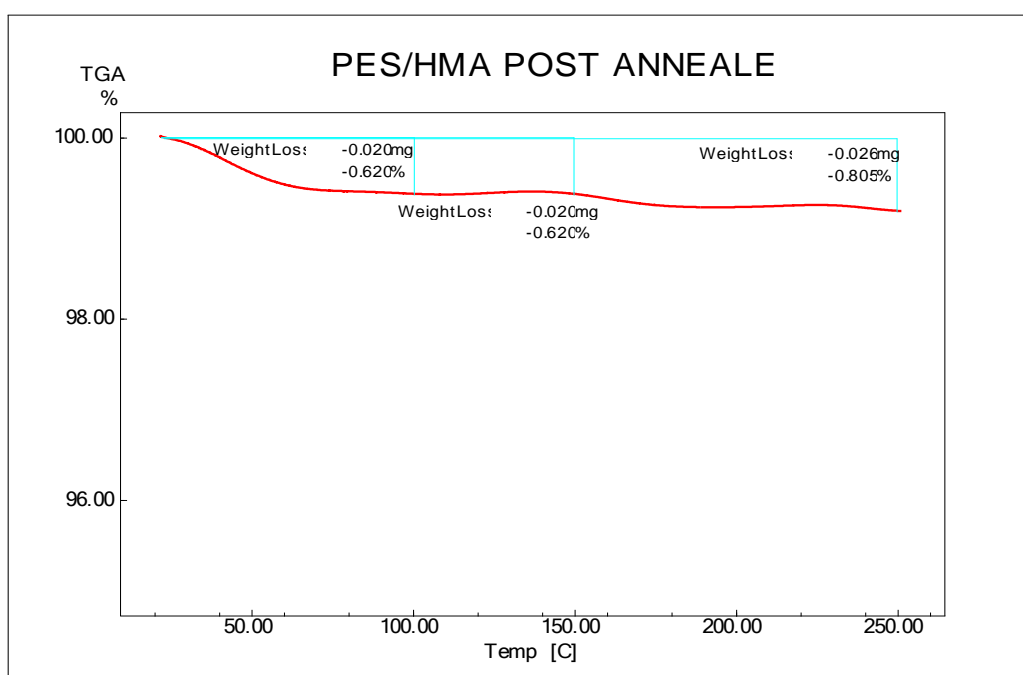


Figure C.4 TGA thermogram for PES/HMA-p membrane.



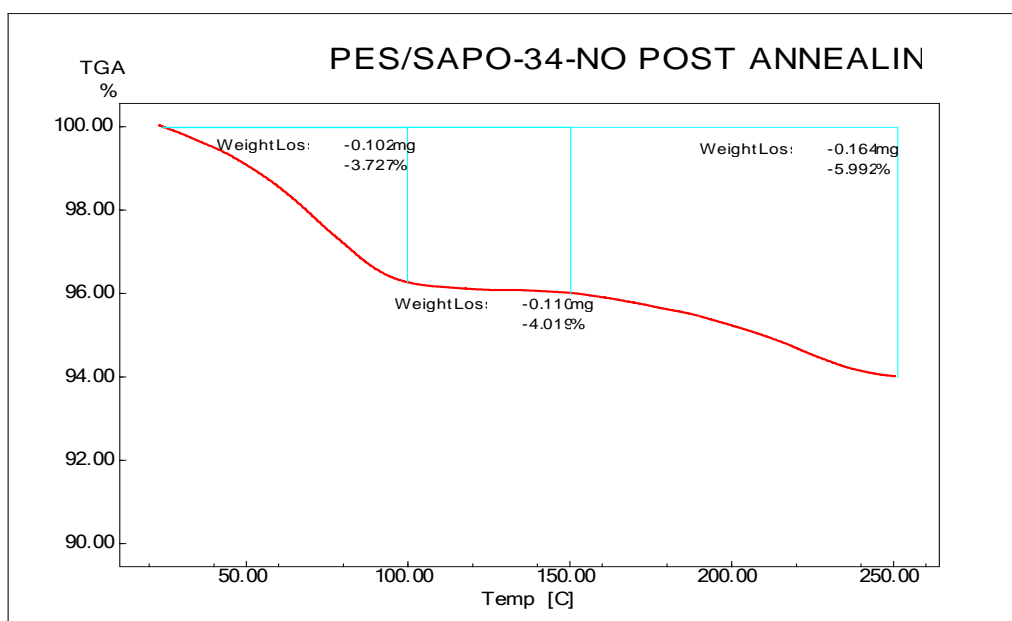


Figure C.5 TGA thermogram for PES/SAPO-34-n membrane.

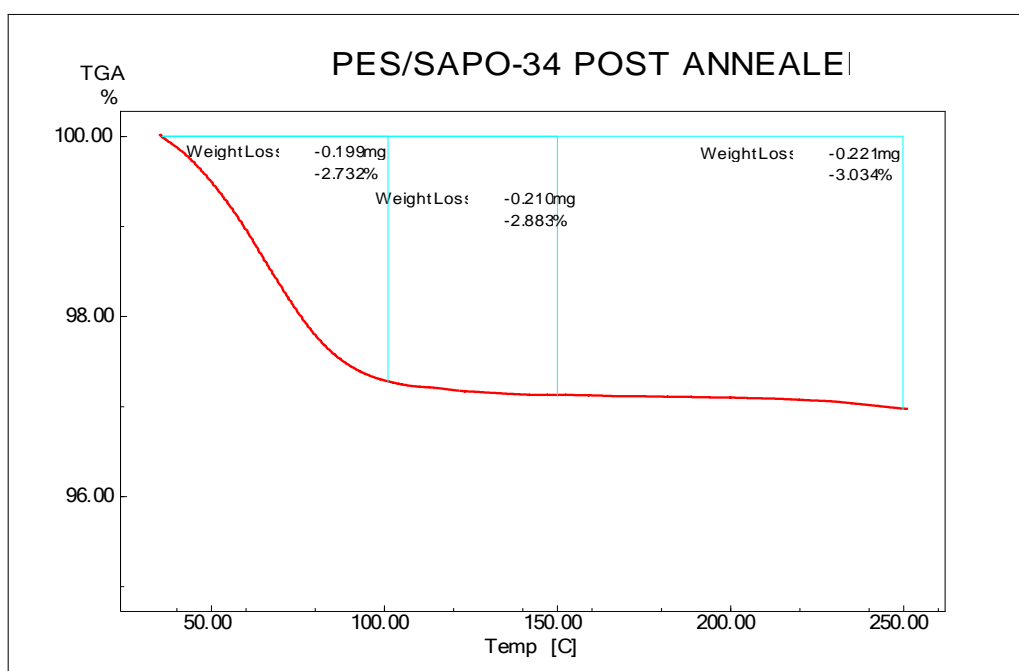


Figure C.6 TGA thermogram for PES/SAPO-34-p membrane.

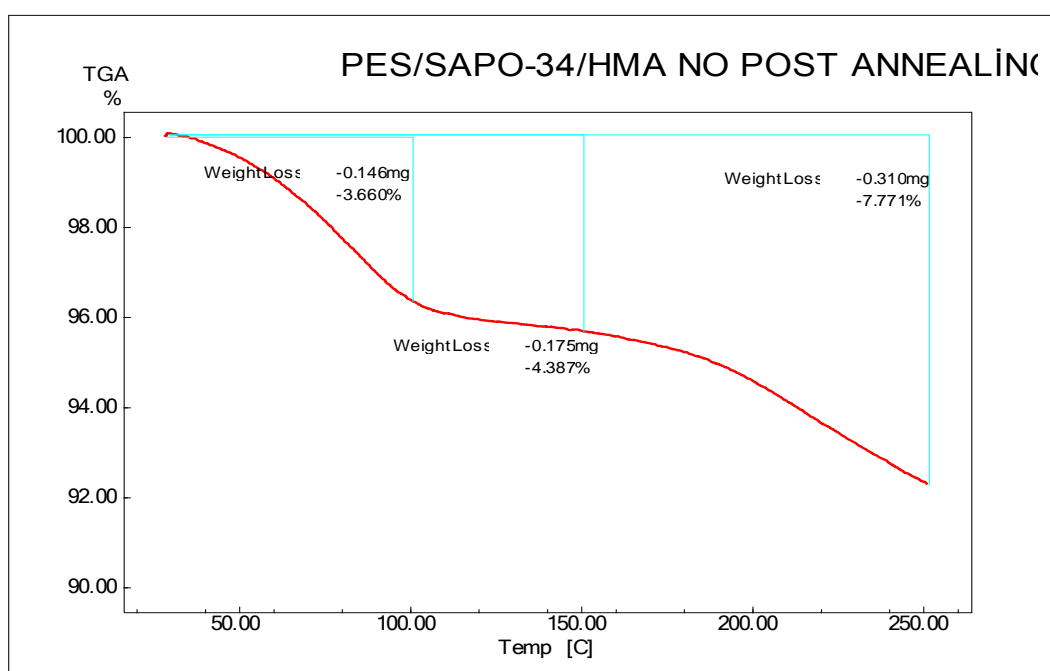


Figure C.7 TGA thermogram for PES/SAPO-34/HMA-n membrane.

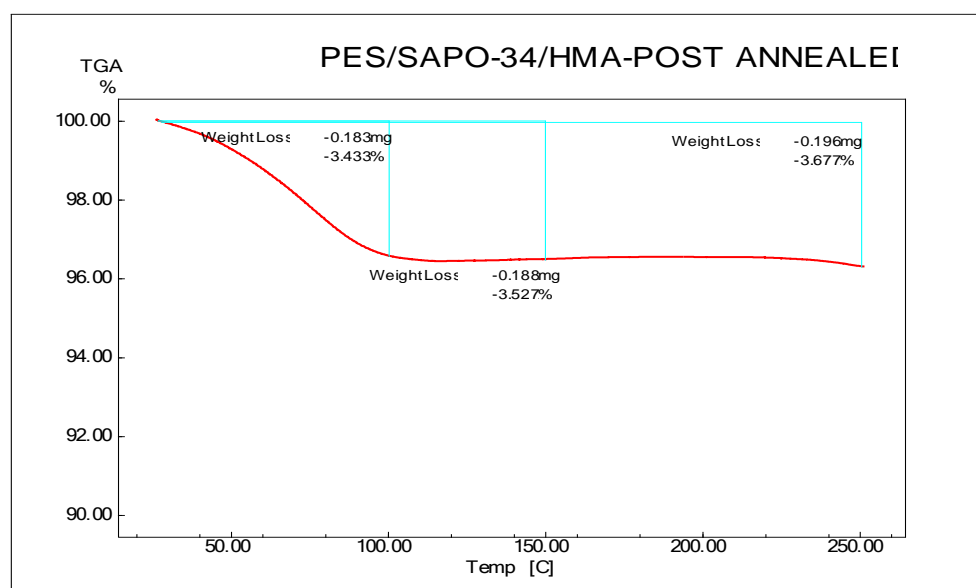


Figure C.8 TGA thermogram for PES/SAPO-34/HMA-p membrane.

## APPENDIX D

### PERMEABILITY AND SELECTIVITY DATA OF TESTED MEMBRANES

Table D.1 Single gas permeabilities of PES-n (M4) membrane obtained from temperature cycles at 35 °C and 90 °C, 1month long period.

	1 <sup>st</sup> Cycle		2 <sup>nd</sup> Cycle		3 <sup>rd</sup> Cycle		4 <sup>th</sup> Cycle	Δ%	Δ %
	35 °C	90 °C	35 °C	90 °C	35 °C	90 °C	35 °C	35 °C	90 °C
H <sub>2</sub>	7.95	20.07	8.03	19.58	7.9	18.98	8.01	0.63	5.43
CO <sub>2</sub>	3.75	7.68	4.0	7.68	4.03	7.39	4.03	7.47	3.78
CH <sub>4</sub>	0.11	0.39	0.11	0.39	0.11	0.4	0.11	9.18	2.04

Table D.2 Selectivities of PES-n (M4) membrane obtained from temperature cycles at 35 °C and 90 °C, 1month long period.

	1 <sup>st</sup> Cycle		2 <sup>nd</sup> Cycle		3 <sup>rd</sup> Cycle		4 <sup>th</sup> Cycle	Δ%	Δ %
	35 °C	90 °C	35 °C	90 °C	35 °C	90 °C	35 °C	35 °C	90 °C
Selectivities									
H <sub>2</sub> /CO <sub>2</sub>	2.12	2.61	2.01	2.55	1.96	2.57	1.99	7.55	2.30
CO <sub>2</sub> /CH <sub>4</sub>	38.27	19.59	37.38	19.49	37.66	18.48	37.66	2.33	5.67
H <sub>2</sub> /CH <sub>4</sub>	81.12	51.20	75.05	49.70	73.83	47.45	74.85	8.99	7.32

Table D.3 Permeabilities of PES-SAPO-34-n (M3) membrane obtained from temperature cycles at 35 °C and 90 °C, 2 month long period.

	1 <sup>st</sup> Cycle		2 <sup>nd</sup> Cycle		3 <sup>rd</sup> Cycle		4 <sup>th</sup> Cycle		5 <sup>th</sup> Cycle		6 <sup>th</sup> Cycle		Δ%		Δ %	
	35 °C	90 °C	35 °C	90 °C	35 °C	90 °C	35 °C	90 °C	35 °C	90 °C	35 °C	90 °C	35 °C	90 °C	35 °C	90 °C
Gas	10.58	26.76	12.67	29.96	14.20	31.31	14.69	32.02	14.73				39.22	19.66		
H <sub>2</sub>	4.58	10.36	5.72	11.35	6.80	12.02	6.96	11.91	7.09				54.80	14.96		
CO <sub>2</sub>	0.13	0.81	0.24	0.94	0.28	0.95	0.33	0.98	0.89	1.20	1.08	1.48	712.0	82.72		

Table D.4 Selectivities of PES-SAPO-34-n (M3) membrane obtained from temperature cycles at 35 °C and 90 °C, 2 month long period.

	1 <sup>st</sup> Cycle		2 <sup>nd</sup> Cycle		3 <sup>rd</sup> Cycle		4 <sup>th</sup> Cycle		5 <sup>th</sup> Cycle		Δ%		Δ %	
	35 °C	90 °C	35 °C	90 °C	35 °C	90 °C	35 °C	90 °C	35 °C	90 °C	35 °C	90 °C	35 °C	90 °C
Selectivity	2.31	2.58	2.22	2.64	2.09	2.60	2.11	2.69	2.08	2.69	10.06	4.08		
H <sub>2</sub> /CO <sub>2</sub>	34.44	12.79	23.83	12.07	24.29	12.65	21.09	12.15	7.97	76.87	4.98			
CO <sub>2</sub> /CH <sub>4</sub>	79.55	33.04	52.79	31.87	50.71	32.96	44.52	32.67	16.55	79.19	1.10			

Table D.5 Single gas permeabilities of PES/SAPO-34-p (M5) membrane obtained from temperature cycles at 35 °C and 90 °C.

	1 <sup>st</sup> Cycle		2 <sup>nd</sup> Cycle		3 <sup>rd</sup> Cycle		Δ%	Δ %
	35 °C	90 °C	35 °C	90 °C	35 °C	90 °C	35 °C	90 °C
H <sub>2</sub>	13.97	30.60	13.92	30.91	13.71	30.58	1.86	0.07
CO <sub>2</sub>	6.29	10.73	6.33	10.62	6.41	10.50	-1.91	2.14
CH <sub>4</sub>	0.19	0.70	0.20	0.69	0.20	0.69	-4.26	1.00

Table D.6 Ideal selectivities PES/SAPO-34-p (M5) membrane obtained from temperature cycles 35 °C and 90 °C.

	1 <sup>st</sup> Cycle		2 <sup>nd</sup> Cycle		3 <sup>rd</sup> Cycle		Δ%	Δ %
	35 °C	90 °C	35 °C	90 °C	35 °C	90 °C	35 °C	90 °C
H <sub>2</sub> /CO <sub>2</sub>	2.22	2.85	2.20	2.91	2.14	2.91	3.70	-2.12
CO <sub>2</sub> /CH <sub>4</sub>	33.46	15.37	32.13	15.41	32.70	15.20	2.25	1.15
H <sub>2</sub> /CH <sub>4</sub>	74.31	43.84	70.66	44.86	69.95	44.25	5.87	-0.95

Table D.7 Effect of operating temperature on permeabilities of PES-n (M4) membrane.

Gases	35°C	50°C	70°C	90°C	35°C
H <sub>2</sub>	7.60	9.72	13.45	17.4	7.55
CO <sub>2</sub>	3.66	4.31	5.25	6.35	3.65
CH <sub>4</sub>	0.106	0.165	0.265	0.42	0.103

Table D.8 Effect of operating temperature on selectivities of PES-n (M4) membrane.

Selectivities	35°C	50°C	70°C	90°C	35°C
H <sub>2</sub> /CO <sub>2</sub>	2.08	2.26	2.56	2.74	2.07
CO <sub>2</sub> /CH <sub>4</sub>	34.52	26.12	19.81	15.11	35.43
H <sub>2</sub> /CH <sub>4</sub>	71.69	58.91	50.75	41.42	73.30

Table D.9 Effect of operating temperature on permeabilities of PES/HMA-p (M7) membrane.

Gases	35°C	90°C	35°C	50°C	70°C	90°C	35°C	90°C	120°C
H <sub>2</sub>	6.22	15.52	6.07	7.96	11.60	15.64	6.11	15.12	22.56
CO <sub>2</sub>	2.09	4.00	2.16	2.59	3.22	3.97	2.20	3.98	5.39
CH <sub>4</sub>	0.06	0.22	0.06	0.08	0.13	0.22	0.06	0.21	0.42

Table D.10 Effect of operating temperature on selectivities of PES//HMA-p (M7) membrane.

Selectivities	35°C	90°C	35°C	50°C	70°C	90°C	35°C	90°C	120°C
H <sub>2</sub> /CO <sub>2</sub>	2.97	3.88	2.81	3.07	3.60	3.94	2.78	3.80	4.18
CO <sub>2</sub> /CH <sub>4</sub>	37.32	18.18	39.27	33.63	24.77	18.05	38.60	18.95	12.83
H <sub>2</sub> /CH <sub>4</sub>	111.1	70.54	110.4	103.4	89.23	71.09	107.2	72.0	53.71

Table D.11 Effect of operating temperature on permeabilities of PES/SAPO-34-p (M5) membrane.

Gases	35°C	50°C	70°C	90°C	35°C
H <sub>2</sub>	13.71	17.58	23.59	30.58	13.81
CO <sub>2</sub>	6.41	7.60	9.17	10.47	6.46
CH <sub>4</sub>	0.20	0.28	0.44	0.69	0.20

Table D.12 Effect of operating temperature on selectivities of PES/SAPO-34-p (M5) membrane.

Selectivities	35°C	50°C	70°C	90°C	35°C
H <sub>2</sub> /CO <sub>2</sub>	2.14	2.31	2.57	2.92	2.14
CO <sub>2</sub> /CH <sub>4</sub>	32.70	27.05	20.65	15.15	33.12
H <sub>2</sub> /CH <sub>4</sub>	69.95	62.56	53.13	44.25	70.8

Table D.13 Effect of operating temperature on permeabilities of PES-SAPO-34/HMA-p (M8) membrane obtained, 2 month long period.

Gases	35°C	50°C	70°C	90°C	35°C	90°C	35°C	50°C	70°C	90°C	105°C	120°C	35°C
H <sub>2</sub>	7.74	9.63	14.24	19.09	8.03	19.06	7.96	10.03	14.20	18.70	22.59	26.50	8.11
CO <sub>2</sub>	2.41	2.93	3.73	4.55	2.45	4.58	2.49	3.05	3.72	4.42	4.95	5.76	2.51
CH <sub>4</sub>	0.060	0.090	0.137	0.239	0.062	0.233	0.060	0.095	0.144	0.229	0.318	0.420	0.064

Table D.14 Effect of operating temperature on selectivities of PES-SAPO-34/HMA-p (M8) membrane obtained, 2 month long period.

Selectivity	35°C	50°C	70°C	90°C	35°C	90°C	35°C	50°C	70°C	90°C	105°C	120°C	35°C
H <sub>2</sub> /CO <sub>2</sub>	3.21	3.29	3.82	4.19	3.28	4.16	3.20	3.29	3.80	4.23	4.56	4.60	3.23
CO <sub>2</sub> /CH <sub>4</sub>	40.17	32.56	27.23	19.78	38.88	19.66	41.64	32.11	25.83	19.30	15.56	13.71	39.21
H <sub>2</sub> /CH <sub>4</sub>	129.0	107	103.94	83	127.46	81.8	132.77	105.5	98.6	81.67	71.04	63.5	126.72